STRONG MOTION ACCELEROGRAPH EVALUATION

Thesis by

Rex Bredesen Peters

In Partial Fulfillment of the Requirements

For the Degree of

Mechanical Engineer

California Institute of Technology
Pasadena, California

1969

(submitted February 14, 1969)

ACKNOWLEDGMENTS

The author wishes to thank Professor D. E. Hudson for his guidance and assistance throughout the investigation and in the preparation of this report. Thanks also are due to the other members of the advisory committee, Professors W. D. Iwan and J. Miklowitz.

The cooperation of H. T. Halverson, R. Obenchain, and L. H. Mauk of Earth Sciences, a Teledyne company, in making developmental changes suggested by the author during testing of the RMT-280 strong motion accelerograph is greatly appreciated.

The author is grateful for financial assistance provided by the Engineering Division of the National Science Foundation, as well as by the Ford Foundation and the California Institute of Technology, in carrying out this investigation.

ABSTRACT

A brief study is made of the effect of common instrument errors on the accuracy of data obtained from strong motion earthquake accelerographs. Error sources considered include zero drift, tilts, nonlinearities, cross-axis sensitivity, lack of initial conditions, noise, and time base errors. It is concluded that most data of current engineering interest are not critically affected by the level of errors found in existing accelerographs. Techniques are suggested for reducing or eliminating many of these errors by instrument design changes.

An experimental study is made of a new strong motion accelerograph during its engineering development. This new accelerograph is designed to record an FM analog of ground acceleration on magnetic tape, providing a record which may be rapidly and automatically converted to digital form. The accuracy limits of the accelerograph are explored and the design reasons for these limits investigated. The more significant findings may be briefly summarized:

(1) Static accuracy. The sensitivity and linearity of the instrument are found to depend critically on a series of interdependent adjustments. Reasonable care will bring errors in both of these quantities to within ±2% of 1/2 g full scale. Higher accuracies

are possible, but require much more time and care, primarily due to the limiting effect of mechanical drift in the accelerometers.

(2) Zero point drift. Uncertainties in the accelerometer zero point arise from both mechanical and electronic drifts. Long term drifts may be related to temperature or relative humidity, or may be entirely random. Short term drifts of up to 2% of full scale may occur during the course of a typical record. The total variation may be as much as ± 30% of full scale for a 100°F range of temperatures. These variations require adjustment of the data before processing, but are not sufficient to interfere with operation of the accelerograph.

(3) Noise. Random noise in the system as tested amounted to 1.4% of full scale, RMS, and was mostly due to the tape recording system. By comparison with optical accelerographs, this noise figure is marginal, but acceptable, and can be improved by changes to the compensation system.

(4) Timing. The advantages of an effectively continuous time base over discrete time marks were discovered and means devised to obtain such a base from the test accelerograph. This method of timing is a qualitative improvement over the best system which is practical on optical recorders.

The overall performance of the test accelerograph is adequate to yield acceptably accurate acceleration vs. time records and Fourier spectra within the range of frequencies which are of current engineering interest. It is able to produce useful displacement records only for periods shorter than several seconds. The reasons for this latter limitation are sufficiently fundamental that markedly superior instruments are not expected to be available within the next ten years.

TABLE OF CONTENTS

1. INTRODUCTION

For about the last century, geophysical studies have been aided by systems of sensitive instruments for the measurement of earth motions. Set up in well supervised seismological stations around the world, these instruments record continuously the faint motions caused by earthquake activity throughout the earth. The high sensitivities which make this long range monitoring possible unfortunately prevent these instruments from giving useful data on the strong motions associated with nearby earthquakes, since the recorders then simply go off scale. This shortcoming has not been considered to be of great importance for geophysical reasons since nearby earthquakes are comparatively rare.

If local earthquake effects differed only quantitatively from those recordable at greater distances, this attitude might still prevail. It has long been suspected, though, that such is not the case, and that the local effects which are responsible for the major economic impact of large earthquakes are worthy of study in their own right. The pursuit of this study soon led to the development of a new class of instruments - strong motion seismographs.

Strong motion seismographs have to meet a number of rather special requirements, the most trivial of which is reduced sensitivity compared to their predecessors. A more significant difference is

dictated by the very nature of their task: to give a good indication of local effects there should be at least several of them, spread over an area surrounding an earthquake epicenter. To have a reasonable probability of detecting an earthquake they must be located in as many as possible of the areas where earthquakes occasionally occur. Since the instruments must thus be rather numerous, they must be individually relatively inexpensive. Since they must be spread over large areas, they cannot be continuously supervised, and must be capable of reliable automatic operation after long periods of sitting unattended.

The numerous field instruments produce automatic records which are then analyzed at relatively few data reduction centers. Figures 1 and 2 show block diagrams of several such instrumentation systems either currently in use or undergoing active development. These systems differ considerably in their mechanical details, but they all show quite similar system organization and are subject to similar analysis.

Each of the boxes in these two figures stands for a transfer operation, and each may be represented by a transfer function showing the relationship of input to output. Some parts of this relationship may be functionally described, e.g. frequency or impulse response of a viscously damped accelerometer. Others are best related in terms of statistical properties, e.g. distortion of photographic paper during chemical processing and drying. The product of all these transfer functions describes the distortion which the input acceleration on the left undergoes in the process of being translated to the outputs

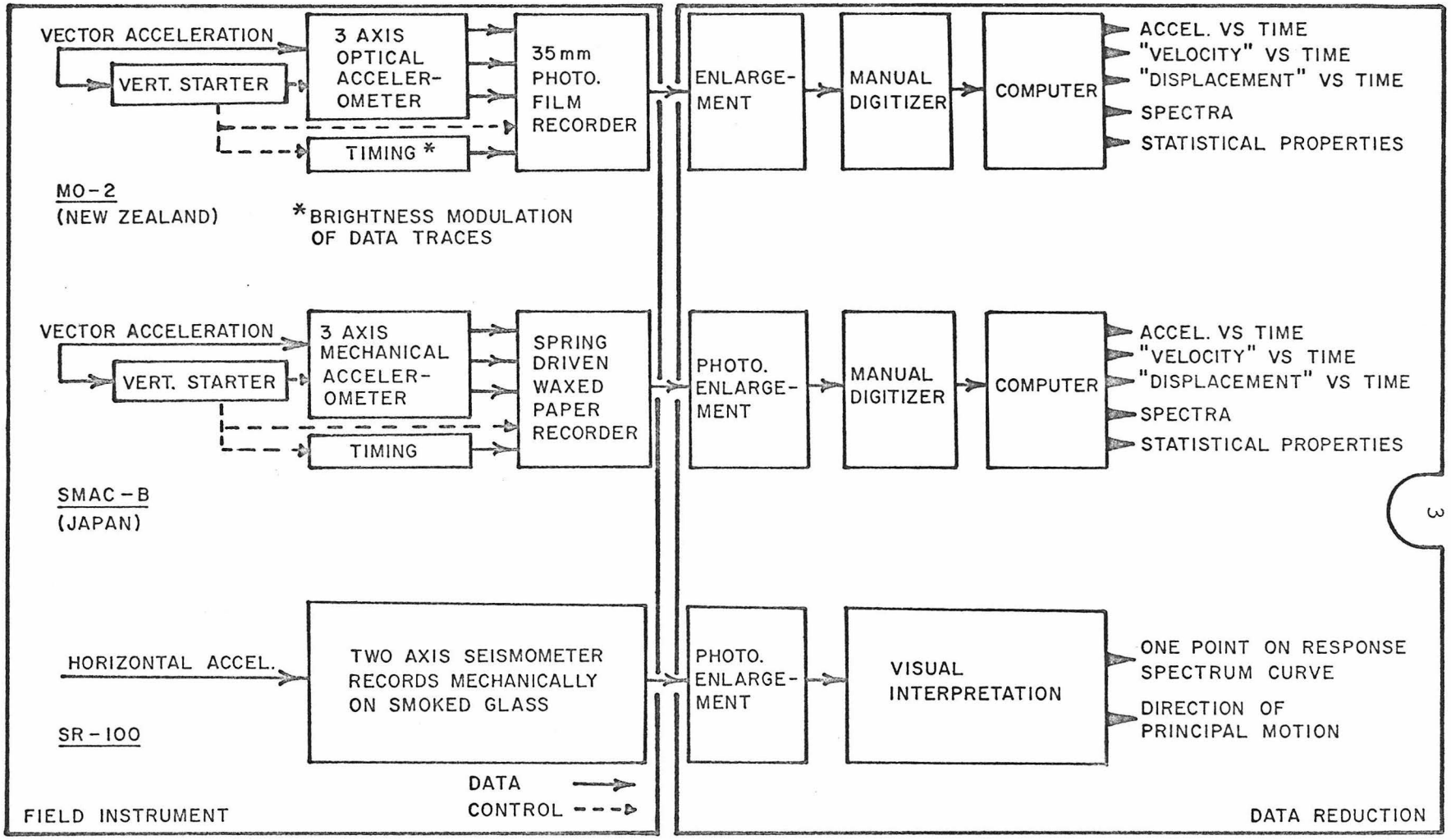

Figure 1: Block Diagrams of Several Representative Strong Motion Earthquake Recording Systems

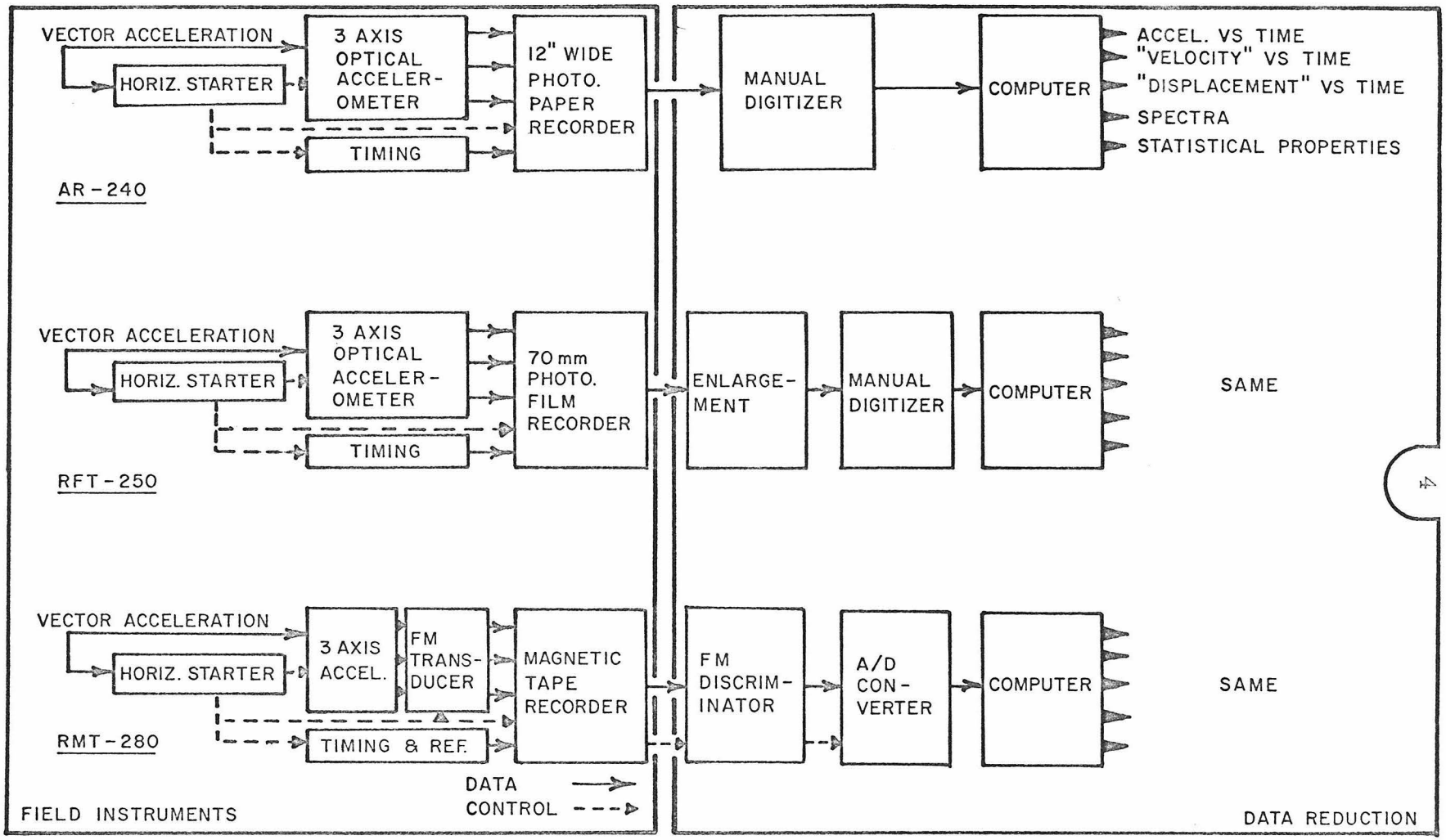

Figure 2: Block Diagrams of the Test Accelerograph and Its Immediate Ancestors from the Teledyne Corporation

on the right. Considerable work has been devoted to studies of the data reduction area of these systems, comparing outputs at the far right for a given record input to several data reduction systems, but comparatively little has been done about the left half and especially about box by box analysis of the overall system.

Studies of the right half of these diagrams have had their effect on the left half, however, in that human judgment has been identified as a principal variable in all of these systems, and that, plus the sheer man-hours required for manual digitization of a record of any length, has led to development of systems which permit data flow from extreme left to extreme right with no significant human intervention. An important step in this direction is the development of magnetic tape recording instrumentation, and this report is largely concerned with an analysis of such a system.

In analyzing the operation of an instrument system it is necessary to keep in mind the information which is to be obtained from it and the use to which that information will be put. Presently available systems produce acceleration/time records and response spectra which are of great value in assessing possible damage to an instrumented building following an earthquake, and for use in design criteria for new buildings in a given area. They also may yield statistical properties which are of value, for instance, in the defining of model earthquakes for theoretical and experimental studies of structure responses. And they produce "velocity"/time and "displacement"/time records which are of value in helping to

identify the mechanisms of strong earth motions.

The quotation marks around the words "velocity" and "displacement" are significant. Presently used or considered instrumentation systems are able to define velocities and displacements only to within a long period component whose amplitude is not accurately known and whose period may be as short as about one-half the record duration. This uncertainty reflects to some extent the lack of initial conditions in the records of existing instruments and also the accuracy limits of the overall systems. It is of little consequence in the parts of the response spectra curves which are of interest in determining the response of most engineering structures. But in a few cases, such as seiches in harbors and reservoirs, and breakage of underground structures, it is a significant limitation. It is also something of an impediment to studies of earthquake mechanisms, since it prevents any easy measurement of the grosser ground motions associated with an earthquake.

One desirable direction for instrument development, then, is in the direction of what might be called an "ultimate" instrument: one which is in effect a cross between the usual strong motion seismograph and an inertial navigation system, and capable of recording the actual motions in an earthquake with an uncertainty of an inch or so, rather than many feet, and with corresponding improvements in the reliability of the velocity and acceleration data. The basic system studied in this report is capable, at least conceptually, of producing such performance with only minor changes. Practically, however, the difficulties are

immense, as this study shows. The problems which stand in the way of the improvement of current instruments up to the "ultimate" system are indicative of the difficulty of development and probable expense of any such system, barring an unforeseeable dramatic breakthrough in instrument technology.

2. ACCURACY CONSIDERATIONS IN STRONG MOTION EARTHQUAKE RECORDING

2.1 Response of a Single Degree of Freedom System to a Transient Input Such as an Earthquake

The instruments traditionally used for earth motion recording are single degree of freedom, mass-spring-dashpot devices. The basic system with its equations of motion is shown schematically in the figure:

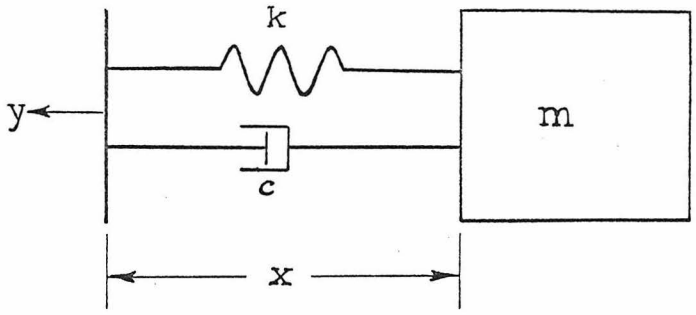

$$m(\ddot{x} - \ddot{y}) + c\dot{x} + kx = 0$$

$$\ddot{x} + 2\omega_o \zeta \dot{x} + \omega_o^2 x = \ddot{y}$$

where: m = seismic mass

k = spring constant

c = dashpot constant

$$\omega_o = \sqrt{k/m} = \text{radian natural frequency}$$

$$\zeta = \frac{c}{2\sqrt{km}} = \text{fraction of critical damping}$$

For a record starting at t = 0 with known initial conditions an integral solution of this equation is:

$$y(t) = y(0) + t\dot{y}(0) + x(t) + 2\omega_o\zeta \int_0^t x(\tau)\, d\tau + \omega_o^2 \int_0^t \int_0^\tau x(s)\, ds\, d\tau \qquad (1)$$

In seismic instrumentation, the motion y of the support is the ground motion, and the relative displacement x the measured quantity. Seismic instruments fall broadly into three categories, depending on the choice of ω_o and ζ. These choices are reflected in the relative importance of the last three terms in equation (1). When the instrument period is longer than the longest period in the motion y, the x term predominates (displacement meter). When the frequencies contained in y are near ω_o and ζ is several times larger than unity, the middle term predominates (velocimeter). When the frequencies contained in y are all below ω_o, the last term predominates (accelerometer). In common usage, strong motion instruments for earthquake engineering are nearly always of the accelerometer type, whereas seismographs for teleseismic use usually fall somewhere between the displacement and velocity classes. Some of the advantages of the accelerometer for strong motion use are:

(1) Because the transducer element has a relatively high natural frequency, accelerometers are smaller, lighter, and more rugged than either displacement meters or velocimeters.

(2) Accelerometers provide records which measure directly the quantity which is of primary interest to earthquake engineers. From the acceleration-time record, response spectrum curves can be computed.

(3) Displacement meters have the difficulty that earth motions near earthquake epicenters sometimes reach amplitudes of a few yards. Such large relative displacements cannot be accommodated in an instrument of reasonable size.

(4) The sensitivity of velocimeters is critically dependent on the value of ζ , while that of an accelerometer depends only on ω_o . Where a range of temperatures is involved, precise control of ω_o is relatively easy, whereas a corresponding precision in the control of ζ is much more difficult.

The transient response of a mechanical system may be written as:

$$x(t) = \int_0^t \ddot{y}(\tau)\, h(t - \tau)\, d\tau$$

where h(t) is the impulsive response. For a damped single degree of freedom system, initially at rest, this response is given by:

$$x(t) = \int_0^t \ddot{y}(\tau)\, \frac{e^{-\omega\zeta (t - \tau)}}{\omega_o \sqrt{1 - \zeta^2}}\, \sin \omega_o \sqrt{1 - \zeta^2}(t - \tau)\, d\tau \qquad (2)$$

As a representative input function, $\ddot{y}(t)$ will be taken as:

$$\ddot{y}(t) = \sum_{n=1}^{N} a_n \sin \frac{n\pi t}{T} \tag{3}$$

where: a_n = real constants

T = record duration

Substituting (3) into (2) gives

$$x(t) = \sum_{n=1}^{N} a_n \frac{e^{-\alpha t}}{\beta} \int_0^t \left(\sin \beta t \sin m\tau \cos \beta\tau e^{\alpha\tau} - \cos \beta t \sin m\tau \sin \beta\tau e^{\alpha\tau} \right) d\tau$$

where: $\alpha = \omega_o \zeta$

$\beta = \omega_o \sqrt{1 - \zeta^2}$

$m = \frac{n\pi}{T}$

Performing the indicated integration then gives

$$x(t) = \sum_{n=1}^{N} a_n \frac{1}{\beta\left(s^2 - 4m^2\beta^2\right)} \left\{ \left(\beta s - 2m^2\beta\right) \sin mt - 2m\beta\alpha \cos mt \right.$$

$$\left. + \left[\left(ms - 2m\beta^2\right) \sin \beta t + 2m\beta\alpha \cos \beta t \right] e^{-\alpha t} \right\} \tag{4}$$

where $s = m^2 + \beta^2 + \alpha^2 = \frac{4n^2\pi^2}{T^2} + \omega_o^2$.

For a typical strong motion accelerograph the exponentially decaying terms in equation (4) are of little importance. Common values are $\zeta = 0.6$, $\omega_o = 75$ radians $\sec^{-1}$, so that $\alpha = 45$ $\sec^{-1}$. If the start-up time is .1 seconds, which is also common, these terms are already decayed to 1% of their initial amplitude by the start of the accelerogram, which is less than 1% of the remaining terms.

The remaining terms in x can be described by the Fourier

coefficients in a series of the form:

$$x(t) = \sum_{n=1}^{\infty} b_n \sin \frac{n\pi}{T}(t + \varphi_n) \tag{5}$$

and it will be found that

$$b_n = \frac{a_n}{\sqrt{s^2 - 4m^2\beta^2}} = \frac{a_n/\omega_o^2}{\sqrt{\left(1 - \frac{n^2\pi^2}{T^2\omega_o^2}\right)^2 + \frac{4n^2\pi^2}{T^2\omega_o^2}\zeta^2}} \tag{6}$$

The form of the denominator in the righthand side of equation (6) is the same as the well known steady state response of a damped single degree of freedom system to a sinusoidal input at frequency $\omega = \frac{n\pi}{T}$. From this it is clear that the Fourier amplitude coefficients of $x(t)$ may be made approximately equal to those for $\ddot{y}(t)$, to within the multiplicative constant ω_o^2, to any desired degree of accuracy by proper choice of ω_o and ζ to make the denominator of b_n approximately 1.

Even if the denominator in equation (6) were always exactly 1, the numerical value of $\ddot{y}(t)$ would depend upon the variable phase shift term in equation (5). This term has no effect on the Fourier amplitude spectra, but does modify the instantaneous acceleration values. This effect can be minimized by taking $\zeta \simeq 0.7$, which leads to an approximately linear relationship between φ_n and n. In this case the phase shift produces a simple time shift in the record, combined with the already noted transient terms. For typical modern recorders, which do not record the transient part of the response and have no absolute time reference, the effect is negligible.

If displacements are to be calculated from the acceleration vs. time record, though, the possibility remains that errors may still be produced by the effect of double integrating the initial transients. To investigate this possibility, assume that the denominators in equation (6) are unity and multiply x by ω_o^2 to get the recorded acceleration. A measure of the displacement error would then be:

$$\text{displacement error} = \int_0^t \int_0^t \omega_o^2 x(t)\, dt^2 - y(t)$$

Using equation (4) for $x(t)$ and carrying out the algebra then gives:

$$\text{displacement error} = -\sum_{n=1}^{N} a_n \left[\frac{2\zeta T}{\omega_o n\pi} \left(1 - \cos\frac{n\pi t}{T} \right) \right] + O\left(\frac{1}{\omega_o^2} \right)$$

This error is non-decaying. For a typical term having $a_n = 50$ in/sec^2, $n = 100$, $\zeta = 0.7$, $T = 50$ seconds, and $\omega_o = 75$ rad/sec, the coefficient is 0.15 inches. The total effect depends on the particular record considered, since the coefficients a_n as originally defined can be mixed positive and negative and may either add or cancel. The possibility exists, however, especially for long records, that a significant difference could appear. Any such difference could be eliminated either by applying the inverse transform of the mechanical system to the record, if the transient part is included, or by taking the value of ζ/ω_o sufficiently small in the original design. Ordinarily, other factors cause the accuracy of displacement calculations to be so low that this effect is not a significant one.

2.2 Common Accelerograph Errors

The discussion so far has covered a few of the things which must be considered in evaluating the processing of an accelerograph record because of mechanical characteristics of an idealized accelerometer. Real instruments are subject to departures from ideal behavior which introduce additional factors. These departures may be of great or minor consequence depending on the intended use of the records. A few of the most significant ones follow, with estimates of their effects on (1) instantaneous accelerations, (2) Fourier spectra, and (3) the displacement calculated at t = 50 seconds.

Baseline Shift. Uncertainties in the record value corresponding to zero acceleration can arise in many ways; for example, accelerometer drift, record/playback errors, or simple lack of resolution. For a baseline error consisting of a simple small translation:

(1) Instantaneous acceleration: error = shift. Typically not significant.

(2) Fourier spectra: Ideally affects lowest order term only, which is of no concern, but may have shorter period effects through interaction with common computing techniques, one of which is discussed briefly in Section 2.3.

(3) 50 second displacement: If the transduction process is

assumed linear, this error term may be treated independently of the remainder of the signal. In this case a displacement error will occur which reaches a maximum value at the end of the record and is given by:

$$\text{displacement error} = 1/2\,(\text{baseline error})T^2$$

For a 50 second record duration and one inch permissible displacement error, the permissible baseline error is 1.2×10^{-6}g, or about .0004% of 1/2 g full scale. This is several orders of magnitude beyond the capabilities of existing recorders.

Instrument Tilt. If the instrument's orientation with respect to gravity changes between the final in-place calibrations and the taking of a record, a condition identical to the just mentioned baseline shift will occur. It is mentioned separately here because of its special consequences as regards instrument design. Tilts of the earth's surface have been observed which were sufficient to close the starting pendulums of AR-240 earthquake recorders and run out the paper supply. That calculates to be in excess of .002 radians, or sufficient to produce a 50 second displacement error of more than 75 feet in a horizontal accelerometer. The obvious conclusion is that instruments intended for displacement computations must have means to nullify such tilts, such as a servo leveling system, or perhaps use of accelerometers which do not have true static response but rather are sensitive only to motions with period less than several minutes.

Transduction Nonlinearities: If the overall transfer function of an instrument system from accelerometer relative motion to playback is nonlinear in a way which cannot conveniently be compensated for, errors will result. The question is pertinent here because such nonlinearities have been observed in the RMT-280, which is the principal subject of this report. (See Section 3.5.)

(1) Instantaneous acceleration: Since the subject here is transduction nonlinearities rather than mechanical nonlinearities, the error at any level is simply the difference between the actual instrument transfer function and the straight line which is chosen to approximate it.

(2) Fourier spectrum: The effect of nonlinearities on Fourier spectra does not lend itself to easy, generalized analytical representation. An estimate of the effect for small nonlinearities may be obtained by considering one simple case involving an unsymmetrical nonlinearity similar in nature to one which sometimes occurs in the RMT-280. (For purposes of this report, an unsymmetrical nonlinearity will be defined as one which cannot be approximated by a single straight line which is simultaneously best for both positive and negative accelerations, e.g. one which has significant even power terms in its power series expansion.) Take the idealized case of a record consisting of a single frequency fixed amplitude wave, and a transfer function which

contains just a linear and a quadratic term:

$$\ddot{y} = A \sin \omega t$$

$$\ddot{y}_{indicated} = \ddot{y} + \frac{\delta}{\ddot{y}_{max}} \ddot{y}^2 = A \sin \omega t + \delta A \sin^2 \omega t$$

$$= A \sin \omega t + \frac{\delta A}{2} - \frac{\delta}{2} A \sin 2\omega t \qquad (6)$$

For this simple case, the effect of the non-linearity has been to introduce an additional coefficient into the Fourier spectrum at twice the original frequency with an amplitude of the same order as the per unit nonlinearity. The only general conclusion which should be drawn from this is that Fourier spectra do not appear to be critically sensitive to small nonlinearities in the range of engineering interest. However, behavior remarkably similar to this simple example was actually observed in the system tests described in Section 4.

(3) 50 second displacement: A similar simplified example may also be used to estimate the effect of nonlinearity on displacement. An idealized earth motion consisting essentially of a step change in displacement is shown in Fig. 3. The acceleration associated with this idealized motion is a single cycle sine wave. A one second period and an amplitude of 6.28 feet second^{-2} would produce a displacement of one foot. If this signal is subjected to the same nonlinearity which has just been applied in equation (6), the constant

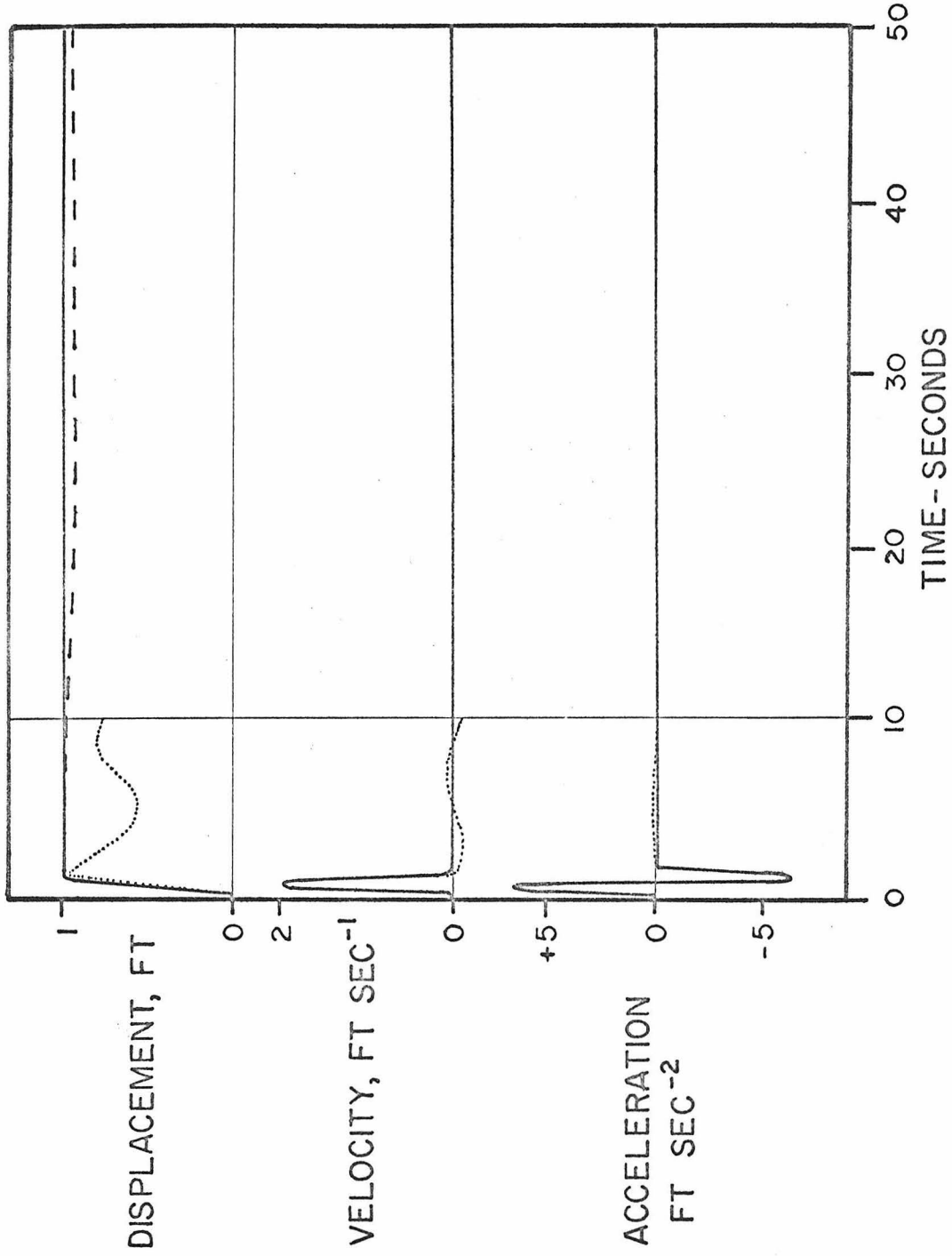

Figure 3: Idealized Earth Movement

term generated in the indicated acceleration will produce a velocity error which leads to a displacement error which increases linearly with time:

$$y_{indicated} - y \approx \left(\frac{\delta A}{2} \text{ ft sec}^{-2}\right) (1 \text{ sec})(T \text{ sec}) = \frac{\delta A T}{2} \text{ ft}$$

If $y_{indicated} - y = 1$ inch when $T = 50$ seconds, then $\delta = .0004 = .04\%$. Extrapolated to 1/2 g full scale, the permissible nonlinearity grows to:

$$\left| \frac{\ddot{y}_{indicated} - \ddot{y}}{\ddot{y}} \right| = 0.1\%$$

The simple example chosen represents a worst case for an unsymmetrical nonlinearity, but would produce at most a displacement error of the same order as the nonlinearity (no velocity error) for a symmetrical nonlinearity. This difference in sensitivity is the reason for making a distinction between the two kinds of nonlinearity. Both cases are applied to a more typical record in the system tests of Section 4.

Cross Axis Sensitivity: There are two kinds of cross axis sensitivity: The first is a small misalignment of the accelerometer sensitive axis, so that the acceleration axes recorded are not quite in their intended directions. The second is a change in the direction of the sensitive axis as a function of applied acceleration, e. g. a pendulum accelerometer whose most sensitive axis rotates with the sensing element.

In the first case, the measuring error is given approximately by:

$$\frac{\ddot{y}_{indicated} - \ddot{y}}{\ddot{y}} \approx \frac{\ddot{y}_{\perp}}{\ddot{y}_{||}} \theta - \frac{\theta^2}{2}$$

where: $\ddot{y}_{||}$ = acceleration parallel to intended sensitive axis

$\ddot{y}_{\perp}$ = acceleration perpendicular to intended sensitive axis

θ = misalignment angle, radians

In the second case, for a pendulum accelerometer:

$$\frac{\ddot{y}_{indicated} - \ddot{y}}{\ddot{y}} \approx \alpha\ddot{y}_{\perp} - (\alpha\ddot{y}_{||})^2$$

where: α = sensing element rotation constant, radians per unit acceleration (any consistent units).

When the angles are small enough that the quadratic terms may be neglected, these errors may be related to the results for nonlinearities by considering the special case where $\ddot{y}_{\perp} = \ddot{y}_{||}$. Then, for the first case, the effect is a simple error in sensitivity, which can be thought of as the simplest possible symmetrical nonlinearity. In the second case, the per unit error is proportional to the applied acceleration, which is precisely the unsymmetrical nonlinearity described just above. For the test accelerometers, $\alpha = .016$ radians/g, so the equivalent nonlinearity, referred to 1/2 g, is 0.8%, unsymmetrical.

Initial Conditions: Many practical problems stand in the way of continuously recording strong motion instruments, and all instruments now in use in the United States are of the stand-by type. Precise data on the effect of missing the first part of the motion are therefore not available. Some useful estimates can be made, however.

(1) Instantaneous acceleration: no effect.

(2) Fourier spectra: Comparative calculations for some specific cases have shown that the omission of short sections of the accelerograph record at the beginning and end of typical earthquake records have negligible effect on the Fourier spectra (Reference 5).

(3) 50 second displacement: The pendulum starter used on USCGS accelerographs has been developed empirically to do a satisfactory job of separating significant seismic events from normal background motions. The starter in the RMT-280 was designed to have the same dynamic characteristics. Half sine pulse tests on the USCGS starter, reported in Reference 4, indicate that the initial ground displacement at first contact closure is small, on the order of 0.05 inch, but that initial velocities may easily be of the order of 0.5 inch/sec. This velocity is small compared to the maximum velocities encountered in an earthquake record, but is nevertheless sufficient to account for a 25 inch error in the 50 second displacement if neglected.

Random Noise: Random noise can be added to an acceleration record by reading errors in the case of photographic records, or by any of a long list of noise sources in the case of electronic recorders. The most important contributors to this problem in the test accelerograph are described in Section 3.2.

(1) Instantaneous acceleration: The uncertainty in this value is the peak value of the added noise.

(2) Fourier spectra: If the sampling rate during digitizing is sufficiently high so that the highest significant frequency components of the added noise are below the Nyquist frequency, then there will be errors in the Fourier coefficients whose maximum magnitudes are equal to the corresponding coefficients of the noise spectrum. If the Nyquist frequency is lower than a significant component of either the noise or signal, then additional errors will be generated by aliasing. One of the major advantages of an all-electronic system is the practicality of removing unwanted high frequencies by filtering and then using a sufficiently high sampling rate to assure proper representation of the remaining information.

(3) 50 second displacement: The effect of random noise on displacement calculations is a principal subject of Reference 6. In that paper, the following equations are developed:

$$E\left\{\underline{X}(T)\right\} = x(T)$$

$$S.D.\left\{\underline{X}(T) - x(T)\right\} \approx 0.645 \frac{\sigma T^2}{\sqrt{N}}$$

where: $\underline{X}(T)$ = computed displacement

$x(T)$ = true displacement

T = record duration

σ = standard deviation of added random noise

N = number of equally spaced samples taken in time T

The conditions assumed in deriving these equations are satisfied by the present case of noise added to the signal before digitizing as long as the Nyquist frequency associated with N does not exceed the highest significant frequency component in the added noise. Higher values of N add no additional information, and so the assumption of independence of the samples breaks down, and there is no further improvement.

For a typical, carefully digitized, photographic record:

$\sigma = 0.2$ in/sec^2

$T = 50$ seconds

$N = 500$

$S.D.\left\{\underline{X}(T) - x(T)\right\} = 22.4$ inches

For a typical RMT-280 record, filtered at 25 Hz (see Section 3.2):

$\sigma = 1$ in/sec^2

$T = 50$ sec

$$N = 2500$$

$$\text{S.D.} \left\{ \underline{X}(T) - x(T) \right\} = 50 \text{ inches}$$

The RMT-280 figure is somewhat worse than that for the optical recorder but not as much as the higher noise level would lead one to believe, and since neither figure is acceptable at this duration it makes little real difference.

Time Base Errors: Time base errors may be conveniently divided into two groups: the D. C. term, or average error, and higher order terms in the Fourier expansion of instantaneous timing error vs. time.

For the D. C. term:

(1) Instantaneous acceleration: No effect on the actual peak values of acceleration.

(2) Fourier spectra: Coefficients are unchanged, but all frequencies are scaled by a percentage equal to the percent timing error, e.g. timing standard 1% fast will cause all frequencies to be 1% low.

(3) 50 second displacement: For small errors there will be a percent error in the final displacement equal to twice the percent timing error, e.g. timing standard 1% fast will cause computed displacement to be 2% too large.

For the higher frequency terms:

(1) Instantaneous acceleration: Still no effect on peak values.

(2) Fourier spectra: This effect does not lend itself to easy analytical representation, but some qualitative observations are in order. When a change in the indicated rate of time flow occurs, there is an apparent shift in all data frequency components exactly analogous to frequency modulation of each data frequency. For the case of a single data frequency and a single frequency variation in the indicated time scale, an expression for the spectrum which is generated by this modulation is derived in Reference 2:

$$M(t) = A_c \sum_{n=-\infty}^{\infty} J_n \left(\frac{\Delta\omega_c}{\omega_v} \right) \cos \left[(\omega_c + n\omega_v)t + \frac{n\pi}{2} \right] \qquad (7)$$

where:

$M(t)$ = modulated wave

A_c = data wave amplitude

ω_c = data wave frequency

$\Delta\omega_c$ = amplitude of apparent frequency change due to time base error

ω_v = frequency of time base perturbation

When both the data signal and the time scale perturbation have multiple term Fourier expansions, equation (7) becomes a triple sum, and is too complicated to draw conclusions from easily. Taking it as it stands, several pertinent observations may be made:

(a) Since $J_1(z) \approx \frac{z}{2}$, and higher terms higher orders, for $z << 1$, the spectrum error is approximately two new terms for each pair of interacting frequencies with resulting per unit errors which are of the same order as the per unit time scale variation.

(b) The spectrum is more sensitive to long period perturbations than to shorter periods.

(c) It should be noted also that the effect of a change in the speed of the recording medium which is not detected by the time standard is exactly the same as the effect of an error in the standard itself. This observation is particularly pertinent to existing photographic recorders which provide time pips only at intervals of one half second. Thus, chart speed variations with periods of one second or longer may be detected and corrected for, but shorter period components are not only not properly accounted for, but will in general be illegitimately reflected into the more sensitive long period part of the spectrum by aliasing. This shows another great advantage of the electronic recorder, in which it is practical to provide a clock signal which operates at a frequency many times higher than the highest frequency which will be used in any derived Fourier spectrum. The result is an effectively continuous time base whose stability can easily be made many times better than

any mechanical recorder drive mechanism.

(3) 50 second displacement: The exact analysis of the effect of random time base variations on displacement computations is another problem whose complexity places it beyond the scope of this report, but the remarks just made about discrete vs. effectively continuous timing marks are equally valid here.

2.3 Some Remarks on the Standard Baseline Adjustment Technique

As was mentioned at several points in Section 2.2, there are good physical reasons for believing that the mean value of the acceleration during a typical seismic event is considerably smaller than the values which would be calculated from unadjusted readings of the accelerograms. It has become common practice, therefore, to apply some sort of baseline adjustment to all accelerograph records before data processing is attempted. The presently accepted standard technique, which is described in detail in Reference 3, is, briefly:

$$a^*(t) = a(t) - C_o - C_1 t - C_2 t^2$$

where: $a^*(t)$ = adjusted acceleration

$a(t)$ = recorded acceleration

C_o, C_1, and C_2 are constants chosen so that the integral

$$\int_0^T \left[\int_0^t a^*(s)\, ds \right]^2 dt$$

is minimized.

The coefficients generated are nonlinear functions of the original acceleration record, so that superposition may not be used in discussing the total effects of this correction technique.

Even though superposition is not strictly valid for this technique, it is possible to gain some insight into its operation by examining some highly simplified cases. For example, consider an unadjusted acceleration record which may be represented exactly by a second degree polynomial. The adjusted acceleration from such a record would be identically zero. This does not mean that the adjusted acceleration is necessarily more accurate than the unadjusted record, since the unadjusted record could conceivably have been right to begin with. The adjustment process can not, of course, provide any new information which was not contained in the original record. The example does indicate, however, that if a real record contained such a component, it would be reduced to a small value by the adjustment technique.

There are several ways in which such components may be introduced into a record, such as accelerometer drift, either mechanical or electronic, chart paper distortion, and chart misalignment on a digitizing table. As indicated in Section 2.2, the sensitivity of displacement calculations to long period accelerations is such that amplitudes which are commonly found in unadjusted records, can lead to computed displacements several orders of magnitude larger than any which are considered as physically possible.

The adjusted records, in general, give displacements which are at least physically reasonable, and so these records are certainly more accurate than the unadjusted ones, even though the displacements may still contain comparatively large errors.

An indication of the possible size and nature of these remaining errors may be given by another simplified example. In Fig. 3 is shown the acceleration, velocity and displacement associated with a highly idealized ground motion, consisting of a single displacement step (a fault slip, for example) which occurs in a short period of time at the beginning of the record. Shown in broken lines are the shapes which these curves would take if the acceleration record were adjusted by the standard technique for two cases:

(1) Record length ten seconds (ten times duration of displacement).

(2) Record length fifty seconds (fifty times duration of displacement).

From these curves, several observations may be made.

(1) When the duration of the displacement is an appreciable fraction of the record length, errors of 50% or more in the computed displacements are quite possible.

(2) There is a tendency for adjusted displacements to fall toward zero toward the end of the record, much as though a high pass filter had been used on the data.

(3) Long, roughly periodic components are introduced into the record. A quadratic correction in the acceleration will introduce terms of the fourth degree into the displacement, with three horizontal tangents possible in the record, and an associated fundamental period on the order of one half the record duration. This sort of behavior was also observed in the system tests reported in Section 4.

(4) All of these effects are rapidly diminished as the record length is increased. This behavior is in marked contrast to the effect of a high pass filter, and suggests a reason for preferring this method of adjustment. It also suggests the possibility of improving the long period accuracy of records by allowing the recorder to run for some time, say a minute or more, after large motions have ceased. With photographic recorders, limitations imposed by record storage capacity and digitizing man-hours made such prolonged recording impractical, but with tape recording devices such as the test accelerograph, the idea seems worth further investigation.

Until recording systems are developed which provide zero point definition several orders of magnitude better than those now available some form of baseline adjustment will continue to be necessary. The current standard scheme has characteristics of complexity and nonlinearity which make general statements about its

effectiveness difficult to prove, but it seems to serve well enough to ensure its continued use. Even in the worst case, the errors in the adjusted acceleration record are of the same order as the accuracy limitations on accelerographs which are now in use or expected within the next ten years. It must always be recognized, however, that displacements computed from such adjusted records will contain long period errors which may be quite large, no matter how good the unadjusted record may be.

2.4 An Idealized FM Seismographic Recorder

The preceding paragraphs have shown how zero line drifts and lack of initial conditions in existing strong motion accelerographs can lead to unacceptable errors in calculated displacements. In principle, it should be possible to eliminate drift problems by producing an instrument whose output is measured with respect to some standard signal which drifts in the same way as the measured signal. In the case of an FM system such as the test accelerograph, this can be accomplished by providing a reference oscillator which is arranged so that its drift characteristics are essentially the same as those of the transducer oscillator. In such a case the phase differences only become significant, and in addition a means is available for determining the initial velocity, as can be shown by an example.

Suppose that the signal applied to the recorder has a frequency f_o modulated by an acceleration signal $a(t)$ such that instantaneous frequency is given by

$$f = f_o + \alpha a(t) = \frac{d\theta}{dt}$$

where θ is defined by the instantaneous signal voltage, E:

$$E = E_o U(\theta)$$

$U(\theta)$ is a periodic function of period 2π and unit amplitude (ideally a sine wave, but not necessarily so).

Therefore

$$\theta = f_o t + \alpha \int_0^t a(t)\,dt + \theta_o$$

If there is also available a reference oscillator running at f_o', it will have

$$\theta' = f_o' t + \theta_o'$$

and the phase difference between the two oscillators at any time will be given by

$$\theta - \theta' = (f_o - f_o')t + \theta_o - \theta_o' + \alpha \int_0^t a(t)\,dt$$

In the special case that $f_o = f_o'$ and $\theta_o = \theta_o'$

$$\theta - \theta' = \alpha \int_0^t a(t)\,dt$$

which differs only by the initial velocity, and the known constant α, from the system velocity. If, in addition, $\theta = \theta'$ at some time shortly before the beginning of the recorded event when velocity is zero, then the phase difference divided by α is precisely the system velocity. This condition may be realized by having both oscillators

continuously running and phase locking them together with a circuit whose time constant is long compared to the anticipated record, so that the average phase difference is zero when the average velocity is zero for a sufficiently long period of time, say, several minutes.

An apparent ambiguity arises if the phase difference exceeds π radians at the beginning of the record, since there is in general no way to tell how many multiples of $\pm\pi$ radians separate the two signals at that point. By proper selection of system parameters, however, it may be arranged that this rarely happens and creates no difficulty when it does. For example, if a = 200 Hz/g (the value used in the test accelerograph), then π radians corresponds to 0.5 f.p.s., which is a velocity that would only rarely be exceeded within the start-up time of presently known instruments. In the rare case that it was, an error of 0.5 f.p.s. in initial velocity would integrate to a displacement error of 30 feet in a one minute record; that would surely resolve the apparent ambiguity. The velocities associated with phase differences less than π radians are such that one might use some measure of phase difference, such as instantaneous voltage difference between the continuously running oscillators, as a means of triggering the recorder into operation.

It is important to note that the phase difference between two signals is independent of any irregularity in the motion of the recording medium except skew, and skew effects may be eliminated if necessary by multiplexing two signals on a single track. This system would therefore permit velocity recording, and hence integration to

displacement, with an insensitivity to recording noise comparable to digital techniques. At the same time, analogue acceleration playback to satisfactory accuracy would be readily available by existing techniques described in Section 3.2.

The purpose of this example is to show that a strong motion accelerograph capable of providing meaningful displacement data may be possible without the mechanical complexity and reliability problems of continuous recording or the maintenance costs of large area triggering networks. It is possible, at least in principle, with existing recording techniques and stand-by type instruments, at the expense of a relatively small continuous current drain. Problems of long period drift in the oscillators are overcome by slaving the data oscillators to the reference oscillator so that they all drift together. The major obstacle to be overcome, at the present state of the art, is an economically acceptable upgrading of the quality of the transducers. The remainder of this report will concern itself in large degree with the current status of that problem.

3. TEST ACCELEROGRAPH ANALYSIS

3.1 Instrument Description

The Earthquake Recorder studied uses electromechanical transducers for the recording of strong motion earthquakes on magnetic tape.* It is a battery powered recorder designed to sit unattended in remote locations for periods up to several months, and record earth motions above an adjustable threshold as they occur. To achieve this endurance with a reasonable size battery pack, the recorder was designed to be triggered into operation by the motion itself, and to be turned completely off, drawing no stand-by power whatsoever, between events.

A block diagram of the system has been shown at the bottom of Fig. 2 in the introduction. In this block diagram, elements to the left of the vertical double line are parts of the field instrument, while those to the right remain in the laboratory or data reduction center and are somewhat at the discretion of the individual user. A description of the playback equipment used in this evaluation and the considerations pertinent to its choice will be found in Section 3.2.

The field instrument is an entirely self-contained unit consisting of a three axis FM accelerometer package, a card containing all control functions plus a fixed frequency reference

---

*Teledyne RMT-280 Prototype

oscillator and an independent one-half second interval timer, a magnetic tape recorder, an inverted pendulum starter, and a battery pack. The physical arrangement of these elements is shown in Fig. 4.

The accelerometer package contains three mutually perpendicular Lehner-Griffith (Wood-Anderson) type accelerometers, each with a moving coil in a permanent magnet field to provide both damping and rough calibration, and a variable reluctance transducer. The transducers are connected to three independent circuit cards which produce electrical outputs which are a frequency modulated analogue of the accelerations applied along the sensitive axes of their respective accelerometers. The center frequencies are 1020, 1360, and 1700 Hz, with a deviation of 100 Hz equivalent to 1/2 g. These accelerometers and their associated circuitry are described in greater detail in Section 3.3.

The control card contains relays for switching all circuits on in response to a contact closure in the starting circuit, a time delay which maintains power for 7 seconds after the last such closure, and two independent timing and reference systems. Provision is made for starting from either the unit's own pendulum starter or from some external source, such as another unit's pendulum starter or a relay in a radio link. The timing and reference circuitry provides a fixed frequency of 2040 Hz and an independent flip-flop circuit driving a relay which amplitude modulates the 2040 Hz signal in a square wave pattern with a 500 millisecond period (see Fig. A3 in Appendix A).

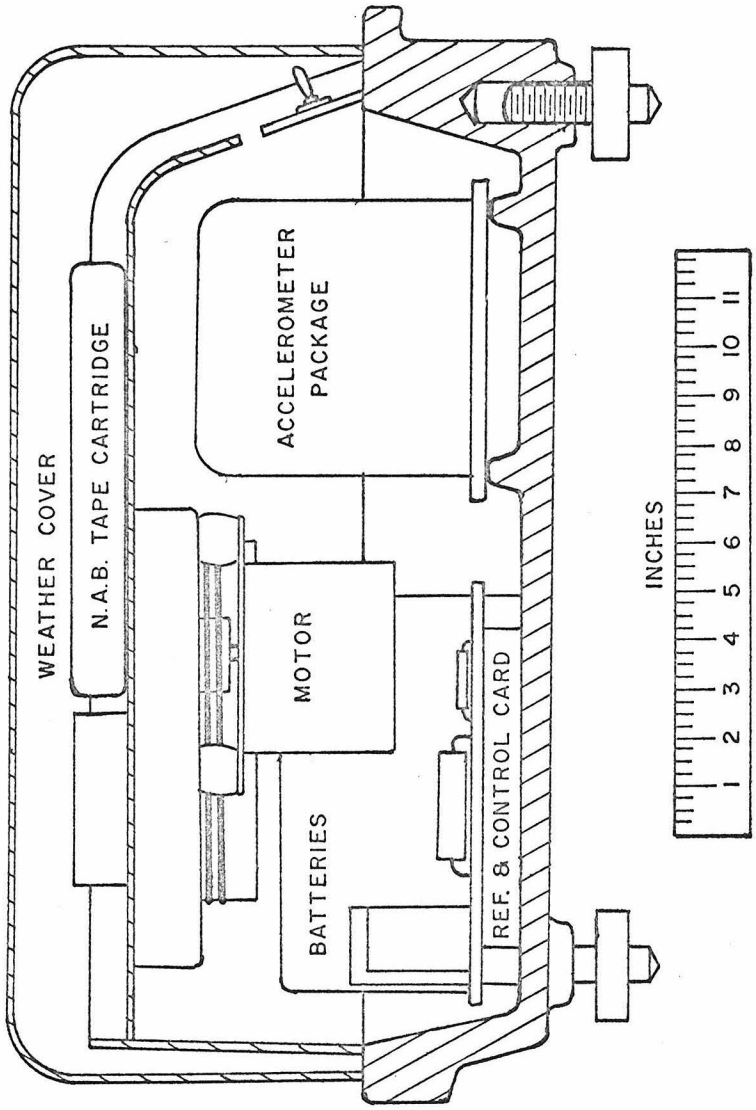

Figure 4: Interior View of Test Accelerograph

Provision is made also for driving this relay from an external source, such as another recorder, in order to provide several recorders with a common time base for correlation of their records.

The magnetic tape recorder uses standard NAB 1/4" tape cartridges with a capacity of 48 minutes at 3-3/4 inches per second. Signals are recorded on four tracks, one for each acceleration channel and one for the 2040 Hz reference. Use of separate tracks permits recording in the direct mode with no bias. The FM acceleration signals are recorded into saturation and the reference signal just far enough below to preserve the amplitude variations which carry the time pip information. The D. C. drive motor is speed controlled by a mechanical governor and operates at twice normal voltage to reduce start-up time.

The pendulum starter is dynamically equivalent to that used in the original USCGS accelerograph. It is more compact that its predecessors, but is virtually identical in performance, with a one second period and approximately critical damping. It responds to inputs in the horizontal plane, including static inputs such as instrument tilt. The choice of period, damping, and contact clearance in this starter probably is not in any sense optimized, owing to a marked scarcity of design data (i. e. strong motion records which begin before the arrival of the initial waves), but many years of operating experience indicate that it performs its task of sorting out significant seismic events from normal background motions with a high degree of reliability and in a reasonably short starting time.

The battery pack consists of four 6-volt rechargeable batteries giving 24 volts for recorder operation and ± 12 volts for the solid state electronics. The battery capacity is adequate for approximately 2-1/2 hours of continuous recording and the anticipated self discharge loss in storage is less than 40 percent per year. After a year of inactivity, the battery should have more than sufficient remaining capacity to use up the recording tape.

The analysis in this report is based on two accelerograph units*, and on the first prototype of the FM accelerometer which is the basis of the instrument.

3.2 Short Period Noise Generation in the Accelerograph System

Unwanted and unpredictable low-level signals are generated at every stage in the system, from the transducer itself through analog to digital conversion of the magnetic tape records. Many noise sources were identified in early testing and have been controlled by minor redesign. In its present state, the system is capable of performance closely approaching that of standard optically recording accelerographs.

The most natural division of noise sources in the system is not by system components but rather by frequency, with a dividing line placed at roughly one cycle per second. Above this frequency are most of the problems associated with noise introduced by the recording and playback process, analog to digital conversion, and mechanical,

---

*RMT-280, Serial Nos. 101, 102

electrical and magnetic interactions between the various parts of the field instrument. Below it are a collection of deviations from ideal behavior which take place over periods ranging from several seconds to several weeks and which are sufficiently distinctive in character to be treated in a separate section. The phenomena associated with start-up are roughly on the border in terms of frequency but fit more naturally with the long period phenomena and will be included there.

The greatest single source of short period noise in the system in its present form is the record/playback process. To appreciate the sources of this noise, a brief digression into the state of the art of FM tape systems is necessary.

An ideal FM discriminator may be considered as a device which produces an output voltage proportional to the instantaneous frequency of its input signal, and then subtracts a D. C. voltage to produce a null output when the input is at the center frequency:

$$V(t) = Af(t) - Af_o = A\left[f_o + F(t)\right] - Af_o = AF(t)$$

where $V(t)$ = output voltage

A = a constant of the discriminator

f_o = center frequency

$F(t)$ = a frequency function (departure from center frequency) which carries the information signal.

When the signal is recorded on magnetic tape as an intermediate step, the picture is complicated by the fact that the tape does not run

through the transport me chanisms at a precisely constant speed. If the per unit speed variations are called $a_1(t)$ for the record pass and $a_2(t)$ for the playback pass, all frequencies in the original signal will be multiplied by the quantity $(1 + a_1)(1 + a_2) = 1 + a_1 + a_2 + a_1 a_2 = 1 + a(t)$. The output signal of the discriminator will be changed correspondingly to

$$V' = A\left(1 + a(t)\right) f(t) - Af_o = a(t)Af_o + A\left(1 + a(t)\right) F(t)$$

producing an error component or noise voltage:

$$V' - V = a(t)Af_o + a(t)\,AF(t)$$

If a constant frequency f_1 is recorded on the tape at the same time as the data signal $f_o + F(t)$ and played back into a separate discriminator set for that center frequency, a signal proportional to $a(t)$ will be produced ($F(t) = 0$ in this case) by means of which a degree of compensation may be accomplished. The simplest technique is to scale this speed variation signal to match the first term of the error component above, and then subtract leaving only the second term. This provides very good compensation for signals $F(t)$ which do not deviate very far from zero, but the quality of the compensation declines rapidly as $F(t)$ becomes an appreciable fraction of f_o.

A better technique, and the one which is used in the playback equipment employed for this evaluation, is to use the speed variation signal to control the gain of the data channel discriminator:

$$V'(t) = A'(a)\left(1 + a(t)\right)\left(f_o + F(t)\right) - Af_o$$

$$V'(t) - V(t) = \left[A'(a)\left(1 + a(t)\right) - A\right]\left[f_o + F(t)\right]$$

$$\text{Then, if } A'(a) = \frac{A}{1+a}\ , \quad V' - V = 0$$

It is possible, in principle at least, in this way to provide perfect compensation for "flutter" (the name given to tape speed variations). Circuits which accomplish the desired change in gain are available and are not prohibitively complicated. A block diagram of such a compensated system is shown in Fig. A1 located in Appendix A.

Certain practical difficulties remain, however. In the output circuitry of an FM discriminator it is necessary to provide a low-pass filter in order to suppress the carrier frequency of the input wave. A low pass 2nd order linear filter which is designed for minimum distortion of complex wave forms has a time delay between input and output which is nearly independent of frequency within its pass band and whose magnitude is given approximately by:

$$\Delta t = \frac{\pi}{2\omega_o}$$

where: Δt = time delay, seconds

ω_o = corner frequency, radians/second

For example, the 25 Hz filter which was used in the data channel of the discriminator used for evaluation of the accelerograph system has a delay of approximately 10 milliseconds.

Such small delays are significant because the compensation signal must be filtered, and hence delayed, before it is applied to the

compensation input of the data channel. It can be easily shown that the result of such a delay is a residual noise signal which is proportional both to the time derivative of the uncompensated noise signal and to the time delay. With the 25 Hz filters originally included in both channels of the discriminator system used in these tests, the resulting transfer function, rising linearly with frequency, had unit amplitude at 14 Hz, with noise frequency components higher than that actually being amplified. Changing the compensation channel filter to 70 Hz corner frequency moved this unit gain frequency to 39 Hz and improved performance considerably. Further boosts in the filter frequency appear impractical due to beat frequencies generated when the data and compensation carriers are allowed to mix. A large order of improvement is still possible, however, by introducing a time delay into the data channel, as indicated in Fig. A1. For reasons which will be seen shortly, the total improvement from such added complication is limited, and the system appears acceptable without it.

The RMT-280 system introduces a further complication into the compensation problem by recording the reference signal and data signals on separate tracks so that they do not necessarily see the same instantaneous speed variations. The test accelerographs were originally equipped with two head assemblies of two tracks apiece, staggered vertically to produce four tracks on the tape. About an inch of tape separated the point at which the reference signal was recorded from that at which two of the three data signals were recorded. A simple calculation showed that fluctuations in tape tension of as little

as .01 lb rms could produce uncompensable errors greater than those commonly accepted in previous optical recorders. Early testing proved that excessive tape stretch did indeed occur and the final version of the accelerograph has a single four element head. This arrangement is still subject to errors due to tape skew, i.e. tape not crossing the head at a constant angle, but this error has proved experimentally to be acceptably small.

All such errors could be avoided by frequency multiplexing a reference signal and three data signals on a single track, and this is commonly done. The necessity of separating the four frequency components applied on the track when the tapes are played back would preclude the use of the present simple but highly nonlinear recording process and add substantially to the complexity of individual field units. Fortunately, this additional complexity is unnecessary in the present instrument.

The noise output of the system was assessed by introducing various signals into an FM discriminator and measuring the resulting noise output with a B&K true RMS voltmeter set for a time constant of 10 seconds. In the case of noises generated within the instrument, a single discriminator sufficed. In the case of noises generated by the record/playback process a variety of combinations involving one "data" channel and one compensation channel were tried.

All record/playback tests were made on the two head stack version of the instrument. These tests provided the data which dictated the later change to a single stack of four heads, and also

included one set of tests which are valid for either case, so that it was not necessary to repeat the tests when the heads were changed. Test tapes were prepared by connecting all four heads of the recording machine in series with a stable oscillator in order to record four identical tracks which could then be used in various combinations as data and compensation tracks. The normal arrangement of tracks for both head configurations is shown in Fig. A2, Appendix A. Playback was always by the same machine: a Viking cartridge tape deck which is similar in design to the RMT-280 transport mechanisms, except that it uses a hysteresis synchronous AC motor in place of the governor controlled D. C. one and has correspondingly better speed regulation.

In some cases noise outputs were analyzed by passing them through a Kron-Hite variable active filter used in the low-pass mode. Band-pass filtering is a more conventional way of assessing noise spectra, but filters of sufficiently narrow band width to be used in the 2-25 Hz range are not easily obtained, and the low pass filter used has the advantage of being a realistic simulation of a possible actual operating condition.

When it seemed desirable to obtain separate values for noise sources which could only be measured in combination with other noises, it has been assumed that the noises dealt with are approximately Gaussian so that their noise powers add algebraically. In most cases the corrections obtained are of the same order as the scatter in the measurements, so that the precise validity of this

rather reasonable assumption is not critical. An example is the total flutter of the tape transport, which was obtained by deducting the noise generated during playback from the total noise.

For convenience, noise values are reported as percentages of 1/2 g full scale. One percent thus corresponds to a one Hz frequency deviation (100 Hz = 1/2 g).

The results of these measurements are summarized in Fig. 5 and in Table 1. The solid curves in the figure represent tapes prepared on Accelerograph No. 1 and played back on the Viking deck. Dashed curves represent tapes both prepared and played back on the Viking deck. In both cases, the following combinations were used:

U. C.: This is the uncompensated output of a single track. It is not necessary to specify which track was used, as all tracks gave substantially the same result.

D. S.: The initials stand for "different stacks". This output was obtained by playing track 2 (in stack 1) and compensating it by means of track 3 (in stack 2). In this combination skew effects are minimized, but tape stretch effects are present.

S. S.: These initials stand for "same stack". Track 1 was played back with track 3 again used for compensation. Stretch effects are eliminated, but skew effects are maximized.

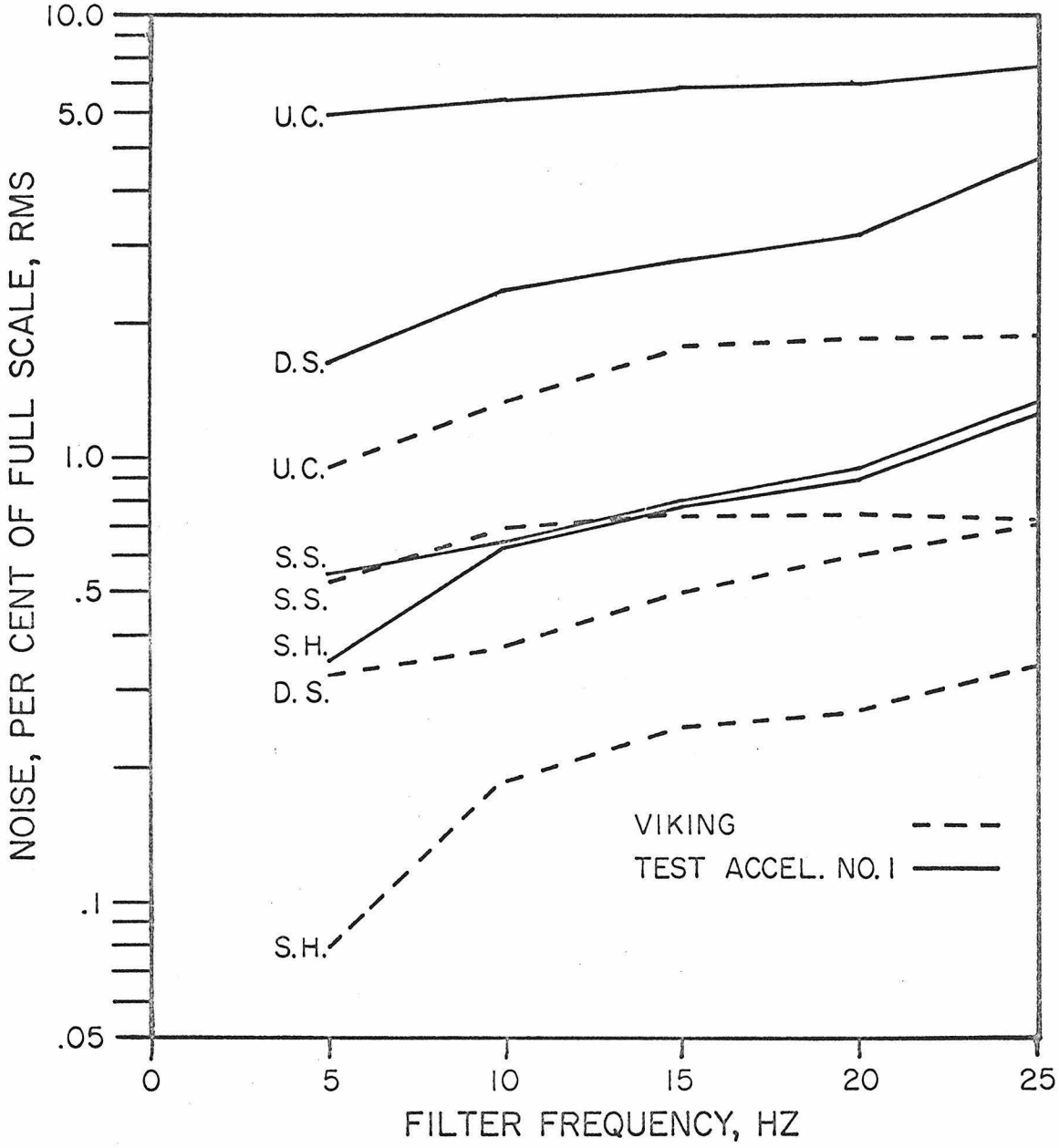

Figure 5: Summary of Noise Levels Generated by Recording System

TABLE 1

SUMMARY OF NOISE LEVELS

	AC Deck, Record & Playback %RMS*	db	RMT-280 Record, AC Deck Playback %RMS*	db
Uncompensated				
25 Hz	1.84	0	7.50	0
10 Hz	1.35	0	6.50	0
Different Stacks				
25 Hz	0.73	-8.0	4.70	-4.1
10 Hz	0.38	-11.0	3.30	-5.9
Same Stack				
25 Hz	0.71	-8.3	1.35	-14.9
10 Hz	0.70	-5.7	0.65	-20.0
Same Head				
25 Hz	0.34	-14.7	1.35	-14.9
10 Hz	0.19	-17.0	0.70	-19.3

*based on 1/2 g full scale

D.C. Compensation: <1% shift in compensated output when compensation and data channels are fed from the same source and shifted 100% (100 Hz); >40 db compensation.

For comparison, typical digitizing errors from photographic records are estimated to be about 0.3% of full scale, RMS.

When related to 1000 Hz center frequency rather than 100 Hz deviation, the wow and flutter figures for the tape decks are:

AC Deck	0.13% RMS
Test Accelerograph	0.74% RMS
Medium priced "Hi-Fi" recorder (typical)	0.2% RMS

S. H.: These initials stand for "same head". Track 3 was played back into both data and compensation channels. This eliminates both skew and stretch effects, and shows what could be obtained by frequency multiplexing the reference frequency on all three data channels rather than using a separate track as at present.

The abscissa of the graph is the corner frequency of the low pass filter, so that the curves are, in effect, cumulative spectra, showing the total response for a given amount of high frequency filtering. The 25 Hz point of each curve corresponds to the 12 db per octave passive filter which is built into the FM discriminator, while lower points were obtained by the series insertion of the Kron-Hite 18 db per octave active filter. The low ends of these spectra were limited to about 2 Hz by the frequency response of the meter.

Several pertinent conclusions can be drawn from these data:

(1) The speed variations produced by the centrifugal governor controlled motor in the RMT-280 deck are some five times worse than those from the AC synchronous motor in the Viking playback deck. This fact is reflected in all the noise measurements and in particular in the large variations in tape tension which necessitated abandonment of the two stack design in favor of the slightly more expensive four heads in a single stack. Such is the price paid for rapid start-up, battery operation, and comparative simplicity in

the field instruments.

(2) The total noise from the present system is such that the noise associated with tape skew is of little consequence, except at very low frequencies. Elimination of the time delay effect in the playback equipment would have a worthwhile effect for a relatively small investment in terms of the overall system, but would be limited to about a factor of two by the tape skew effect. Elimination of both of these effects would be rather expensive because of the added complexity of the field units.

(3) The system as it stands is only slightly worse than the optically recording units it is intended to replace, when filtered at 25 Hz, and about the same when filtered at 10 Hz. Further, the slight edge which the optical system might hold is partly offset by the larger number of points which it is practical to take in a wholly automated digitizing system.

The solution indicated at the end of observation number 2 would make possible a noise attenuation of 40 db or more throughout the 0-25 Hz bandwidth, bringing the total recording noise to less than .1% rms. Since this is not the only noise in the system, the additional complexity is probably not justified.

Several other sources of short period noise have been detected in these instruments, whose causes are in some cases only partially

understood. In Accelerograph No. 2, a random noise output of about 0.8% rms was observed when the recorder motor was operated. Connection of a separate wire direct from the battery to the recorder motor reduced this output to about 0.1% by reducing the magnitude of the voltage spikes applied to the accelerometer package. Both recorders showed an even larger problem from this source (about 2% rms) until voltage regulator circuits were added at the inputs to the accelerometer electronics packages. With this change the noise dropped to below .1% in No. 1, but only by half in No. 2. Both regulator circuits appear to be working equally well. If necessary, this noise can be cured with an additional relay.

In Accelerograph No. 1 a noise amounting to about 0.15% rms has been traced to magnetic coupling between the recorder motor and the nearest variable reluctance transducer (the one on the transverse accelerometer). This noise has not been detected in No. 2, but that may mean that it is small enough to be masked by the electrical noise.

The difference between the two instruments may reflect other differences in the drive motor performance. A factor of two was noted between the currents drawn by the two motors while running unloaded at the same governor controlled speed. These differences are of no practical interest unless the recording noise is substantially reduced.

A third minor problem is shared by both recorders. Since all FM discriminators are at least slightly amplitude sensitive, the step changes in amplitude which occur four times a second on the output of the reference oscillator to provide timing marks produce small

noise spikes in the output of the compensation discriminator, which are then reflected in the data channel. At present, keeping the amplitude change to no greater than 20% limits the spikes to a size which is barely detectable in the overall noise. A substantial reduction in other noises would make this solution impractical, and might necessitate a new concept for the timing mark system. If all data and compensation signals were put on a single track, for example, the time mark system could then be placed on a separate track and be entirely independent.

The first version of the test accelerographs had all four oscillators designed for the same center frequency. It was found, however, that there was sufficient magnetic coupling between the channels to produce gross beat frequency effects when the oscillators deviated by a few Hz from one another. Shielding proved unworkable, because of the powerful static fields associated with the transducer damping magnets, which simply saturated the shields. It was thus found necessary to convert to four widely separated frequencies for the four oscillators.

3.3 Short Term Drift

Laboratory evaluation of the accelerograph has revealed a number of curious mechanical, electro-mechanical, and electronic phenomena which affect the stability of the zero acceleration output of the accelerometer package, in a manner analogous to a base line shift in the optical recorders. Some aspects of these phenomena

appear to affect only the ease and accuracy of calibration of the devices, and probably are not an essential shortcoming of the instrument as a measuring system. Other aspects, however, show up as an uncertainty in the zero level of the acceleration records produced, and in particular as a change in the zero level during the first few minutes after start-up. These effects are large enough to be significant in terms of overall system accuracy for long period measurements, but appear to be predictable only to the extent of putting a rough upper limit on their size.

The transducer element used in the accelerograph is similar in many respects to those used in previous optically recording accelerographs. The basic construction of this accelerometer is shown in Fig. 6. It will be described in more detail in a later paragraph.

The most noticeable difference between the new accelerometers and earlier versions of the instrument is the addition of a variable reluctance transducer to sense rotation of the accelerometer moving element and so provide, through associated solid state circuitry, a frequency modulated analog electrical output, suitable for tape recording. All instruments tested were set up to provide a frequency deviation of 100 Hz for .5 g's. As before, small variations in output will be expressed as a percentage of 0.5 g full scale, i.e. 1% = 1 Hz deviation = 5 millig's.

Following is a listing of the most important experimental anomalies observed during the testing of these accelerometers, showing the sequence of the investigation.

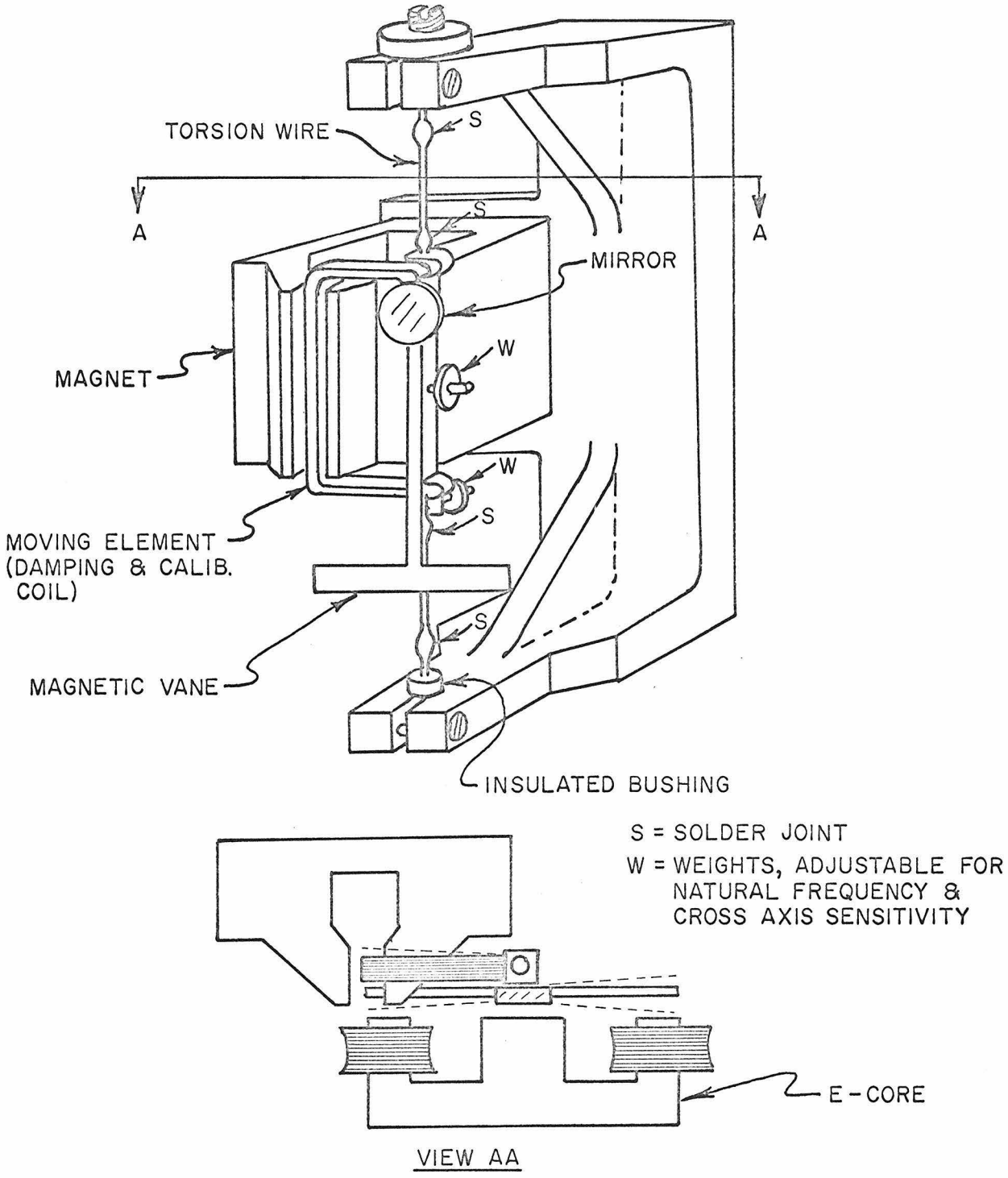

Figure 6: Lehner Griffith Accelerometer as Used in Test Accelerographs

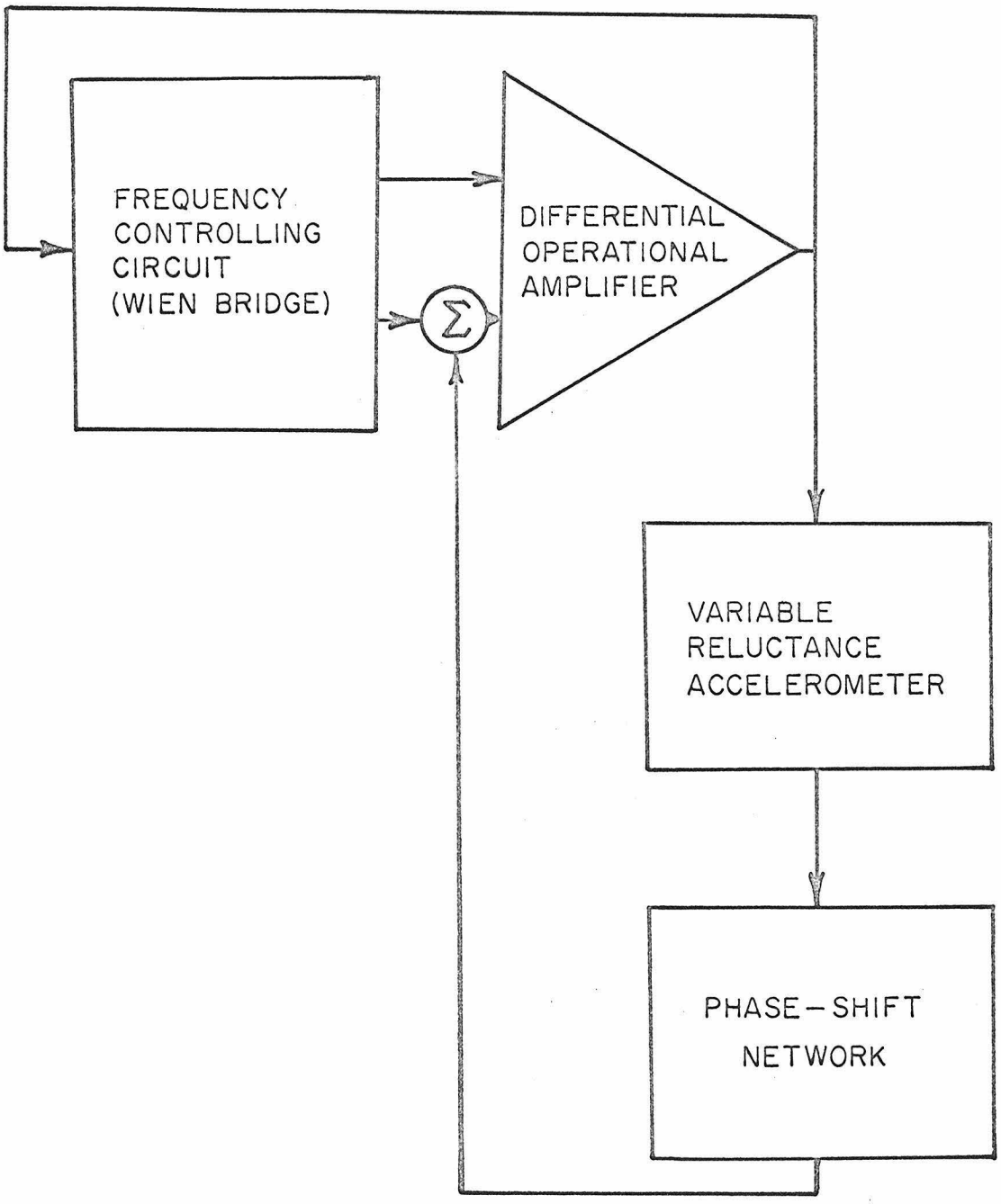

Figure 7: Operational Block Diagram of RMT-280
Acceleration Controlled Oscillator

(1) The Prototype Transducer. The first transducer tested was a rebuilt version of a standard Lehner-Griffith Strong Motion Seismometer element. It differs somewhat in appearance from Fig. 6 but is mechanically almost identical.

(a) It was observed that a step acceleration input produced a step change in output, followed by a slow drift of 2-3% over the next several minutes, and that a return to zero acceleration caused a step change back to an output which differed from the original zero level by about the amount and direction of the drift. The output would then return to zero in an approximately exponential fashion with a time constant of at least several minutes. A typical curve is shown plotted in Fig. 8.

(b) Another Lehner-Griffith accelerometer which still had its mirror attached was tested optically using an optical arm of about 30'. When it was deflected an amount corresponding to about 1/2 g by means of its calibration coil and then allowed to return to zero, an optical offset with a maximum value of about 2% was observed, decaying toward zero with a time constant which varied from trial to trial, but which was typically several minutes.

(c) Long term stability was checked by monitoring frequency changes associated with long term applied acceleration.

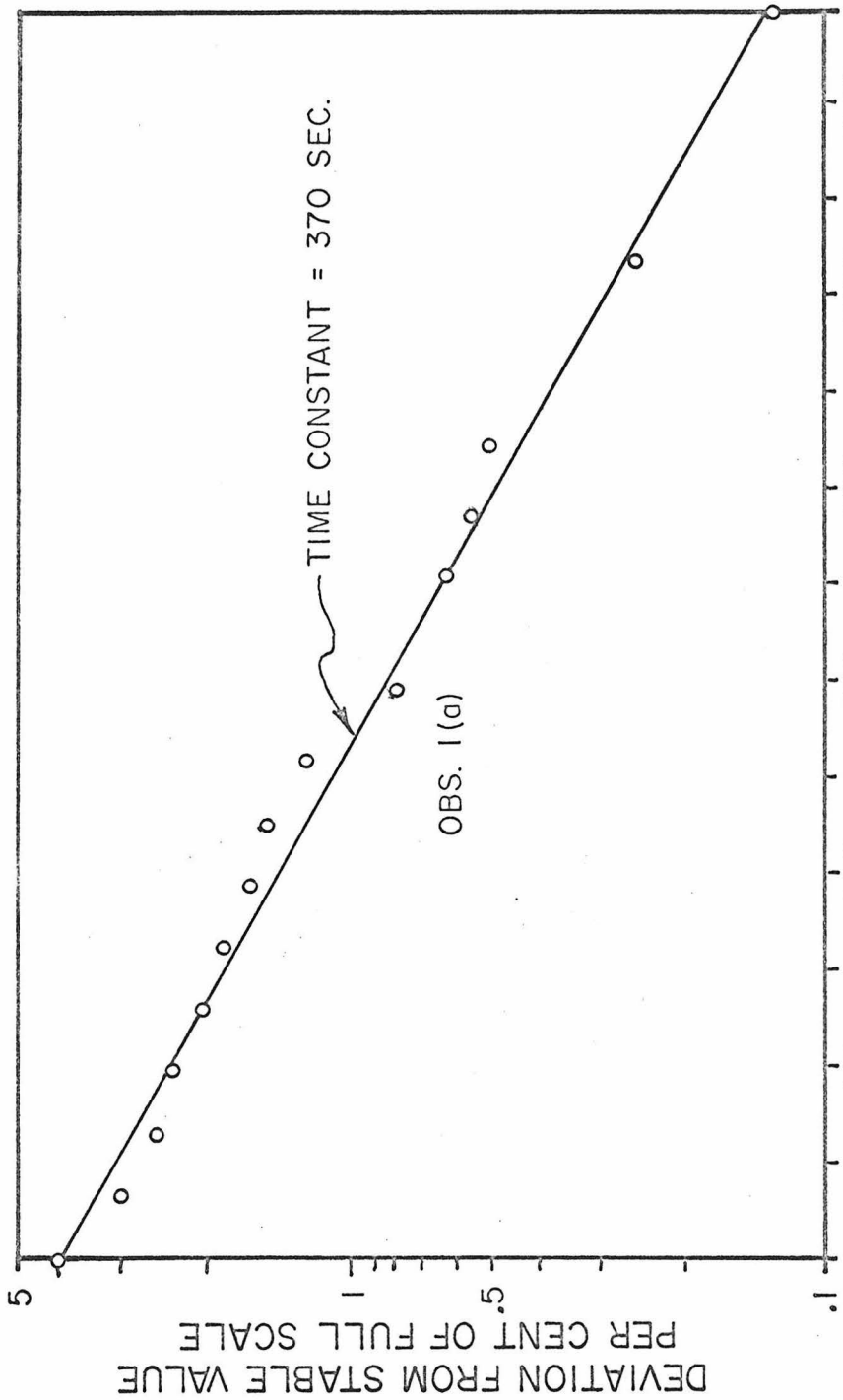

Figure 8: Prototype Accelerometer Recovery from 1/2 g (5 minutes)

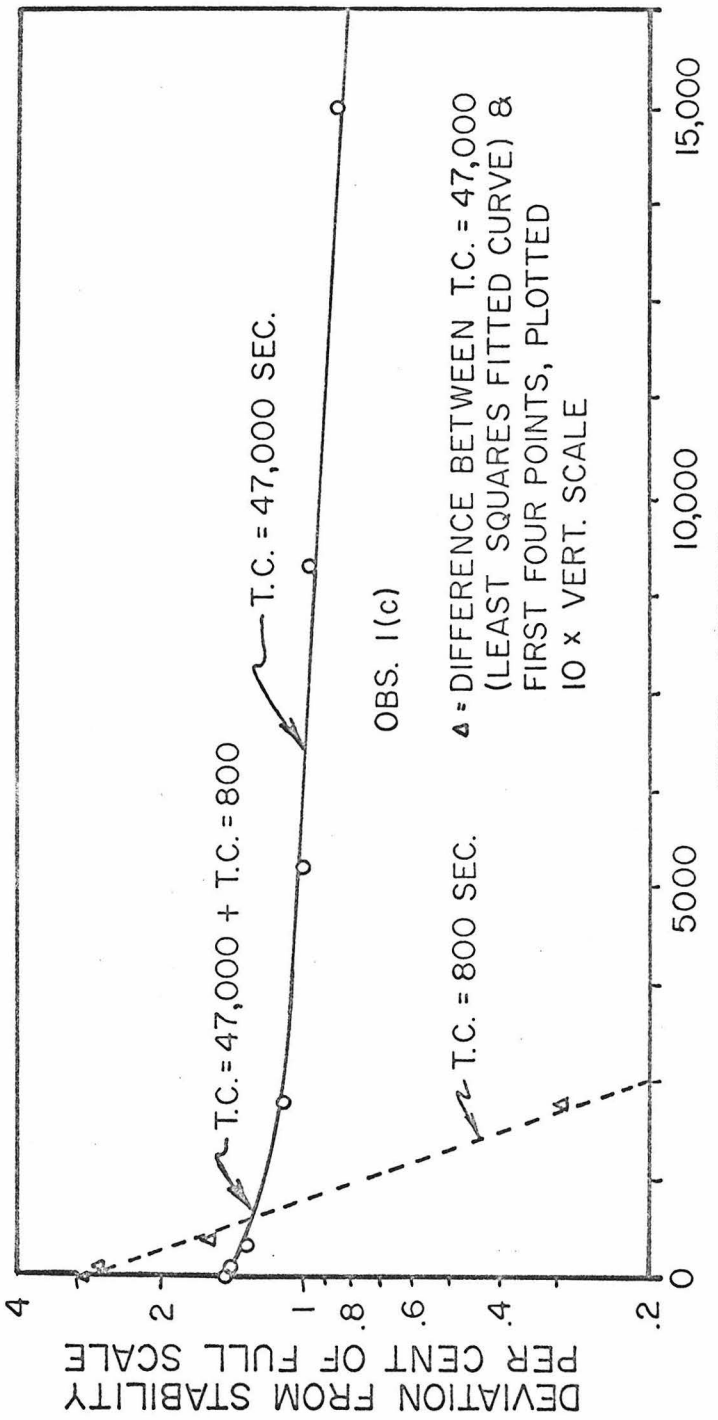

Figure 9: Prototype Accelerometer Recovery from 1/2 g (28 hours)

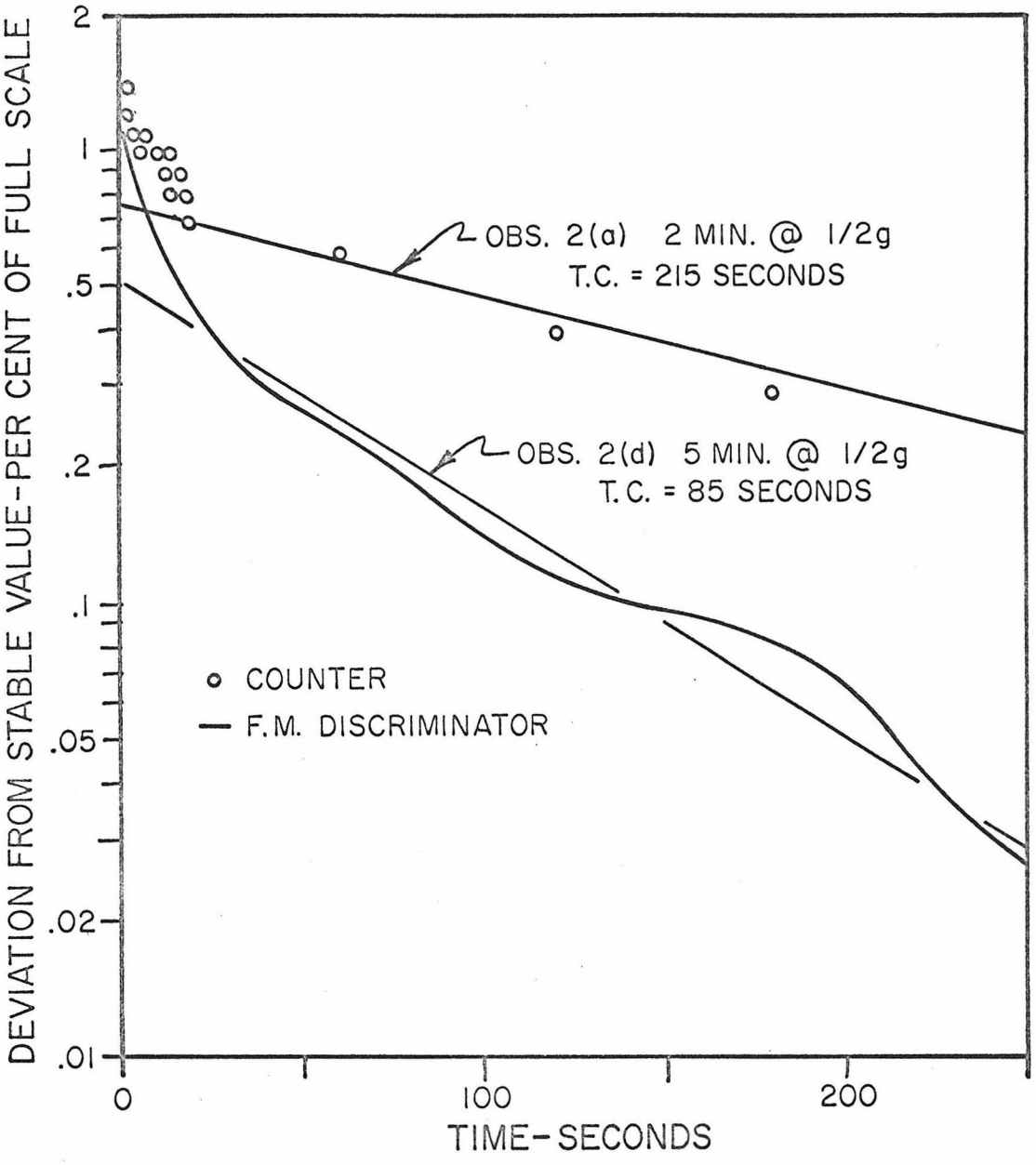

Figure 10: Test Accelerograph Recovery from 1/2 g

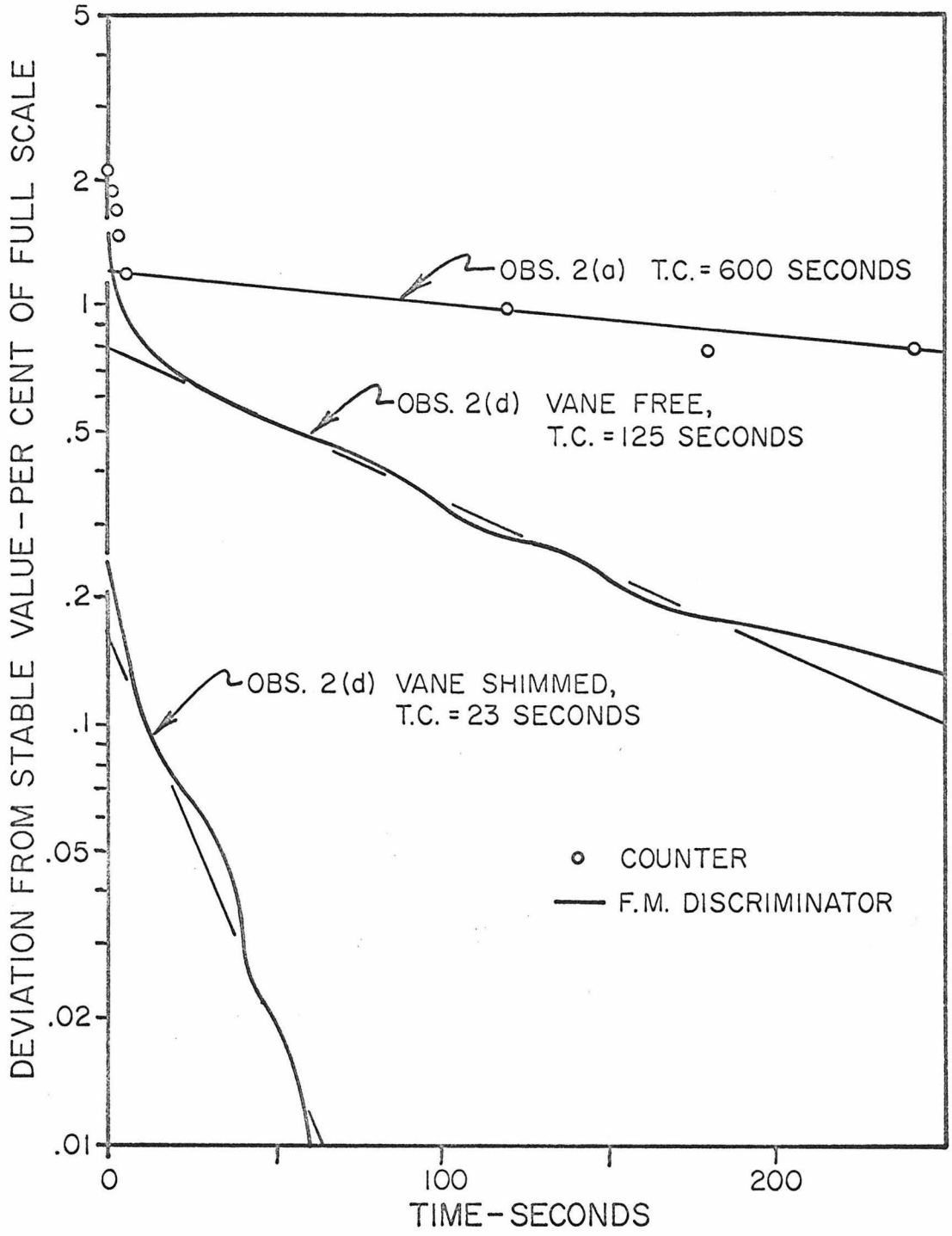

Figure 11: Test Accelerograph Turn-On Drift

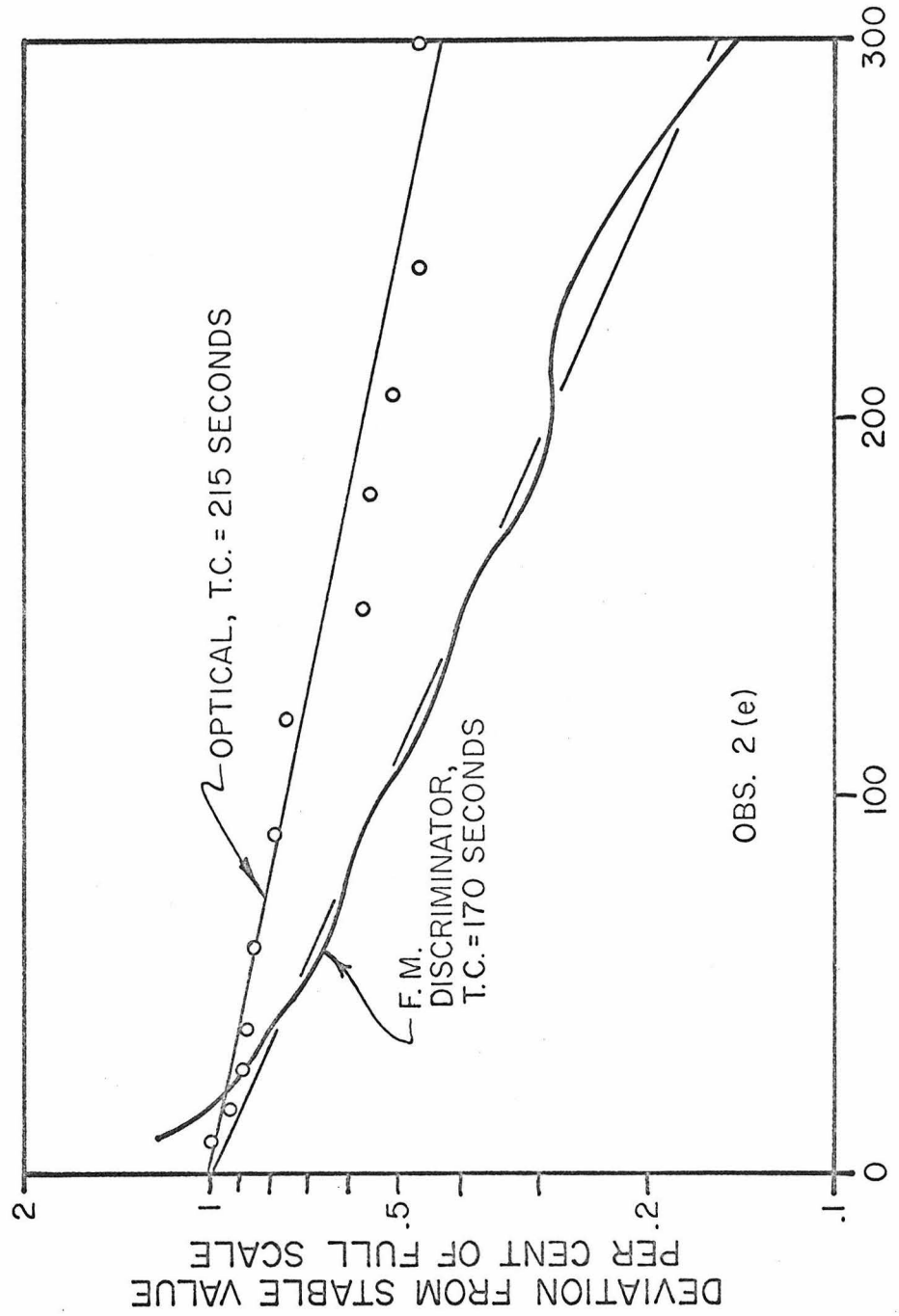

Figure 12: Simultaneous Optical and Electrical Drift Measurements

Deviations in excess of 10% were produced, but the accelerometer repeatedly returned to zero within ± 1% if given sufficient time. The first part of one such return, after 28 hours at 1/2 g, is shown in Fig. 9.

(2) RMT-280 Transducers

(a) The modified transducers in the RMT-280 system showed behavior similar to the prototype transducer when subjected to 1/2 g static acceleration (upper curve, Fig. 10). The magnitudes of the effects are smaller, and the multiple hour decay effect noted in Fig. 9 was absent.

(b) When the instrument was turned on after having been quiescent at zero g for more than about 1/2 hour, a similar type of drift behavior was observed (uppermost curve, Fig. 11). A part of this drift, amounting to about 0.4% with a time constant of about 5 seconds was found to occur even when the accelerometer was removed from the circuit by shorting its output, showing that some of the effect occurs in the associated electronic circuits.

(c) Experience in adjusting the test transducers showed that optimum adjustment requires that the zero position of the accelerometer be set so that the vane of the variable reluctance

is at a noticeable angle to the pole faces. An optical measurement of the gaps showed that the end gaps differed by typically ± 25% with respect to the center one. Although at this stage there was no indication that this asymmetry adversely affected the performance of the accelerometer system, it did make initial set-up unnecessarily difficult and time consuming. Minor circuit changes to alleviate this asymmetry were made, and will be included in future instruments.

(d) Following a period of noise testing, during which the accelerometer suspension was subjected to larger than normal stresses by the insertion of shims between the vane and its E-core, interest returned to the turn-on phenomenon. An attempt to reproduce the top curve of Fig. 11 resulted instead in the middle curve of Fig. 11. A re-run under the same conditions, but with the shims once again in place to eliminate mechanical motion of the vane, produced a much smaller drift, but a highly variable one. The bottom curve in Fig. 11 represents the largest drift observed.

After the shims were removed, a comparison check of the recovery from 2 minutes at 1/2 g was made. The results of this test are shown as the lower curve on Fig. 10.

(e) The accelerometer was set up on an optical bench to permit simultaneous optical and electronic read-out of its behavior. As

a system calibration, the recovery from 10 minutes at a deflection corresponding to 1/2 g was recorded. Results of this test are shown in Fig. 12. Half an hour later a test was conducted to see if there was or was not a mechanical motion associated with the turn-on drift. There was no measurable optical change within the first half-minute, but when a reading was taken seven minutes later a frequency shift of 0.8% and an optical shift of 0.3% were observed; both shifts were in the direction corresponding to the previously observed 0.4% shift that occurs when the system is turned on with the accelerometer shorted out.

Calculations showed that the diameter of the mirrors on the accelerometers imposed a theoretical limit of resolution corresponding to .15% on optical measurements, which would make further tests of limited value.

(f) As an additional test of instabilities in the electronic circuits, the test accelerometer was replaced by another type of mechanical-magnetic instrument, a Schaevitz Linear Variable Differential Transformer. When the resulting system was calibrated by means of a micrometer, it was found that all hysteresis and turn-on phenomena had dropped below the level of readability except for the roughly 0.4%, 5 second time constant turn-on change mentioned earlier. In this case the size and duration of the change appeared the same whether the

transducer was shorted or not.

The key measurements in the above tests are frequencies, or rather changes in frequency. All of the measurements not otherwise noted on the figures were made with a Berkeley Model 5510 electronic counter operated either in the frequency or "10 period average" mode. In either case the highest resolution setting provides a least count equivalent to 0.1%, with an uncertainty of ± 1 count. These limitations introduce digitizing noise sufficient to complicate the interpretation of the smallest effects measured, those on the order of 1%. Some measurements were recorded on a Brush Mark 280 pen recorder after conversion to the voltage domain by means of a Pacific Communications and Electronics, Inc. Type 115 solid state discriminator. This discriminator is subject to drifts which may amount to 0.2% over a period of several minutes, and produces about 0.2% to 0.5% peak to peak of noise when used with the Brush recorder due to an interaction between the small component of carrier frequency which appears in the discriminator output and the chopper which is used on the input to the Brush recorder. Even this slightly noisy record compares favorably to those produced by the optical recorders.

It should not be inferred that the above drift effects are of no importance, simply because they are small enough to be difficult to measure. In Section 2.1 it was shown that errors of this order in the apparent average acceleration level are large enough to make long period displacement computations from typical acceleration records of little or no value. Even the smallest of these effects are of the

same order as the RMS noise level in the recording system, and many times larger than either the short period D. C. stability of that system or the potential overall noise level if it were brought fully up to the state of the art, as described in Section 3. 2.

Before beginning a more detailed discussion of the problems just described some additional details of the mechanical construction of the transducer will be useful.

The Lehner-Griffith seismometer is an accelerometer whose moving element is a spring centered pendulum (see Fig. 6). The pendulum is physically a rectangular coil of wire whose outer side moves in a magnetic field produced by a permanent magnet. In normal operation the ends of this coil are connected to an adjustable resistor so that accurately controllable viscous damping is introduced in a manner analogous to standard galvanometer practice. Passing an adjustable D. C. current through this coil produces forces similar to those caused by acceleration, and permits easy field checks of the system calibration.

The motion of the coil is constrained by a suspension system composed of torsion wires above and below the moving element. Rotation of the coil about this axis is sensed optically by means of an attached mirror in earlier model recorders, and electrically by means of a variable reluctance transducer in the RMT-280. The suspension wires also carry the damping and calibration currents from the moving coil, making it necessary to electrically insulate the lower wire from the frame. This insulator was originally a nylon bushing, which has

been changed in the RMT-280 transducer to a glass feed-through. The mechanical fastenings at the ends of the RMT-280 torsion wires consist of wire wraps secured with 60/40 lead/tin solder. Earlier versions, including the prototype transducer, used a simple solder joint.

The Lehner-Griffith seismometer was originally designed for a natural frequency of about 1.2 Hz, but most versions now in use for strong motion recorders have a natural frequency of about 20 Hz. The change has been accomplished mostly by stiffening the suspension, without significantly changing the design or construction practices. The first transverse resonance ("fiddle stringing") has been kept quite high, about 250 Hz, by applying tension to the support wires, so that the instrument is much stiffer transversely than it is torsionally.

In the RMT-280 the accelerometer becomes an integral part of an acceleration controlled oscillator as shown in block diagram form in Fig. 7. The basic oscillator is a Wien bridge driven from the output of a differential operational amplifier whose input comes from the output voltage of the bridge. The frequency of the system adjusts itself to produce a null at the bridge output. The variable reluctance accelerometer is also driven from the amplifier output, producing a signal whose amplitude is approximately proportional to the applied acceleration and whose phase is either 0° or 180° with respect to the oscillator voltage. This signal is then shifted in phase to produce a component whose phase is $\pm 90^{\circ}$ with respect to the oscillator, which is then fed back to the summing point of the operational amplifier.

This quadrature phase signal forces the oscillator to shift in phase, and hence frequency, to keep the summed input voltage small. The result is frequency modulation, with an overall linearity characteristic determined by a large number of interacting elements, including at least the phase shift vs frequency characteristic of the Wien bridge, the basic linearity of the variable reluctance transducer, and the effect of several significant stray capacitances. Overall sensitivity is controlled by various gain adjustments not shown and amplitude of the oscillation is controlled by an adjustment of the total system losses and by a pair of stabilizing Zener diodes in the bridge circuit.

Discussion of Short Term Drift Effects. To understand the drift phenomena described above, it will be helpful to know the magnitudes of significant forces and moments acting in the transducer system. Details of these calculations are given in Appendix C, and the main results can be summarized as follows:

(1) A magnetic torque with a non-zero average value is generated in the variable reluctance transducer when the E-core is energized with the vane at an angle to the pole faces. The torque increases with increasing angle.

(2) The sign of the torque is such as to increase the vane angle, i. e. increase the larger gap and decrease the smaller one.

(3) For a particular case in which the gaps are asymmetric by ± 10%, the magnitude of this torque is calculated to be 1.7×10^{-7} newton-meters peak, or 8.5×10^{-8} newton-meters average.

(4) Torques associated with the acceleration are calculated to be 1.7×10^{-4} newton-meters per g.

(5) The shear stress in the leading edge of the solder fillets is calculated to be 200 psi at 1/2 g acceleration.

The data presented so far have one obvious common characteristic. They represent an asymptotic approach of the output frequency or mechanical position of an electromechanical system to some stable value. Other than that, they represent a wide variety of conditions and time spans. It is possible, however, to infer a great deal from a proper classification of the similarities and differences.

The best way to begin the classification is to separate by time constants, as follows:

(1) Time constant approximately 5 seconds: The only effect observed on this time scale is a relatively small one, about 0.4% shift, which occurs on turn-on. It is clearly observed when only the electronic circuitry is active (transducer shorted out) or when the Lehner-Griffith accelerometer is replaced by a transducer which does not exhibit hysteresis effects. The effect is thus

electronic, and the duration, which is many times longer than any electronic time constant in the circuitry, implies that it is probably a thermal effect. The most obvious possibility is that some of the frequency determining components in the Wien bridge change value significantly as they warm up, but many other possibilities suggest themselves. For example, the Zener diodes which are included in the bridge to stabilize the amplitude of oscillation make the oscillator dependent on drive level. A change in frequency could thus be tied to many other effects, including transient gain changes in the operational amplifier.

(2) Time constant approximately 1.5 to 15 minutes: At this time scale are found all but one of the large magnitude effects, including both recovery from deflection, and turn-on effects. The grouping of the time constants and the strong similarities in time histories for these two kinds of effects strongly suggest a common or closely related cause (see especially Figs. 10 and 11). A consideration of the third category will serve as a useful introduction to other data which support this idea.

(3) Time constant approximately 12 hours: Changes over this time scale were observed in one extended test of the prototype transducer. The more recent accelerometers do not exhibit this effect. Several observations combine to indicate that the reason for this behavior was the nylon bushing at the lower support:

(a) Optical tests confirmed that the recovery phenomenon was at least partly mechanical in nature.

(b) The effect disappeared when the accelerometers were redesigned to eliminate the nylon bushing. The electronics were not changed.

(c) Data in Reference 1 show that nylon does indeed exhibit creep and recovery phenomena of an approximately exponential nature with time constants on the order of 12 hours.

The total effect observed in Fig. 4 appears to be a simple sum of two roughly exponential effects, one having a 12-hour time constant, while the other fits in the previous category with a time constant of about 13 minutes.

The most interesting phenomena are those associated with category 2, with time constants of a few minutes. All data indicate that effects with this time scale are related by more than just a coincidence of rate, and probably have a common electro-mechanical cause, or at least closely related causes.

The first effects noted were the creep and recovery, or hysteresis, effects. These effects are encountered at every calibration as a progressive zero shift and a tendency for all readings to be time dependent. On two occasions, similar effects have been detected optically. This fact, plus the observation that the effect does not

appear when the accelerometer is replaced in the circuit by a mechanically different magnetic transducer, strongly indicates a mechanical origin. Several observations indicate that this mechanical effect arises from the solder joints, to the virtual exclusion of any other possibility. First, the size of the effect is much too large for any anelastic behavior of the phosphor bronze suspension wires that is compatible with the qualitative nature of the observations. Second, an approximate calculation of the stress level in the solder joints shows a level at which significant creep effects have been observed in similar alloys. Third, the effect is much smaller in the newest accelerometers than it was in the original prototype, and the principal mechanical difference between these two versions is the improved design and workmanship of these joints. The solder joints in the prototype were very porous, had large resin inclusions, and showed evidence of poor wetting. The newer units show traces of porosity, but are otherwise much tidier and have the advantage of a wire wrap for security. All this implies that it is the solder joints, and very likely primarily their imperfections, that cause the trouble. This idea is supported by the observation that the recovery effect was found reduced in both amplitude and time constant following some tests which subjected the suspension to higher than normal stresses (Fig. 10).

Of even greater interest is the turn-on effect, both because it is potentially more bothersome in its influence on system accuracy and because it is more difficult to understand. The evidence suggests that this turn-on effect is closely related to, though perhaps not

entirely explained by, the creep and recovery phenomenon. First, the positive evidence may be summarized as:

(1) The two sets of curves (e.g. Figs. 10 and 11) are quite similar in shape and time constant, and even show a similar reduction in both amplitude and time constant following experiments which substantially exceeded the normal stress levels in the suspension.

(2) Both effects were totally absent in the LVDT version of the instrument.

(3) There are mechanical torques acting in the accelerometer when it is turned on with the vane at an angle to the E core, as shown in the computations in Appendix C. These torques increase with increasing vane angle, which agrees qualitatively with the fact that all observations of the effect after minor circuit changes permitted reduction of this vane angle were of much smaller magnitude than those made before. In addition the 0.3% shift which was finally confirmed optically was consistent in sign, at least, with the magnetic torques predicted from theory.

Among the items of evidence of more questionable import are:

(1) The magnetic torques computed are not sufficiently large to

account, by themselves, for the actual motions observed. In the one case where a turn-on drift was detected optically, for example, the magnetic torque computed from measurements of the vane angle, was 1.7×10^{-7} newton-meters peak, or 8.5×10^{-8} newton-meters average, while the mechanical torque necessary to produce the 0.3% offset which was observed should be about 2.5×10^{-7} newton-meters for a linear system. Although this agreement is well within an order of magnitude, it is not close enough to be considered a conclusive argument.

(2) Both the hysteresis and turn-on effects show large variations in apparent time constant from test to test, though they always remain in the 1.5 - 15 minute range of the second category.

(3) Measurements taken with the mechanical motion of the vane blocked (bottom curve, Fig. 11) are similar to the purely electronic effects, although the time constants do not fit any of the three categories exactly.

(4) In the simultaneous optical-electrical measurement of recovery from creep shown in Fig. 12, the two curves are basically similar, although there is a noticeable difference in the apparent time constants.

(5) All accelerometers tested have shown a preferred direction of turn-on drift, but it is not uniform. Some drift mostly up, others mostly down, and all show marked variations from trial to trial even when nothing has apparently been changed between trials.

A further appreciation of the possible complexity of the problem may be gained by considering some of the variables which may be involved which have not been mentioned:

(1) Tests reported in Section 3.4 on temperature and humidity effects indicate that these two factors probably did not change enough to be significant during any of the measurements discussed above. For large variations, they do have an appreciable effect, both electronically and mechanically, and may be important factors in the history of an instrument just prior to any measurement.

(2) The transducers are not very sensitive to changes in the magnetic properties of the E-core and vane because only about 1/2% of the total magnetic reluctance occurs in the iron. Since the measured changes in inductance are also small, however, an unbalanced change of about 5% would suffice to produce the 1/2% of full scale effects noted.

(3) The instrument reaction to the stresses associated with shimming the vanes shows that the mechanical effects are history

dependent. The general trend seems to be toward smaller drifts with increased testing. There are indications of at least a partial return to early behavior when the instrument is left undisturbed for a few months.

Some Other Aspects of the Start-Up Problem. When the accelerograph receives a pulse from the starting system, there is a certain time delay before the instrument can actually record. This delay is another aspect of the start-up problem which is of practical importance. Like the other start-up phenomena just discussed, it is transient in nature, but involves time constants on the order of 0.1 second.

Actually, two equally important effects are involved, one purely electronic, the other mechanical. The former is the time for the electronic oscillators to build up from zero to a reasonably stable oscillation. The latter is the time required for the tape transport mechanism to achieve a speed close enough to nominal so that recorded frequencies near the center frequency will be played back within the input pass band of the FM discriminators and so within the possibility of electronic compensation.

The mechanical behavior of the RMT-280 tape transport is shown in Figs. 13 and 14. Figure 13 is a typical record of tape speed versus time for the first 20 seconds of operation obtained by playing a pre-recorded 1020 Hz tape through the PC&E discriminator with no compensation applied. Figure 14 is a similar typical record expanded to show only the first second. A reasonable value for the

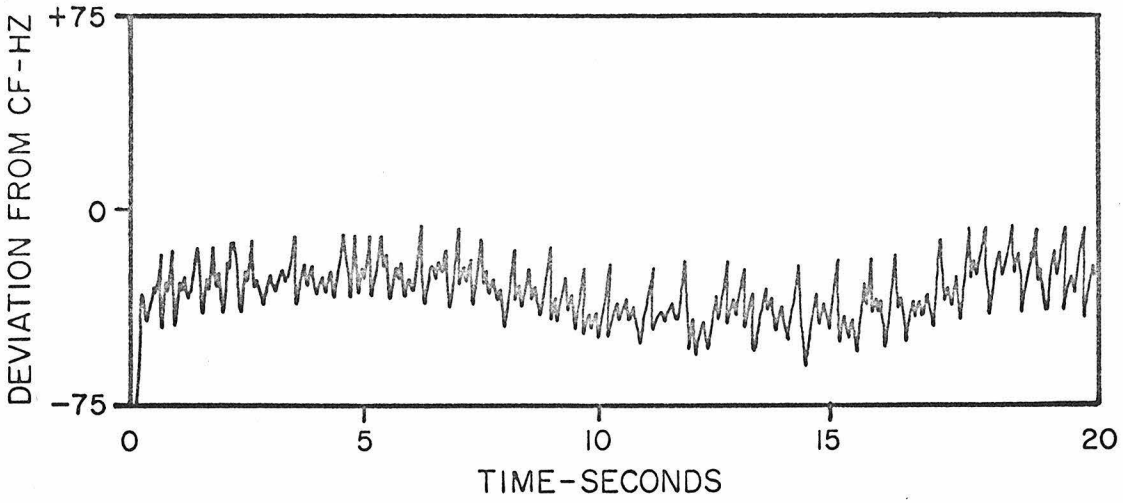

Figure 13: Uncompensated Speed Variations in Battery Powered Recorder

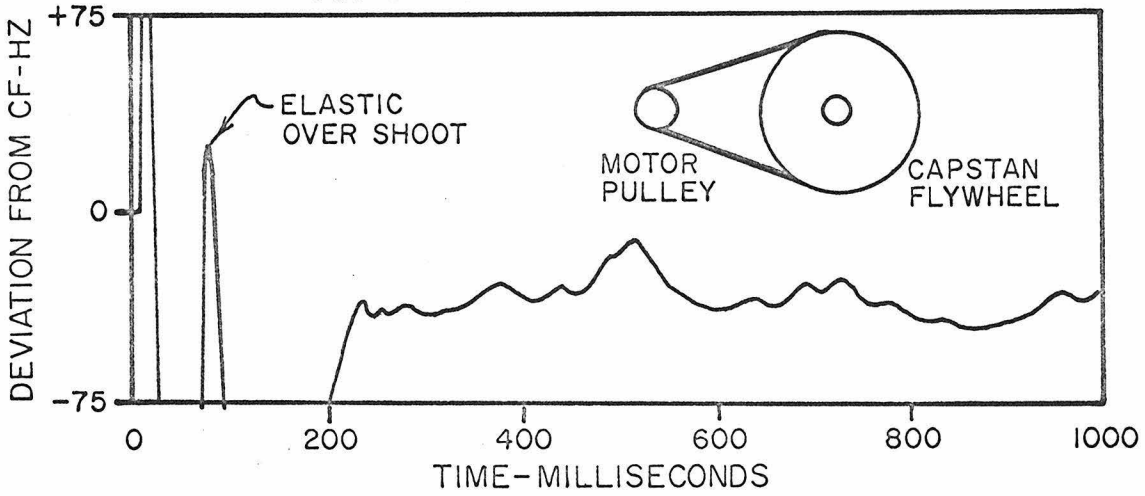

Figure 14: Start-Up of Battery Powered Recorder (First Second of Figure 13, Expanded 20x)

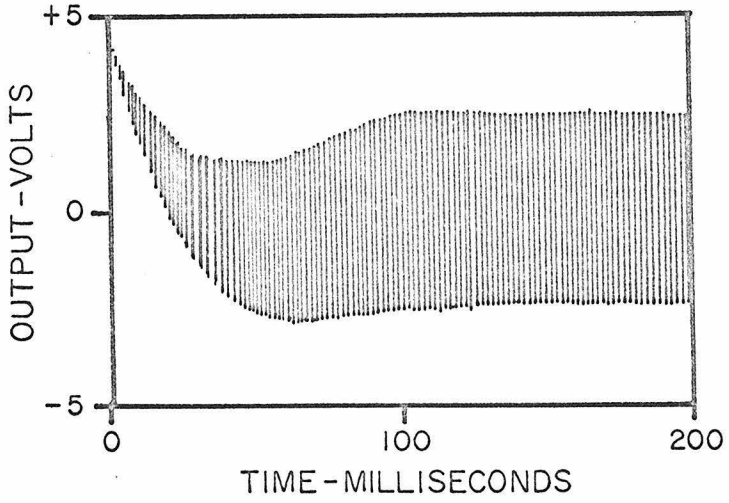

Figure 15: Oscillator Start-Up

start-up time, based on three trials each on two recorders, would seem to be 200 ± 25 milliseconds, though the speed does indeed pass through nominal somewhat earlier, at about 80 milliseconds. The explanation of this behavior may be found in the design of the capstan drive, shown schematically as an inset in Fig. 13. The capstan is attached to a flywheel, which is driven by a governor controlled D. C. motor through rubber belts. If the motor pulley is held fixed and the flywheel deflected approximately 15° and then released, the flywheel will exhibit damped oscillations corresponding to roughly 4 Hz natural frequency and about 20% of critical damping. When the motor is accelerated quickly to governor speed, this elastic system receives approximately the angular equivalent of a velocity shock. The flywheel exhibits decaying oscillations about its eventual stable speed, with a strong overshoot followed by a strong undershoot. The dominance of these oscillations in determining start-up time was demonstrated by tests in which the drive motor was subjected to only 12 volts instead of 24 volts. The time increased by only 50%, and the difference probably would have been even smaller if the elastic properties of the drive belts were perfectly linear. Rubber bands, as springs, normally become stiffer and show higher hysteretic losses with increased extension, which would be compatible with the observed behavior.

In these tests, the motor has demonstrated sufficient torque to accelerate the flywheel to nominal speed in less than 100 milliseconds if the drive system were stiffened. This would almost

certainly result, however, in a marked increase in the presently marginal steady state noise level, unless steps were simultaneously taken to improve the compensation system.

The electronic phenomena associated with starting the system from rest are represented in the oscilloscope observation reproduced in Fig. 15. It may be seen that the oscillations achieve amplitude stability in somewhat less than 100 milliseconds. Tests with the FM discriminator are not capable of high precision in the under 100 millisecond range because of starting transients generated in the output amplifier; reasonable stability is apparently achieved within 80 milliseconds. Tests with an electronic counter show that stability within 0.2 Hz (0.2% of 1/2 g) is achieved within 200 milliseconds. Since all these figures are comparable to or less than the mechanical starting time of the tape transport, no further refinement of this measurement is necessary.

3.4 Long Term Drift and Temperature Response

Since a strong motion accelerograph must operate after long periods of several months or more of unattended waiting, it is important to know how stable the center frequencies of the accelerometers are over long periods of time. Any small shift in these frequencies will cause uncertainties in the zero level for acceleration, and large shifts could reduce the available dynamic range by shifting operation too near one edge of the frequency band. To aid in investigating this stability, a piece of test equipment was assembled which

periodically turns the instrument on, samples the zero g output of an accelerometer, and then turns off again. This test set up is described in more detail in Appendix A.

All tests were carried out in an air conditioned laboratory to aid in separating long term random effects from those due to temperature variations. Shorter term tests were later conducted in which the temperature alone was varied in order to determine to what extent these long term tests were affected by variables other than time and to aid in predicting the total extent of changes in center frequency to be expected in a less well regulated environment.

The results of these tests are shown plotted in Figs. 16 and 17. The top curve in each figure is the sampled center frequency of one of the three accelerometers. The sampling rate was from four to six times a day with a minimum interval between samples of two hours. At each sample the accelerograph was operated for twenty seconds and a continuous record of zero-g output was made. For consistency, all of the frequencies plotted were read at the end of the twenty second period. The frequency at turn-on differed from the 20 second sample frequency by as much as 1.5 Hz higher or lower (No. 1 generally higher, No. 2 generally lower). There was no readily discernable pattern in the amount of drift recorded during each 20 second period, except that it tended to be somewhat less when the period between samples was reduced to less than one hour. Breaks in the curves represent periods when the strip recorder was on loan for other experiments for more than 24 hours. The periodic operation of the

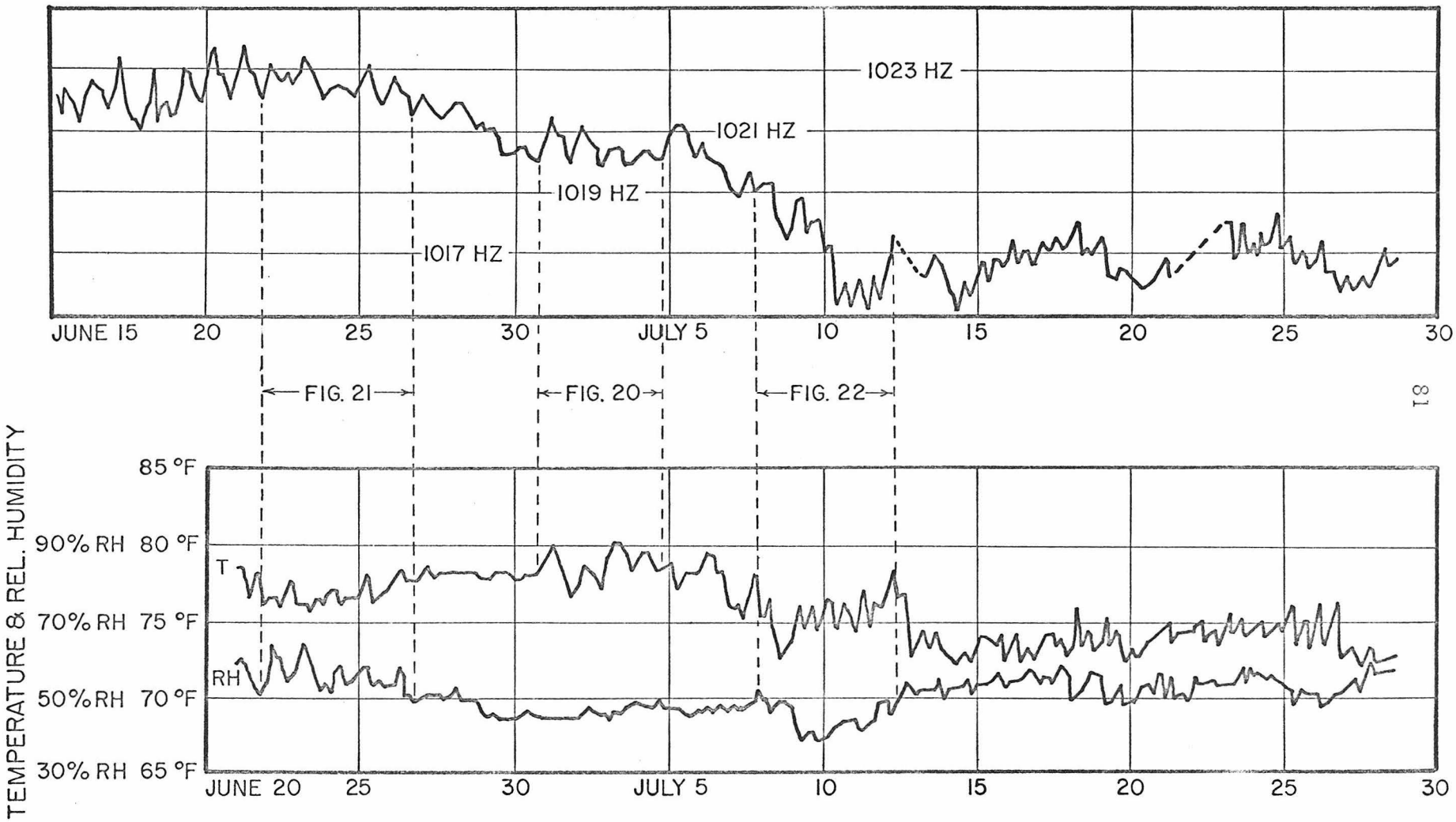

Figure 16: Long Term Center Frequency Stability of Test Accelerograph No. 2, with Temperature and Relative Humidity

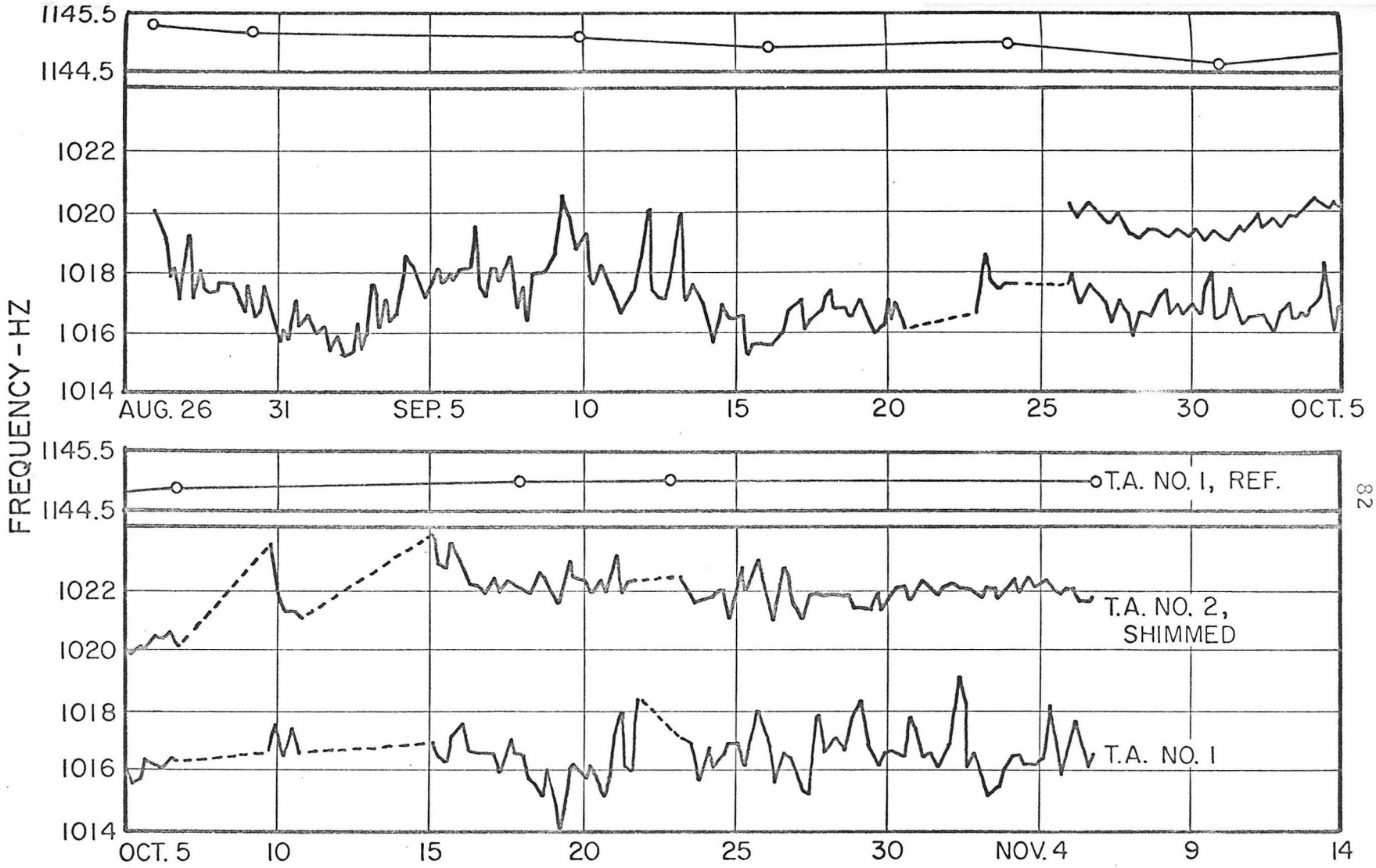

Figure 17: Long Term Stability of Center and Reference Frequencies, T. A. No. 1, and Shimmed Center Frequency, T. A. No. 2

accelerograph was not interrupted during these times.

The two lower curves in Fig. 16 are temperature and relative humidity. The second curve in Fig. 17 shows results of a concurrent measurement on No. 2 with its accelerometer vanes mechanically blocked to prevent motion; the purpose of this measurement was to help separate mechanical effects from electronic ones. The top curve in Fig. 17 shows the result of sampling the reference oscillator of No. 1 at long intervals.

In between the test shown in Fig. 16 and that shown in Fig. 17, both recorders were subjected to a series of temperature tests in which the accelerographs were cycled from room temperature to an upper temperature in the range of 130°F to 165°F and back again in a period of about four hours. One test was conducted to 190°F, but the accelerometer began to drift badly at about 170°F, and returned to room temperature with a 3 Hz permanent set, so this extreme was not repeated. A typical heat run for a complete accelerometer is shown in Fig. 18, and for the same accelerometer with shims in place to prevent mechanical motion in Fig. 19. Average results of these and some other tests are summarized in Table 2.

In studying the long time behavior of No. 2, as shown in Fig. 16, several things stand out. One is the strongly diurnal variation in frequency. Another is the apparent correlation between these frequency variations and parts of the other two curves: in some places the temperature, and in others the relative humidity. To verify the apparently causitive nature of these correlations, three

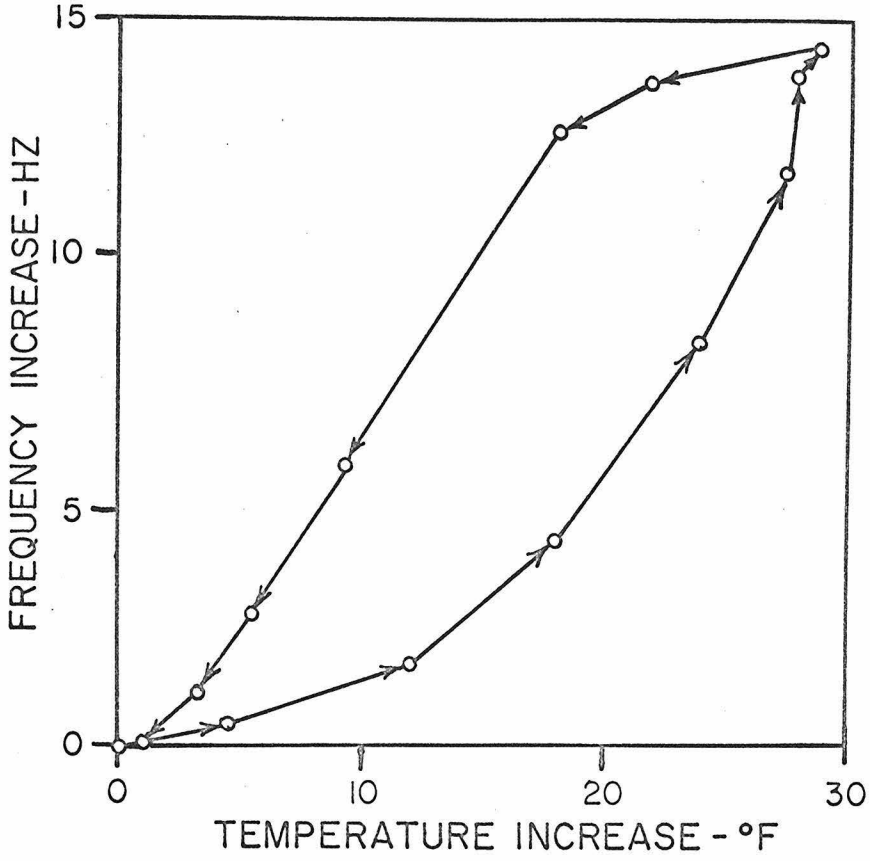

Figure 18: Typical Temperature Run

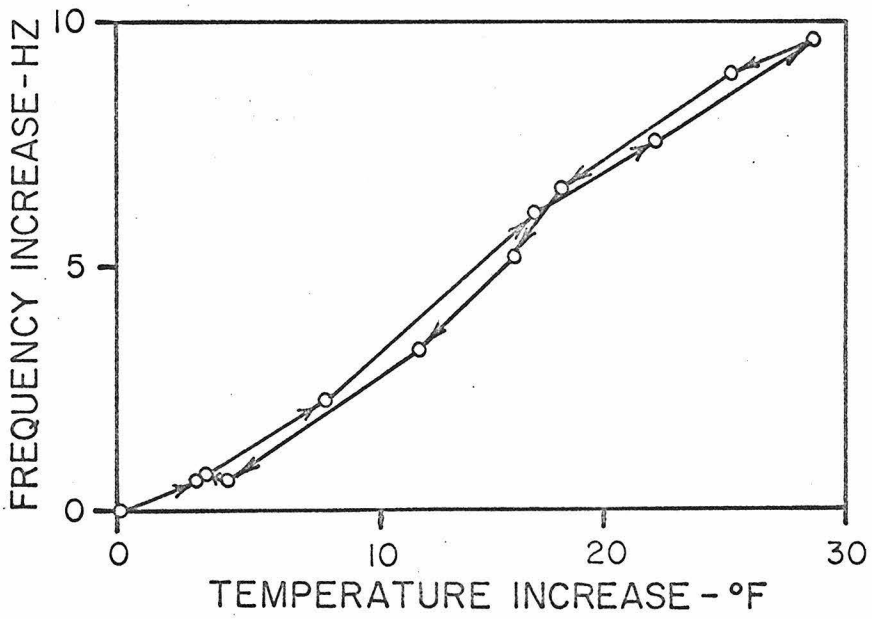

Figure 19: Typical Temperature Run, Vane Shimmed

TABLE 2

SUMMARY OF TEMPERATURE COEFFICIENTS

S/N 101, transverse accelerometer	0.35 Hz/°F*
S/N 102, transverse accelerometer	0.40 ± 0.10 Hz/°F
Same, with accelerometer clamped	0.22 ± .02 Hz/°F
Same, with null point grounded	0.14 Hz/°F*
Timing Channels	0.03 Hz/°F

* single reading

These results show that the temperature coefficient of S/N 102, transverse channel, is composed of approximately the following fractions:

Electronic	35%
Magnetic	15%
Mechanical	50% (variable)

They also show that the electronics for this accelerometer have a temperature coefficient five times as large as for the timing channels, which use the same oscillator circuit, but without complicated shunt impedances.

additional plots were made. The first, shown in Fig. 20, is a plot of frequency against temperature, taken over a five day period when temperature swings were fairly large, but there was very little change in relative humidity. Figures 21 and 22 show plots of frequency against relative humidity over periods of about five days when fairly large changes in humidity were taking place, but the temperature was nearly constant. In the first period, the relative humidity remained almost always above 50%, and in the second almost always below. In the case of these two figures, an adjustment was made for the temperature changes which did occur, based on the earlier short term temperature cycles.

Several important conclusions can be made from these data:

(1) Repeatability in temperature tests, including return to initial conditions, indicates that these accelerometers are not markedly dependent on their temperature histories. In particular, the long time behavior of No. 1, which had been subjected to several 75°F - 165°F temperature cycles before testing, was not materially different from that of No. 2, which had not been cycled.

(2) The hysteresis shown in Fig. 18, which was present in normal tests of all accelerometers checked and absent in all tests where mechanical motion of the accelerometer was not a factor, is the only clearly defined mechanical effect observed in these tests.

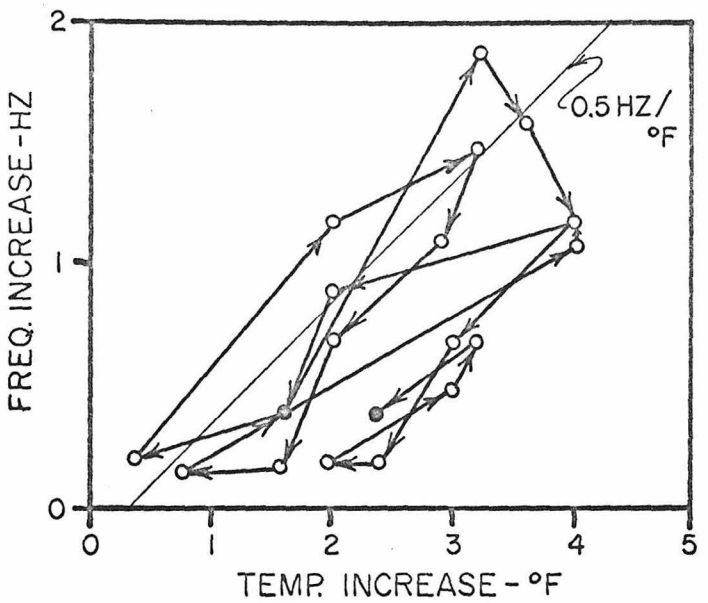

Figure 20: Long Term Temp. /Freq. Plot

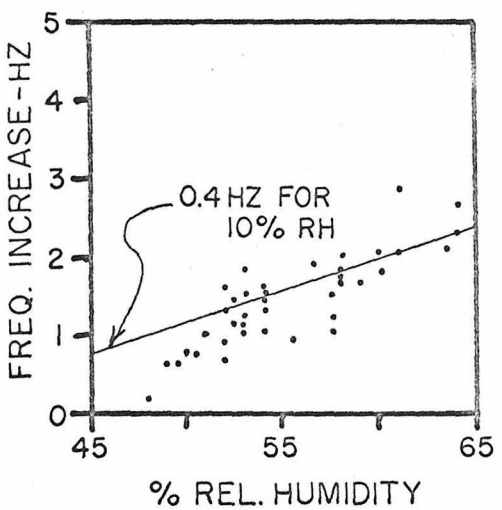

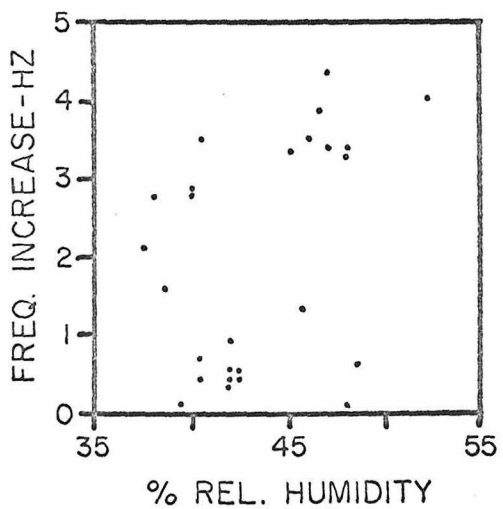

Long Term Temperature/Relative Humidity Plots

Figure 21: R. H. > 50%

Figure 22: R. H. < 50%

(3) The major repeatable source of frequency variation with temperature is the electronics. The temperature coefficient of the Wien bridge oscillator is nearly the same as that of the complete accelerometer. However, the temperature coefficient of the Wien bridge oscillator in the accelerometer package is about five times as large as that of the reference oscillator, which is also a Wien bridge device. The most likely explanation of this difference is the effect of additional circuit elements in the accelerometer circuit, which exert a shunting effect on some elements of the bridge even when the phase-shifter feedback loop is opened at the accelerometer.

(4) The temperature-frequency plot in Fig. 20 is compatible with the shorter run temperature tests, but shows a large random component superimposed. Certain data support the idea that this random component is largely mechanical wandering of the accelerometer suspension; the hysteresis observed during temperature cycling, and the marked improvement in long term stability exhibited by No. 2 when mechanical motion was prevented by shims. (Compare Fig. 16, 9 Hz peak to peak in 20 days, to Fig. 17, 5 Hz peak to peak in a similar period.) In addition, zero drifts of a corresponding magnitude have been observed in several records taken from recorders using the optical versions of these accelerometers.

(5) Similar plots of frequency vs relative humidity indicate a

coefficient of about 0.04 Hz per % R.H. between 50% R.H. and 64% R.H., but no significant correlation below 50% R.H. This result effectively eliminates humidity as a factor in the short term temperature runs, since they all started at less than 50% R.H. and became relatively drier as the temperature was increased.

(6) The total zero-point wandering, from all causes, amounts to about 7 Hz long term random plus .35 ± .15 Hz per degree Fahrenheit, most of the uncertainty in coefficient being apparently a short term mechanical effect. This amount of shift would obviously invalidate double integration of long period data, but is not sufficient to otherwise interfere with operation of the device. It probably is not significantly greater than has been commonly accepted in optical accelerographs.

3.5 Linearity and Adjustment

The linearity of the relationship between applied acceleration and frequency shift in the RMT-280 depends on many interrelated effects. Simplified attempts at an analysis of separate items have not been able to explain the magnitudes of the nonlinearities actually observed. For example, computations similar to those in Appendix C have been carried out on the variable reluctance element, using the simplifying assumption that the permeability of the iron is a constant. They show that this element should be linear to within about 1% of full scale, regardless of how much the initial imbalance in the magnetic

circuit may be. Actual measurements have shown that nonlinearities on the order of 20% at full scale are possible, by using an initial offset sufficient to cause the fluxes in the two halves of the E-core to differ by about 30%. One suspected cause is the variation of μ as a function of H.

Laboratory experience with the RMT-280 has shown that it is possible, by taking sufficient pains, to bring the overall system linearity within acceptable limits of 2%. In fact, during final adjustments, the limiting factor usually is not the remaining nonlinearities, but rather the difficulty in measuring them sufficiently accurately, because of the long period hysteresis effects described in Section 3.3. The technique involves balancing the two major nonlinearities against one another.

Experiments have shown that the two major nonlinearities to contend with in these adjustments are those associated with the phase shift network, controllable by varying the bias on the transistor which drives it, and with the variable reluctance pickup, controllable by varying the initial angle on the vane. Both of these circuits appear capable of linear behavior within about 1/2% of full scale when operated near their optimum settings, but interactions with other controls, and production variations, sometimes require a non-optimum setting of the bias adjustment in order to bring oscillator amplitude and overall gain within required tolerances. When this happens departures from linearity as large as ± 10% of full scale may occur, and these must be corrected by inducing a compensating

nonlinearity in the accelerometer transducer. A typical linearity plot for a carefully adjusted unit is shown in Fig. 23. A plot which is probably typical of the results which could be expected on a production basis, using reasonable, but not elaborate, care is also shown.

After a little practice, curves similar to the better one in Fig. 23 could be achieved in about 1.5 - 2 hours per accelerometer, including a ten point check of the actual linearity. Reducing accuracy requirements to a level compatible with the less accurate curve of Fig. 23 reduced both the number of measurements taken and the time per measurement so that complete adjustment was possible in about twenty minutes per accelerometer. To achieve this time, measurements at the -1/2 g, zero, and + 1/2 g points are taken as proof of linearity.

The effect of nonlinearities of this order on computed displacements has been indicated for an idealized case in Section 2.1. It will be further investigated for a more typical motion in Section 4.1.

The effects of interactions between the various controls, and hence the number of iterations required to adjust an accelerometer, can be reduced by relaxing one of the constraints. The only one which is available, without affecting linearity or recording level (signal to noise ratio), is the overall sensitivity. If that is allowed to deviate ± 20% from its nominal value of 200 Hz per g, but is measured and recorded to the accuracies indicated on Fig. 23, both of the above adjustment times can be reduced by about one third. These recorded

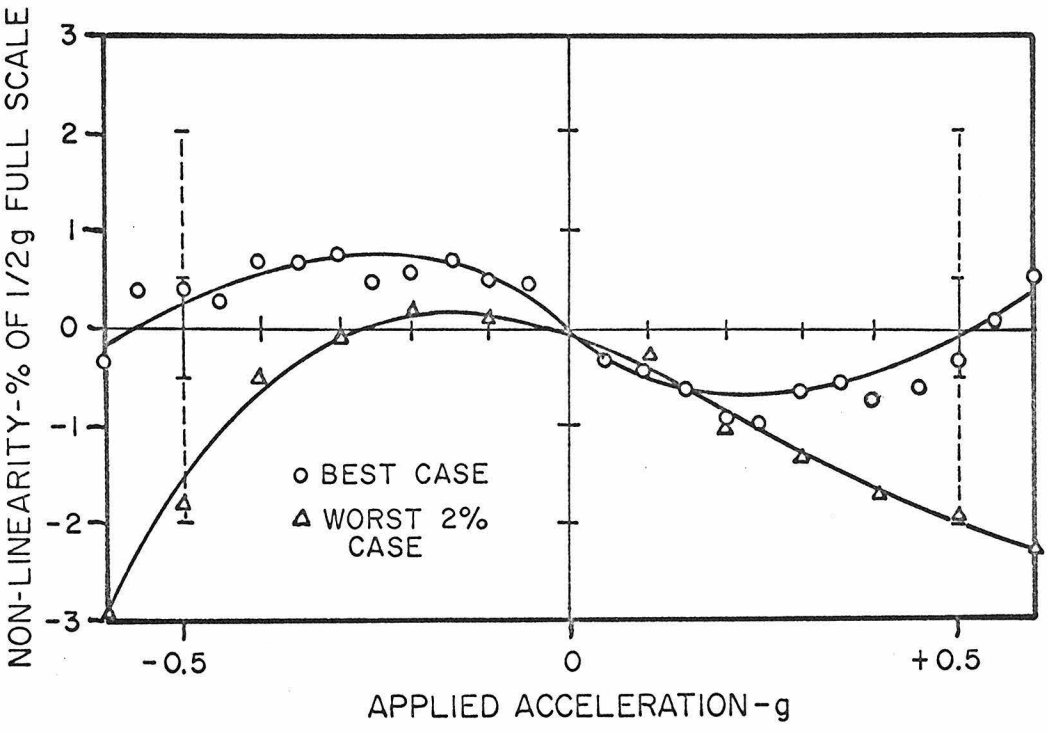

Figure 23: Typical Linearity Plots

sensitivities would have to become part of the data system paperwork, as there is no satisfactory provision for recording the information on the tape. There is a calibration system, described qualitatively in Section 3.3, but non-uniformities in the magnetic field, and low resolution in the rheostat which adjusts the calibration current, limit its accuracy to about ± 3% of full scale.

4. ACCELEROGRAPH SYSTEM TEST

As an overall test, a complete accelerometer package was subjected to a motion similar to a destructive earthquake and its output was recorded on its associated tape mechanism, as in an actual event. At the same time recordings were made of a commercial accelerometer of much higher natural frequency, and of the displacements associated with the motion. A common time base was provided for all recorded data. The various records were then digitized, processed to provide computed displacements and Fourier acceleration spectra, and compared. Further processing was later carried out to get an estimate of the probable effect of small transduction nonlinearities on the computed data.

Test Description. A pseudo-earthquake was generated by driving a low frequency electromagnetic shake table from a filtered random noise source with a high frequency roll-off beginning at 6 Hz.

The shake table was not sufficiently large to accept the entire accelerograph, so the accelerometer package, consisting of three accelerometers and their associated oscillators, was removed from accelerograph No. 1 and attached to the table. Its transverse axis was set parallel to the table motion. A flexible cable connected the accelerometer package to the remainder of the accelerograph so that recordings could be made in the usual fashion.

Table motion was monitored by a Statham 2 g strain wire accelerometer which recorded on a Brush Mark 280 pen recorder. This accelerometer has a nominal linearity better than 1% of full scale, which would make it roughly comparable to the RMT-280 in the zero to 1/2 g range, but has a natural frequency of 100 Hz, some five times higher than the RMT-280.

Table motion was also monitored by a Schaevitz linear variable differential transformer. This instrument was connected into an unused RMT-280 accelerometer oscillator circuit to provide an FM analog of the table displacement having the same center frequency, full scale deviation, and output impedance as the acceleration signal. This displacement signal was recorded on an unused track of the accelerograph data tape.

The displacement and FM acceleration signals shared a common time scale by being recorded simultaneously on the same tape, along with the internally generated timing and compensation signals. The Statham/Brush record was correlated by means of the twice per second timing pulses in the accelerograph, which were applied to the Brush timing pens.

Dynamic calibrations were carried out on the shake table with sine wave signals. The shake table was operated at 5 Hz, 0.313 inches peak to peak (0.4 g peak) and outputs of both the Statham accelerometer and the accelerograph transverse channel (discriminated to voltage analog) were checked on the Brush recorder. When

the FM discriminator was static tested on the same recorder using an oscillator and digital counter, the result was found to agree with a sensitivity measurement of the accelerograph made six months earlier within system resolution, or about 0.5%.

Convenient static calibration levels were provided on the sample earthquake magnetic tape by displacing the table with a micrometer, and by using the built-in calibration circuit of the FM accelerometer while a few seconds of tape were run off. To overcome the ± 3% accuracy limitations imposed on the accelerometer calibrator by nonlinearities and finite resolution adjustments, both plus and minus 1/2 g (nominal) points were compared to the dynamic calibration just described and their actual equivalent acceleration values recorded.

Tape playback was accomplished by means of the system described in Appendix A. The flutter compensated analog signals were fed into an eleven bit Raytheon A/D converter. Discriminator sensitivity was turned down from 2 volts full scale to about .75 volts full scale to permit use of the converter's one volt full scale range. At these settings the converter's resolution was .06% of 1/2 g full scale, so that digitizing noise added was at least an order of magnitude below other system noises.

Since only one pair of discriminators was available, the acceleration and displacement records were digitized in two separate passes. On each pass, samples of the data track were alternated

with samples of the twice per second time pip circuit. This multiplexing provided a means for indexing the time scales for the two data tracks later on. In the final playback system it will be possible to sample all tracks in one pass, so that such indexing is necessary only for correlating tapes from different instruments.

To provide a stable time base which is independent of variations in the speed of the data tape, the reference tone track, which was recorded to compensate the voltage output of the data discriminator, was also counted down and used as a clock pulse for the A/D converter. The reference frequency used in this test was 1135 Hz, and it was counted down 4:1, so that 284 samples per second, or 142 samples per second per track, were taken. This sample rate corresponds to a Nyquist frequency of 71 Hz, which is more than sufficient.

The Statham/Brush acceleration record was read manually on the same Benson-Lehner digitizer which is normally used to digitize photographic strong motion earthquake records in the Earthquake Engineering Research Laboratory.

Test Results: The two acceleration records are shown in Fig. 24 as they appeared after being digitized and plotted to the same scale. When superimposed they appear identical except for the noise which was added to the accelerograph record by its tape system. When comparing these records, and the data obtained from them, it should

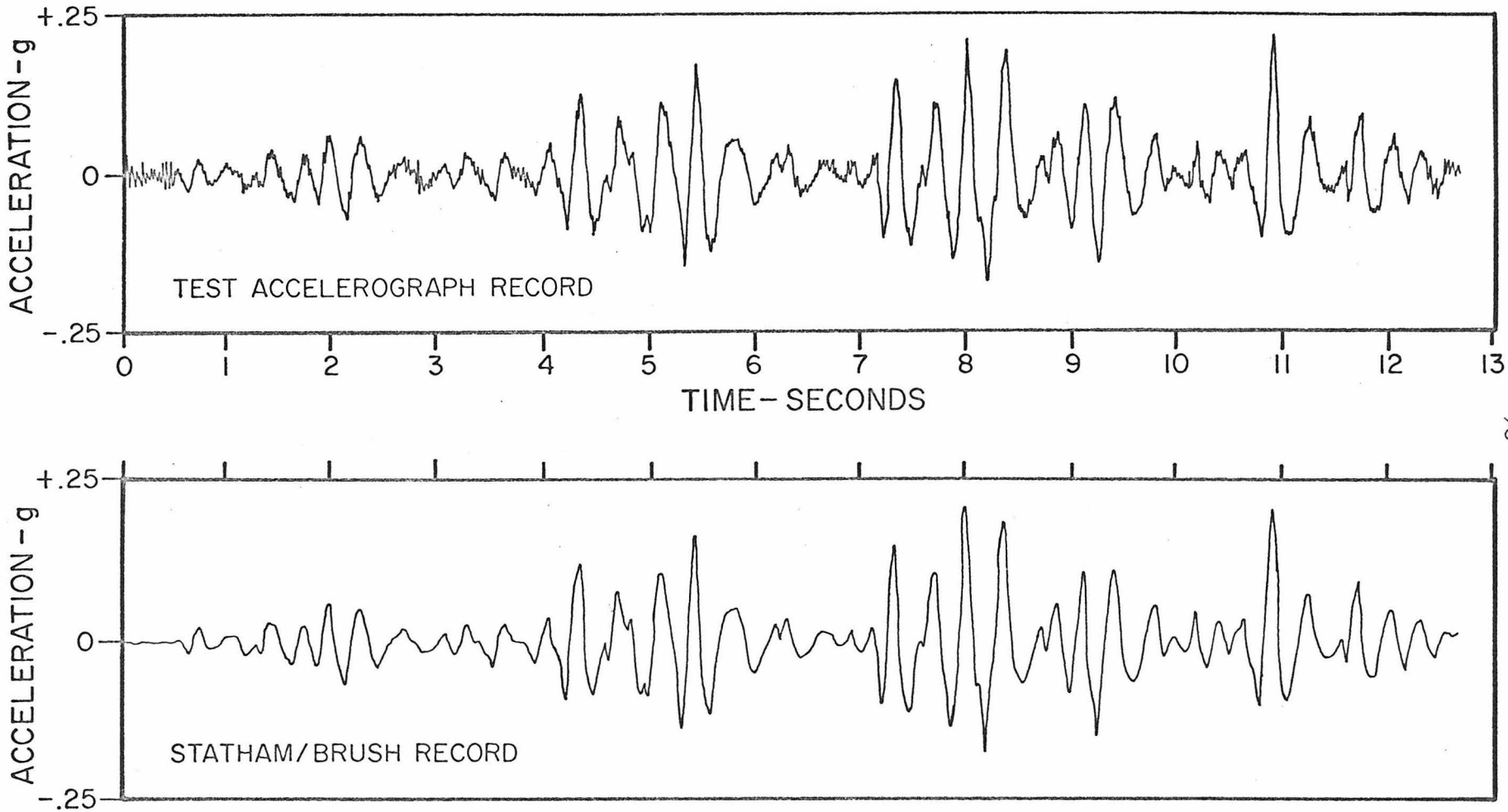

Figure 24: Sample Earthquake Acceleration vs. Time, for RMT-280 System Test

be kept in mind that the Statham/Brush record is of higher quality than a typical photographic instrument record. The trace width was about one fifth as great, and the chart speed was 50mm per second rather than 10-20mm per second, both of which permit more accurate settings of the digitizer cross hairs. Also, the accelerometer had about five times as high a natural frequency, making it less subject to phase distortion. Finally, 579 points were read for a record of 12.68 seconds duration, about five times as many points as would usually be read.

Both records were given the usual baseline adjustment and then doubleintegrated to get displacements. The results are compared to the actual displacements in Fig. 25. Note that both computed displacement records contain long period errors of about the sort expected from the nature of the polynomial adjustment and of a magnitude comparable to the amplitude of the actual displacement. For a less ideal record, that is, one which does not include the beginning of the measured motions and which does not fall toward zero displacement at the end of a comparatively short record, these long period errors would be expected to be much larger. For periods shorter than about 3 seconds, the agreement is good enough to be of considerable help in analyzing qualitative features of earthquake ground motion, such as whether the motion was more or less continuous or consisted primarily of one or more relatively isolated displacement steps.

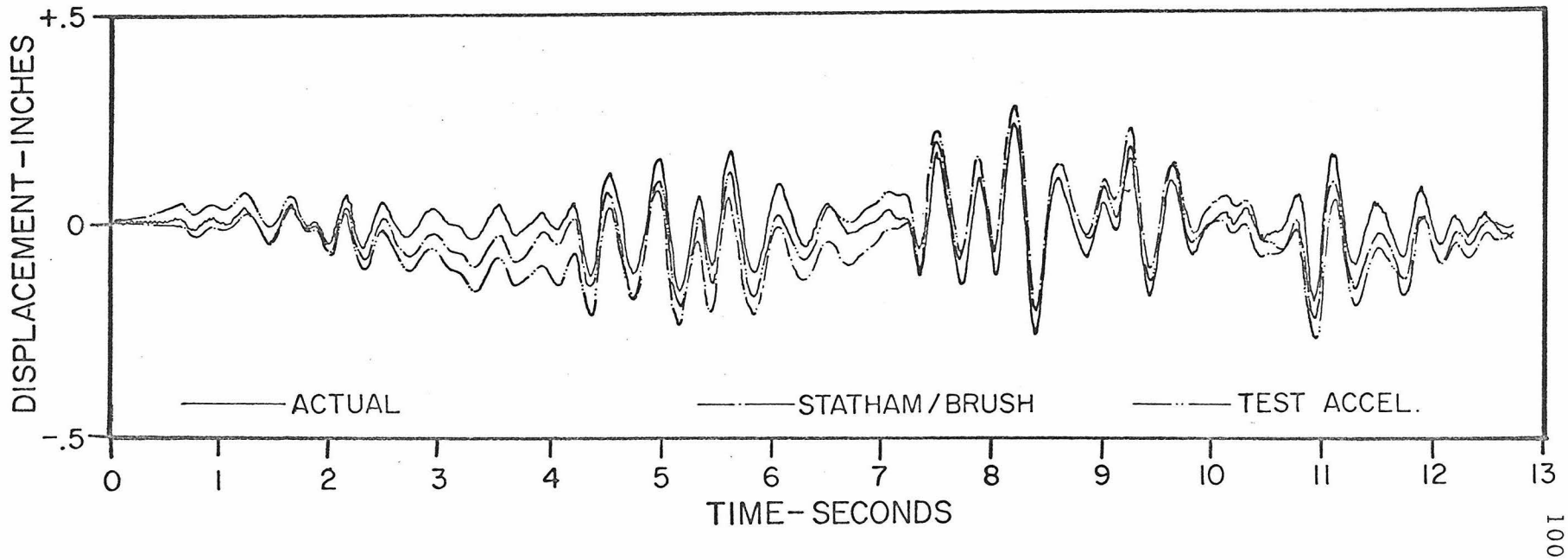

Figure 25: Actual Displacement Compared to Computed Displacements for Sample Earthquake

The coefficients for a Fourier expansion of each acceleration record were next computed with the same adjusted baseline. The two spectra are shown superimposed in Fig. 26. They are virtually identical from 1 Hz to 10 Hz except for a small discrepancy in the vicinity of 5-6 Hz. Above 15 Hz the coefficients for the Statham/ Brush record are essentially zero, while those for the accelerograph show an approximately linear increase to 25 Hz, and a similar slow decline above 25 Hz. This behavior is what would be expected if the accelerograph output above 15 Hz were almost entirely noise. For this particular example, which is typical to the extent that actual earthquake motions usually show little energy above 10 Hz, an improvement in signal to noise ratio would have occurred with no significant loss of information by filtering at 10 Hz instead of 25 Hz. In any case, noise level would seem to be the principal limitation on the test accelerograph's performance above 10 Hz. Improvements to the compensation system suggested in Section 3.2 would make a worthwhile difference. The generally excellent agreement, aside from the noise problem, at frequencies above 1 Hz supports the opinion that long period mechanical hysteresis affects mainly the ease of calibration of these instruments.

Below 1 Hz, the deviation in spectra is believed to be principally due to long period components introduced by the baseline adjustment. Their percentage disagreement is of the same order as the long period errors observed, and instrument nonlinearities are

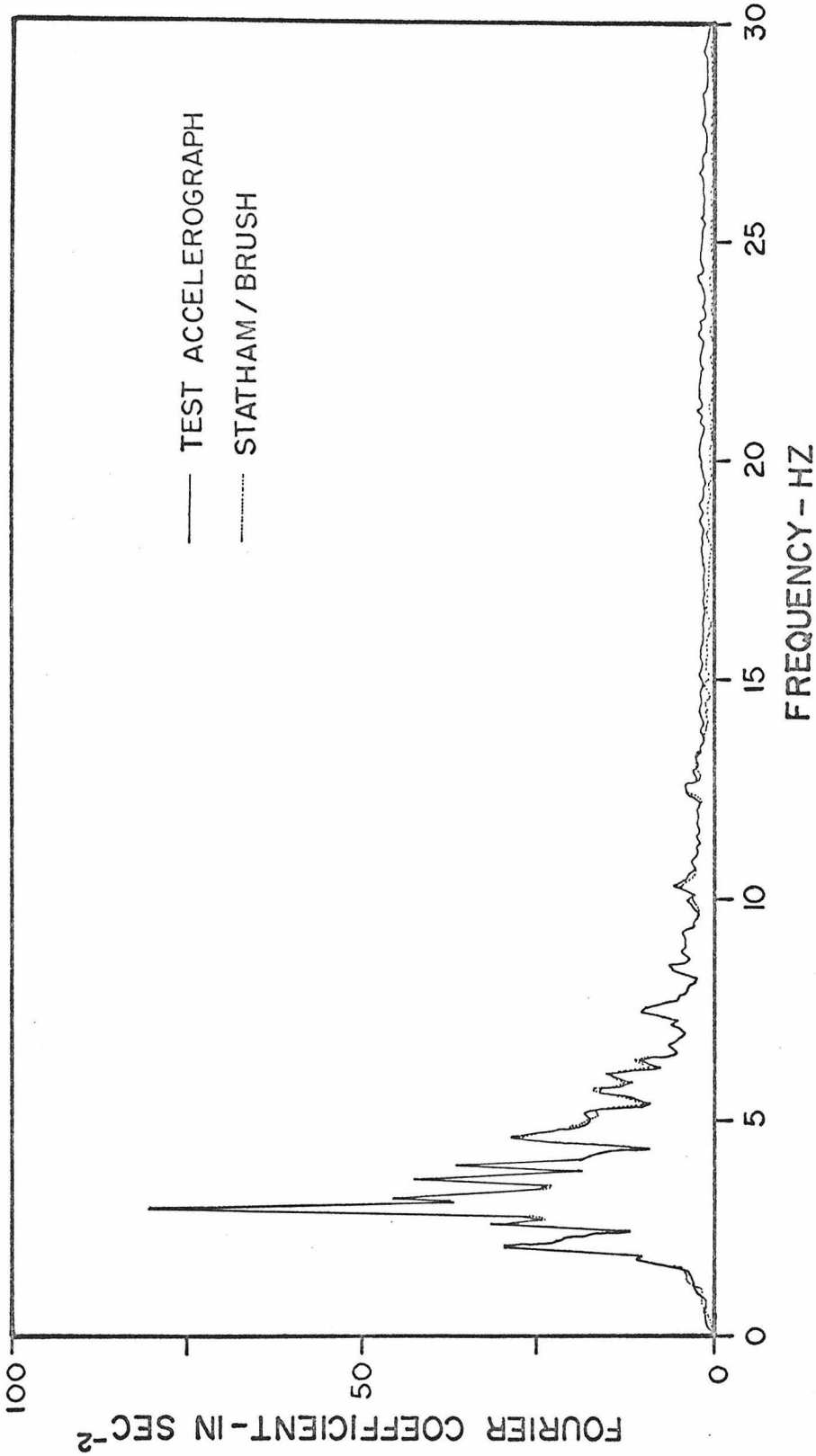

Figure 26: Fourier Coefficients Computed from Two Records of Sample Earthquake

not sufficient to account for such errors. The beginning of marked deviations at 1 Hz is therefore probably due to the short duration of this sample record. Real earthquake records would not be expected to encounter large errors until somewhat longer periods, typically above three seconds.

The discrepancy at 5-6 Hz is too small to be of any real concern as regards instrument accuracy, but it is rather interesting because of its relationship to the large peak at 2.8 Hz. The simple example of a small unsymmetrical nonlinearity considered in Section 2.2 predicted that a single frequency at 2.8 Hz should interact with such a nonlinearity to produce an additional signal at 5.6 Hz with a relative amplitude of the same order as the per unit nonlinearity. That would seem to be essentially what has happened here.

Incidentally, computation of these Fourier spectra by means of a standard computer program which was written primarily for analysis of records from existing strong motion recorders brought about some computer storage problems. Because of the large number of intermediate results which this program is required to generate and store, the size of the computer working storage limits inputs to a maximum of about 1500 data points, and this particular program was written to accept only 1000. This comparatively short record contained 1800 points, which necessitated a smoothing program followed by discarding half the points before the program could be used. That still left the Nyquist frequency at 35 Hz so that

no major harm was done. Automatically digitized earthquake records of the future, at 100 samples per second, may contain 5000 or more points and would require some software revisions, with possible recourse to offline storage. This would not affect the investigation of longer recording times suggested in Section 2.3, since the full record would be used only for the relatively simple computation of an adjusted baseline, while the long uneventful tail of the record could be discarded for all subsequent computations.

Nonlinearity Study. As an additional check on the properties of the test accelerograph, a brief study was conducted to verify the expected effect of the small transduction nonlinearities which it is known to exhibit. The baseline adjusted, 900 point version of the acceleration vs. time record was altered on the computer to simulate the effect of a 1% symmetrical nonlinearity, and then a 2% unsymmetrical nonlinearity. The resulting records were then separately baseline adjusted and used to compute new displacements. The actual nonlinearities simulated and the changes in computed displacements are shown in Fig. 27.

As expected, the errors introduced by these simulated nonlinearities are predominantly long period, and of about the same magnitude as those observed when the test accelerograph and Statham/Brush displacements were compared to the actual displacements. Also as expected, the symmetrical nonlinearity which is

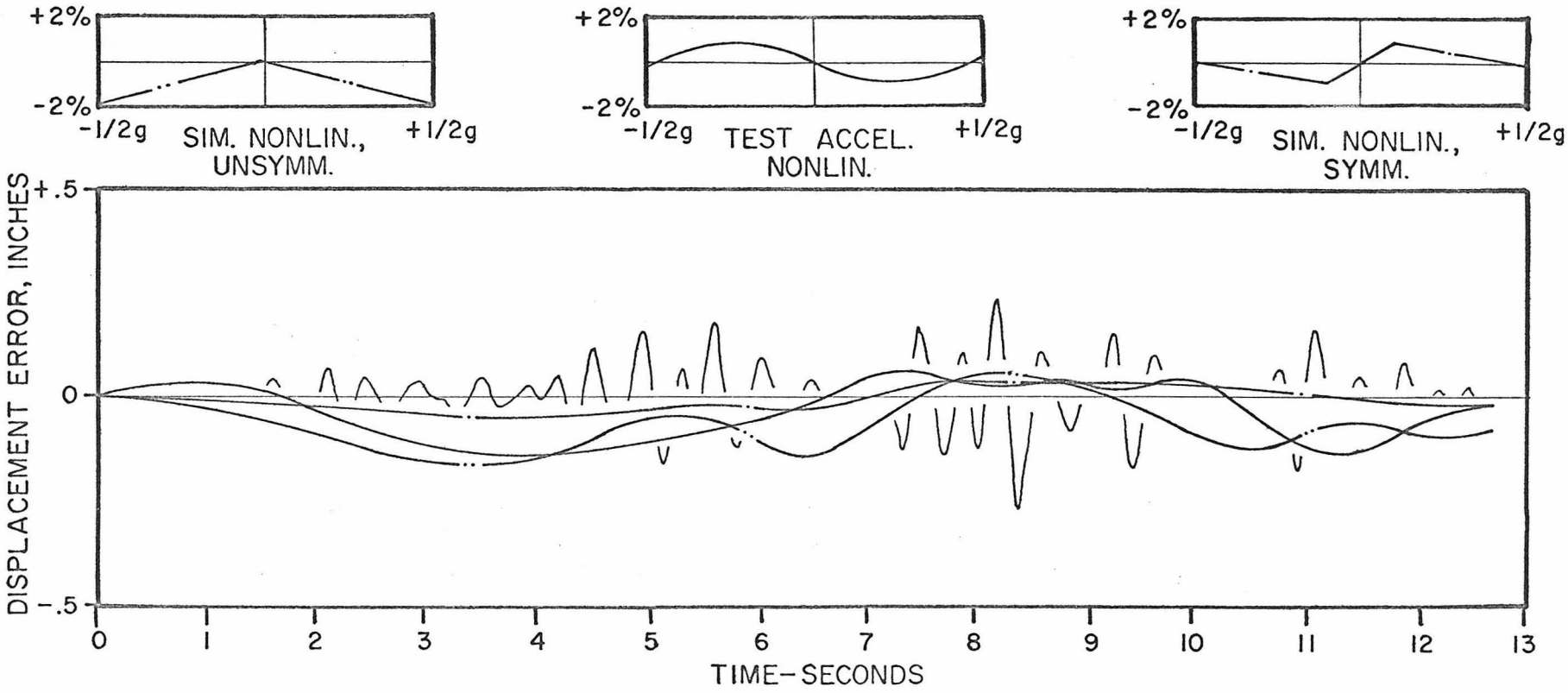

Figure 27: Errors in Computed Displacement Due to Simulated Symmetrical and Unsymmetrical Nonlinearities, Compared to Errors from Test Accelerograph Record. Standard Baseline Adjustment Used in All Cases.

associated with a very carefully adjusted RMT-280 produced smaller errors than the probably more typical unsymmetrical curve. Neither of these simulated nonlinearities produced errors which could be considered as fundamental limitations, since the long period information which they principally affect is already highly unreliable for many other reasons.

5. SUMMARY AND CONCLUSIONS

The RMT-280 Strong Motion Earthquake Recorder converts acceleration to computer compatible output through the following chain of events:

(1) The instrument is activated by an inverted pendulum seismic switch when ground motion above a preset threshold begins.

(2) Three mutually perpendicular linear accelerometers transform acceleration into small angular motions by means of pendulums mounted on torsional suspensions.

(3) A variable reluctance angular transducer on each accelerometer controls the frequency of a local oscillator to produce an electrical output which is a frequency modulated analog of the angular displacement.

(4) The three FM acceleration signals plus a timing and compensation signal are recorded on magnetic tape.

(5) In a separate playback facility, the recorded information is reproduced with compensation for tape speed variations and electronically digitized.

Two of these instruments have undergone a series of evaluation tests in the California Institute of Technology Earthquake Engineering Research Laboratory leading to modifications to bring them to a performance level adequate for their intended use. Then they were given a complete system test using a low frequency shake table which was programmed to produce pseudo earthquakes. The results are conveniently reported in several groups:

Static Accuracy: Performance of the field instruments is dependent on the time and care taken in adjusting them in the laboratory. With 1/2 g taken as full scale, and using a tilt table accurate to ± 0.1%, the following static accuracies were obtained:

(1) Adjustment time approximately 1-1/2 to 2 hours per accelerometer:

Linearity: ± 1% of full scale, symmetrical nonlinearity; less than .5% unsymmetrical.

Sensitivity: Within ± 0.5% of a preselected value at the ± 1/2 g points.

(2) Adjustment time approximately 20 minutes per accelerometer:

Linearity: ± 2% total nonlinearity, typically mostly unsymmetrical.

Sensitivity: Within ± 2% of a preselected value at the ± 1/2 g points.

It is this set of accuracies which is probably typical of field units.

Times in both cases can be reduced by about one-third if the final sensitivity is allowed to fall within ± 20% of the nominal value and calibrated to the accuracies quoted.

A ± 1/2 g calibration circuit is included on each accelerometer, adjustable to ± 3% of the values given by the tilt table.

The sensitivity of the FM accelerometers was found to be stable within 0.5% over a period of six months, the duration of the final phase of these tests.

The long times required for accurate adjustment are due to interactions of several controls, requiring iterative settings, and to a long period mechanical hysteresis in the accelerometers. This mechanical hysteresis has the effect of causing "static" readings to drift steadily with time. In particular, every time a static acceleration is applied for more than a few seconds, a temporary change is induced in the accelerometer zero. This phenomenon causes the number of readings which must be taken during an accelerometer adjustment to increase rapidly with the accuracy and ultimately becomes a limit upon the static accuracy achievable. It also appears to be an important contributor to several other kinds of zero point drift.

Zero Point Drift: Uncertainties in zero point in the RMT-280 arise in four principal ways:

(1) Turn-on drift: When the instrument is activated after a quiescent period, the zero point frequency displays an approximately exponential drift with a time constant of about a minute and a maximum amplitude of about 2% of full scale in that time. The size of the effect is not constant, but varies in a random fashion with repeated trials and may be either positive or negative.

(2) Temperature drift: $+0.35 \pm 0.15\%$ of full scale per degree Fahrenheit.

(3) Relative humidity drift: About 0.4% of full scale increase in zero point frequency for each 10% increase in relative humidity above 50% R. H. No apparent effect below 50% R. H.

(4) Long term random drift: About $\pm 4\%$ of full scale over a period of three months. The maximum sustained drift rate observed was 1% per day for 5 days.

Short Period Noise: The major source of short period noise in the RMT-280 is wow, flutter, and skew effects in the tape recorder and in the compensated playback system. Tests with an interim playback system yielded the following total noise figures:

(1) Low pass filtered at 25 Hz: 1.4% of full scale, RMS.

(2) Low pass filtered at 10 Hz: 0.7% of full scale, RMS.

Improvements to the playback system consistent with the current state-of-the-art are expected to reduce the 25 Hz figure to 0.5% RMS. Improvements in the field recorders could make a further reduction to less than 0.1%, but would significantly increase manufacturing costs.

Timing Accuracy: Use of the compensation oscillator as a time base provides an essentially continuous time base which has:

(1) Linearity: .02% of reading from record starting point.

(2) Accuracy: 1% of reading from record starting point.

An independent two per second timing mark generator of similar accuracy provides a convenient means for correlating records from several interconnected recorders.

Overall System Accuracy: The accuracies quoted above are sufficient for the following accuracies in reduced data from the RMT-280:

(1) Acceleration at any given time can be read to accuracies of ± 3% to ± 5% (depending on adjustment) if standard corrections are made for zero point drift.

(2) Fourier coefficients may be found for the range of periods from 0.1 seconds to 3 seconds subject to two independent sources of error:

± 0.5 in/sec^2 noise level (typically less than 0.3% of the largest coefficients associated with a 1/2 g amplitude earthquake ground motion).

± 3% of reading due to combined effects of nonlinearity and the longer period component introduced by baseline correction.

(3) Double integration to obtain displacements is valid for qualitative conclusions for periods shorter than about 10% of the record duration, or typically about 3 - 6 seconds.

These estimates of overall accuracy are consistent with the results of the full system shake table tests. The results for the two accelerographs tested agreed sufficiently closely to conclude that the measured characteristics are typical.

The performance of the RMT-280 compares favorably with that of the optical recorders which have heretofore been the standard of the field. The RMT-280 produces a slightly noisier record than a carefully digitized optical recorder, but this effect can be minimized by processing techniques which its ten times higher average sampling rates make practical. It also has the marked advantage of an effectively continuous time base.

Recommended Future Development: The noise level of the RMT-280 is presently the principal limiting factor in its performance and the

most promising area for future developmental improvements. Most of the other problems relate primarily to displacement calculations where significant improvement seems unlikely. For example, to extend the period limit on displacement calculations to one minute would require an improvement in the D. C. stability by at least a factor of 10^4. Improvements of this order would likely require a basically different approach. Elimination of mechanical hysteresis, one of the long period problems, would make calibration easier, but would have only a minor effect on overall accuracy.

The RMT-280 in its present form is capable of performing the duties for which it was intended. In most respects it represents a significant advance over the optical recorders now in use. Additional improvements can be attained by minor alterations suggested in the present report. It is not believed that new types of instruments having markedly superior characteristics are likely to be available within the next ten years.

REFERENCES

1. Alfrey, T. Jr. (1948). Mechanical Behavior of High Polymers; Interscience Publishers, Inc., New York.

2. Black, H. S. (1953). Modulation Theory; D. Van Nostrand Company, Inc., New York.

3. Brady, A. G. (1966). Studies of response to earthquake ground motion; Ph.D. Thesis, California Institute of Technology.

4. Hudson, D. E. (1963). The measurement of ground motion of destructive earthquakes; Bull. Seism. Soc. Am. 53, 419.

5. Hudson, D. E., N. C. Nigam and M. D. Trifunac (1969). Analysis of strong motion records; Fourth World Conference on Earthquake Engineering; Santiago, Chile.

6. Schiff, A. J., and J. L. Bogdanoff (1967). Analysis of current methods of interpreting strong motion accelerograms; Bull. Seism. Soc. Am. 57, 857-874.

7. Hathaway Pacific Corporation (1963). Technical Bulletin No. PI500-564-3, Hathaway Pacific Corp., 4055 Fabian Way, Palo Alto, California 94303.

APPENDIX A

TEST INSTRUMENTATION

A1. Commercial Equipment Used

Description	Manufacturer	Model No.	Remarks
Digital Counter	Berkeley	5510	
Digital Counter	Hewlett-Packard	5245M	
Tape Deck	Viking	NAB Cartridge	
Stereo Preamp	Marantz	7T	Used in interim playback facility
FM Discriminator	Pacific Communications and Electronics, Inc.	115	
Pen Recorder	Brush	Mark 280	
Time Switch	Paragon	8035-0	
Interval Time Switch	Eagle Signal Corp.	Microflex	Used in long term stability test set-up
Vacuum Tube Tuning Fork	General Radio	723C(1000Hz)	
Temperature and Relative Humidity Recorder	Foxboro		
Accelerometer	Statham	A5-2-350	
Carrier Amplifier	Brush	4212	Used to monitor table motion in system test
Linear Variable Differential Transformer	Schaevitz	400 HR	

A2. Special Test Set-ups

The figures in this appendix provide additional details of several important test set-ups referred to in the body of this report.

Figures A1 and A2 show details of the system used to compensate the test accelerograph's data tapes for wow and flutter in the record and playback transport mechanisms. An analysis of this compensation technique is carried out in Section 3.2. Figure A1 shows the functional relationship of the important parts of a single compensated channel. The time delay component indicated in the data unit serves to match the time delay of the required low pass output filter in the compensation unit. This component was not used in the interim playback facility used for all testing in this report. Data in Section 3.2 show that the system performance is acceptable without this refinement, but could be significantly improved by its inclusion in future playback facilities.

Figure A2 shows the relative positions of the record and playback tape heads for the test accelerographs and their playback systems. The arrangement on the left is the one which was in use at the time of the tests reported in Section 3.2. The one on the right is the one which has been specified for use in all future production. In both cases track number 3 is the one used for reference. It is easily seen that tests involving track number 1 as the data track, which is the worst skew error condition, are

unaffected by the change in heads. This fact made it unnecessary to repeat the noise testing when the heads were changed.

Figure A3 shows a simplified schematic of the equipment which was assembled to sample the zero-g output of the test accelerometers over long periods of time. Following a typical cycle will illustrate the kind and quality of the data obtained from this set-up. Each cycle is initiated by one of several trippers on the 24 hour dial of the master clock. The clock supplies AC power to the chart recorder, the FM discriminator, the electronic tuning fork and the first of the three interval timers. During the 20 second interval before the first timer trips out, a 1000.0 ± 0.1 Hz signal from the tuning fork is applied to the input of the discriminator. The voltage level recorded on the chart during this interval provides a calibration of any drifts which may have occurred in either the discriminator or the chart recorder since the last operator check of the equipment. As the first timer trips out it removes the tuning fork from the discriminator input and applies power to the second timer. The second timer connects one channel of the accelerograph to the discriminator and leaves it connected when it trips out two seconds later, starting the third timer. The third timer turns on the accelerograph and records 20 seconds of its output on the chart recorder, showing not only the apparent zero for that cycle, but also any drift which may occur during the twenty second period. When the third timer trips out it turns off the accelerograph and

stops the chart recorder. Approximately half a minute later the master clock turns the AC power back off, and all elements automatically reset for the next cycle.

Other similar cycles, involving additional contact pairs, not shown, and in some cases different settings of the interval timers, were used to make simultaneous recordings of the accelerograph battery voltage or to provide sequential recordings of two different accelerographs. Data obtained from these tests are reported in Section 3.4.

Figure A4 illustrates the technique used to detect the timing information which is carried on the reference signal as amplitude modulation. This particular circuit was assembled for laboratory experimental use and is somewhat more complicated than would be necessary for routine data playback. In particular, the relay output stage could be eliminated. In laboratory experiments the relay proved convenient for such things as driving the event marker pens on a chart recorder, but for most purposes the clipped and detected signal will serve equally well.

Figure A5 shows a block diagram of a typical complete playback facility including analog to digital conversion. Important features of this diagram are the use of a single reference channel to compensate three data channels, and use of the reference signal as an external clock input. The value of deriving the A/D

converter clock signal from the recorded reference signal is described in Section 2.2. The overall arrangement of components is identical to the facility assembled for the system tests of Section 4, except that equipment limitations permitted use of only one data channel at a time.

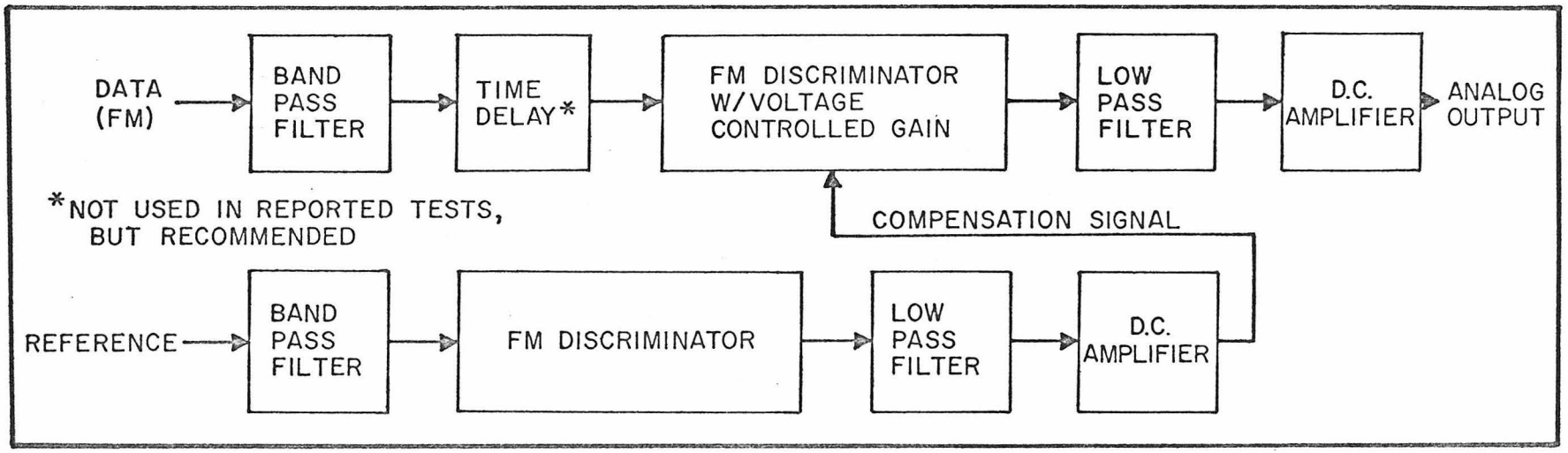

Figure A1: Block Diagram of Compensated Tape Playback System (one channel)

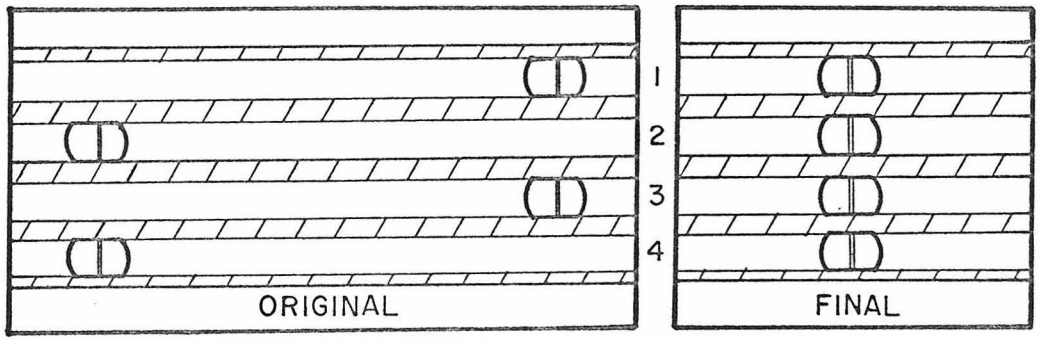

Figure A2: Tape Head Configurations

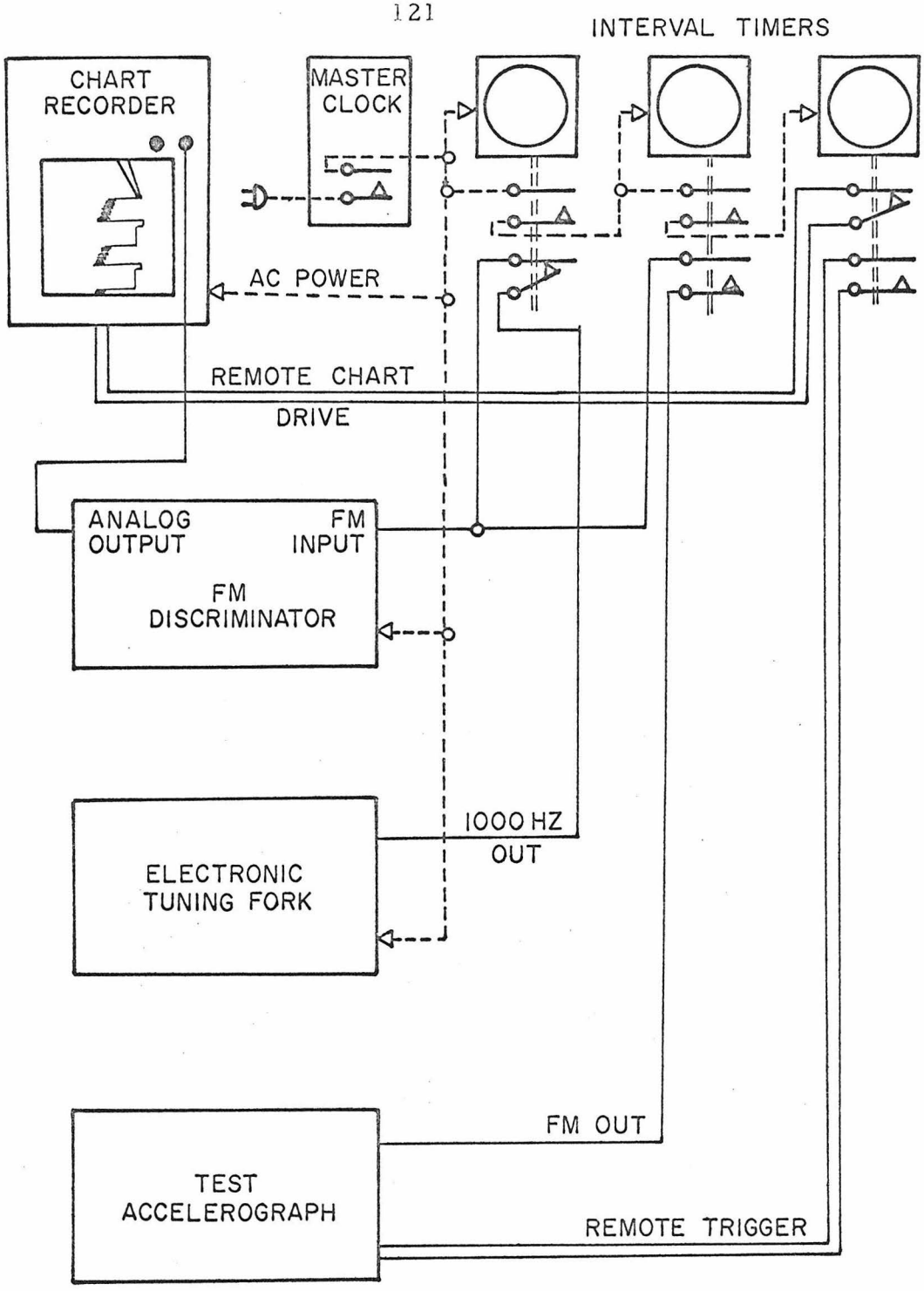

Figure A3: Test for Long Time Stability of FM Accelerometer Zero Point Frequency

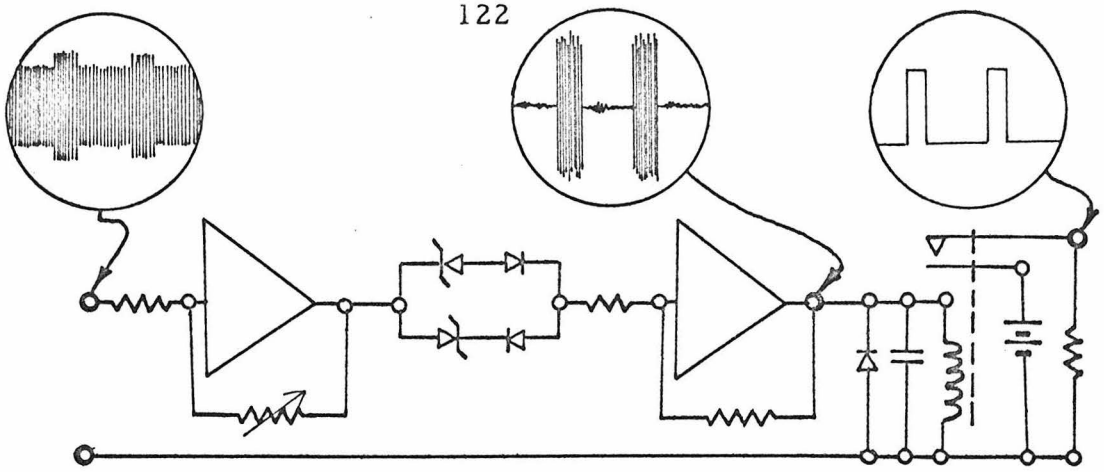

Figure A4: Time Pip Detection Circuit with Typical Signals

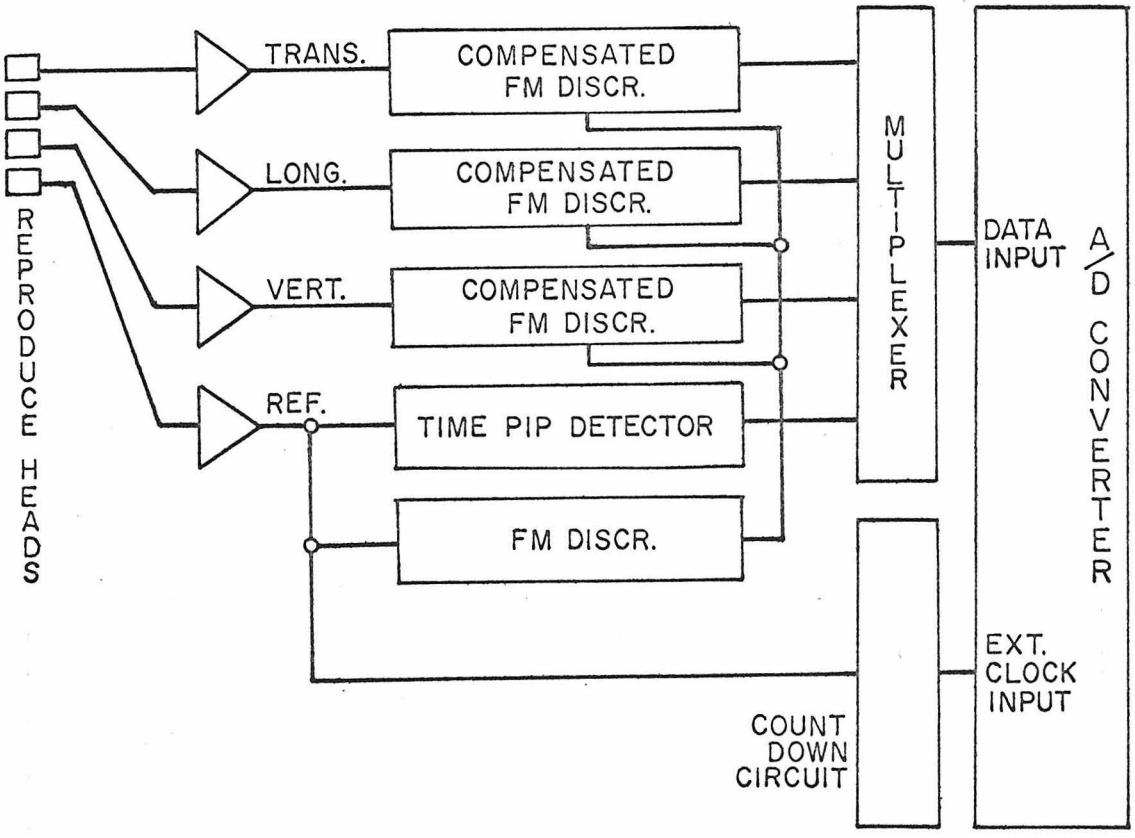

Figure A5: Typical Tape Accelerograph Playback Facility

APPENDIX B

DEVELOPMENT OF A SMALL SHAKING TABLE FOR EARTHQUAKE SIMULATION

Measurement of the dynamic performance of accelerometers for strong motion earthquake recorders requires a shaking device which is capable of clean, closely controlled motion over a range of relatively low frequencies and acceleration levels. A horizontal shake table having these properties was constructed at the beginning of these accelerograph evaluations and used throughout the tests. Its use has been noted particularly in the system tests reported in Section 4.

1. Description

The table is shown in side elevation in Fig. B1. The working surface is an aluminum plate 12" long by 10" wide carried on four flexure mounted arms. It is driven by a modified Goodmans Industries 25 force pound shaker with a maximum stroke of 1/2 inch peak to peak. The length of the flexure arms was chosen to be 12.5 inches to assure that the vertical motion would be less than 1% of the horizontal motion at maximum amplitude. The ratio of vertical to horizontal peak accelerations is slightly less favorable, but can never exceed 2% for sinusoidal motion.

The table is normally instrumented with a Statham accelerometer and a Schaevitz LVDT displacement sensor (details in Appendix A1). The frame also carries a micrometer for ease in checking and recording overall system displacement calibrations when special test set-ups are used.

2. Performance

The performance of the table with a six pound test load is shown in Fig. B2 for constant voltage and constant current drive conditions. The mechanical resonance frequency is clearly shown at 2 Hz by the constant current curve. The table motion for constant voltage input is essentially constant acceleration above 2 Hz and essentially constant displacement below. In view of the 1/2 inch limitation on peak to peak displacements, this mode of behavior has proved convenient for instrument testing, and is also suited to fairly simple displacement limited earthquake simulation.

The 1 Hz lower limit on the curves is imposed principally by the amplifier presently used to drive the shaker, though many other practical problems arise in testing at lower frequencies with such a simple shake table. The small acceleration levels which are possible below 1 Hz even with 1/2 inch travel (less than .03 g) make the acceleration waveform sensitive to extraneous small force inputs, such as anelastic behavior of instrument cables.

The 50 Hz upper limit is purely a matter of range of interest. The system was designed to have no resonances below 200 Hz and

actually has no significant ones below 230 Hz. A very narrow transverse resonance occurs near 40 Hz, but has little effect on the usefulness of the table, since it is observable (through a 40 power microscope) over a band width of only about 1 Hz.

3. Development

Design, construction, and testing of the table proceeded routinely except for the modifications mentioned on the Goodmans shaker. This shaker is manufactured with a bakelite spider at either end of the voice coil to constrain it to axial motion. These perform their function very well over the normal frequency range of the shaker, but at 5 Hz or below, they exhibit a marked "oil canning" effect which produces a major distortion of the acceleration waveform. They were consequently removed, and the voice coil is now entirely supported by the flexure mounted table. There is no mechanical connection to the shaker frame except through the soft braided wires which carry current to the coil.

Removal of these spiders corrected one major problem, but created a series of minor ones. Removal of the rear spider required that the magnet assembly be dismantled to gain access to the interior. This breaking of the magnetic circuit had the fairly common effect of partially depoling the field magnet, so that a very low efficiency was observed on reassembly. A first attempt at repoling produced acceptable performance except that a shift in static position occurred which was roughly proportional to A. C. drive level and sufficient to

cut the available peak to peak displacement in half at frequencies near 5 Hz. It was suspected, finally, that the effect was caused by modulation of the field flux by the current in the voice coil, which would be possible only if the field magnet were not quite saturated. The condition of the field magnet was checked by driving the table at resonance by hand and measuring the voltage output of the open circuited voice coil. When the transducer coefficient computed from these measurements was compared to that computed from the manufacturer's nominal value for current required to produce 25 pounds force, it was found to be about 25% low. A second repoling was performed on a more powerful machine. The measured coefficient was then found to be only 1.4% below nominal, and the static shift problems disappeared.

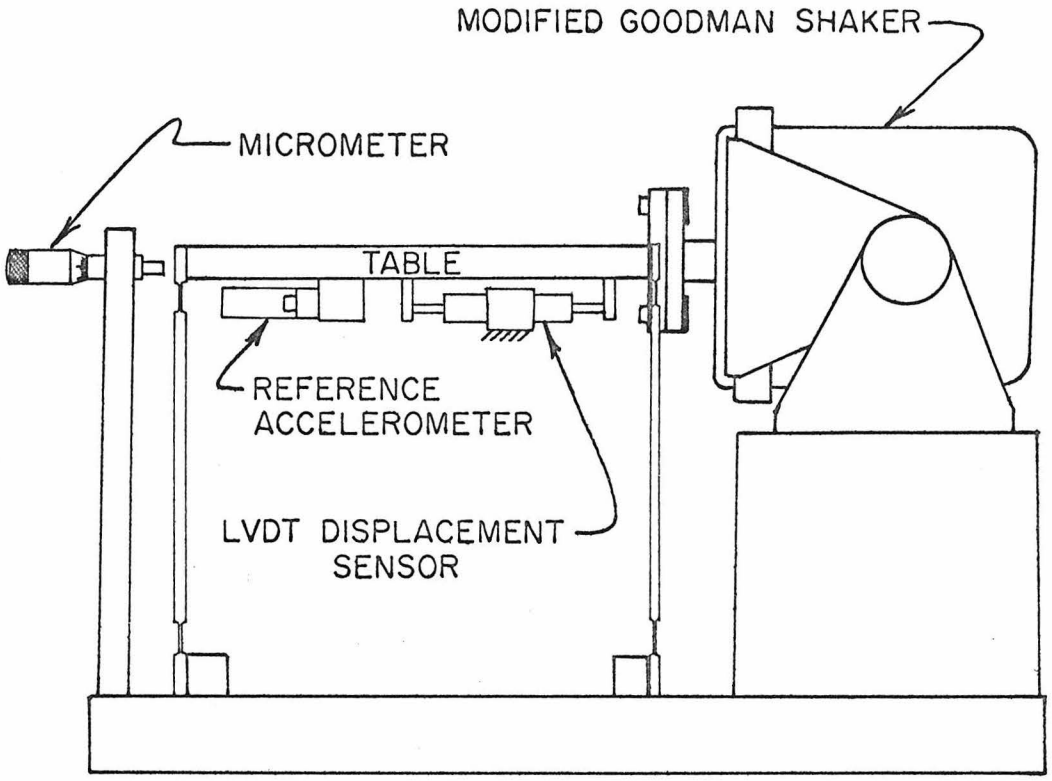

Figure B1: Flexure Mounted Experimental Low Frequency Shake Table

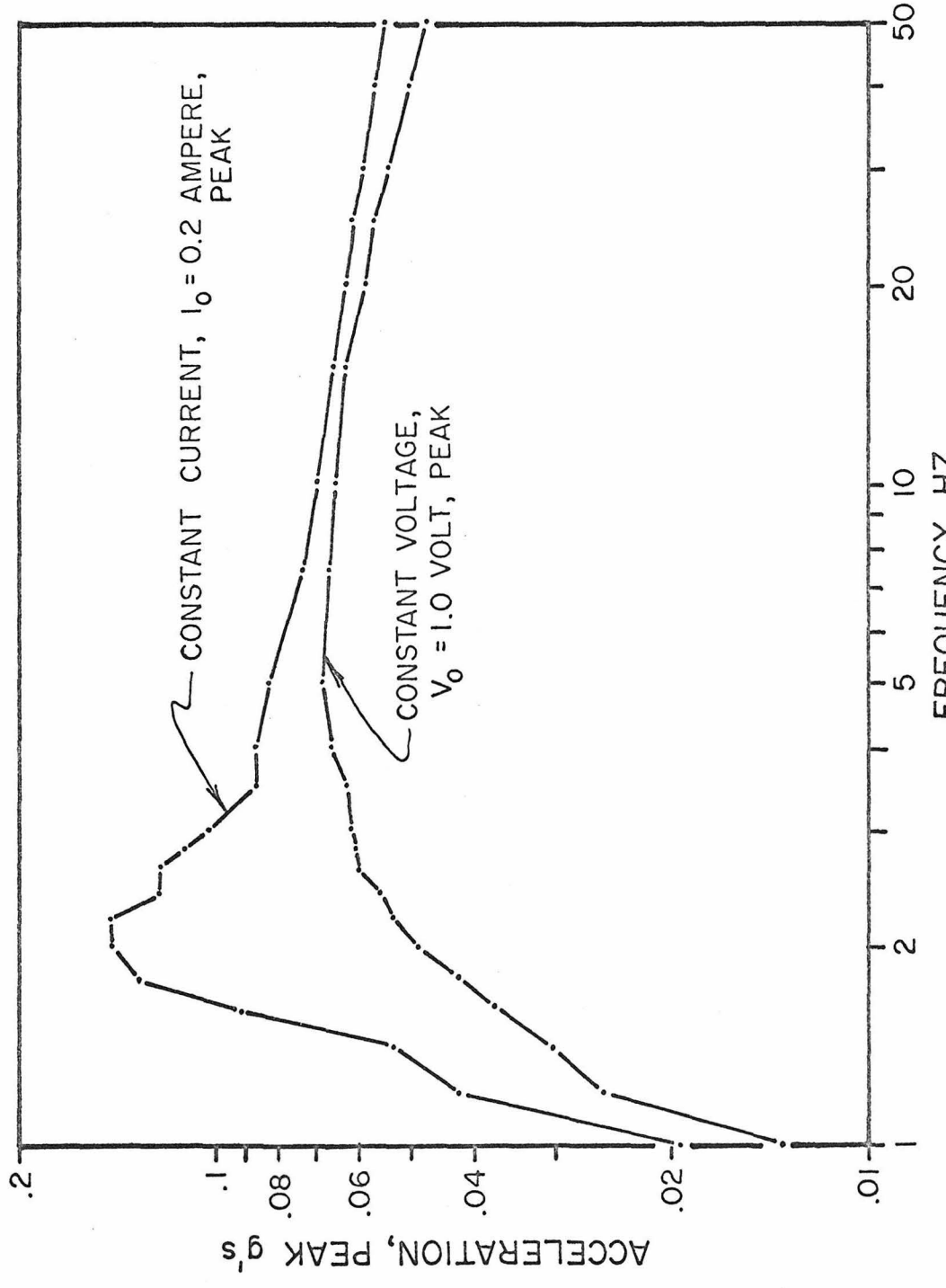

Figure B2: Sinusoidal Frequency Response of Low Frequency Shake Table with 6 Lb Test Load

APPENDIX C

MAGNETIC AND MECHANICAL FORCES ACTING IN THE TEST ACCELEROMETERS

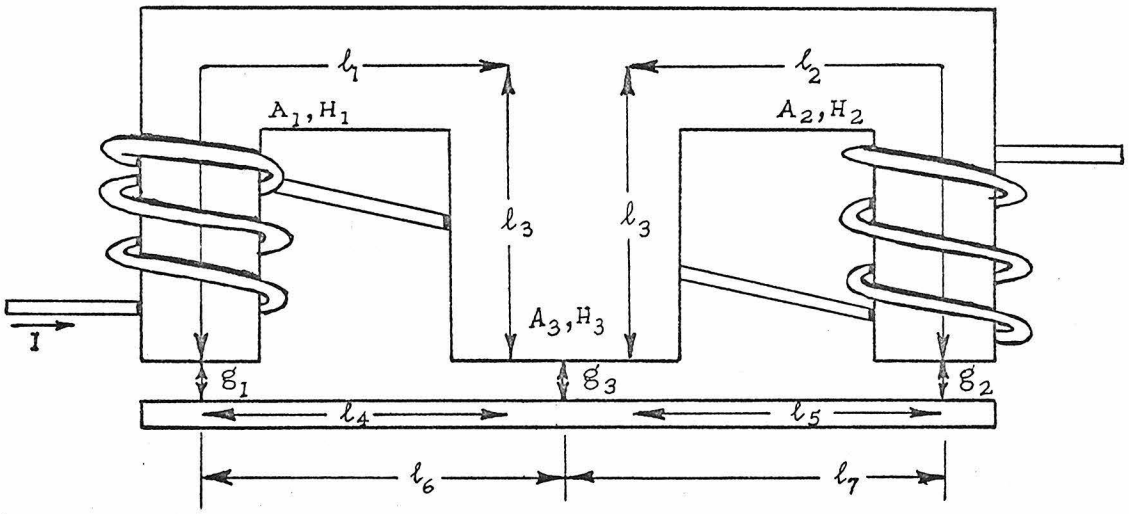

A_i = Areas

H_i = Magnetomotive Forces

To simplify the calculations, all magnetic properties will be approximated by the linear term. The expressions are written for rationalized MKS units.

Neglecting $\frac{\partial D}{\partial t}$ (eddy currents) compared to J (applied currents) (since the cores are laminated to keep eddy currents small):

$$\nabla \times \vec{H} = \vec{J}, \qquad \text{or, in integral form} \quad \oint \vec{H} \cdot d\vec{\ell} = \int_s \vec{J} \cdot \vec{n}\, da$$

for the left side:

$$\oint \vec{H} \cdot d\vec{\ell} = \ell_1 H_1 + g_1 Hg_1 + \ell_4 H_4 + g_3 Hg_3 + \ell_3 H_3 = \int_s \vec{J} \cdot \vec{n}\, da = NI$$

for the right side:

$$\oint \vec{H} \cdot d\vec{\ell} = \ell_2 H_2 + g_2 Hg_2 + \ell_5 H_5 + g_3 Hg_3 + \ell_3 H_3 = \int_s \vec{J} \cdot \vec{n}\, da = NI$$

where N = number of turns on each coil, I = coil current. Neglecting fringing:

$$\Phi_1 = \mu H_1 A_1 = \mu_o Hg_1 Ag_1 = \mu H_4 A_4$$

$$\Phi_2 = \mu H_2 A_2 = \mu_o Hg_2 Ag_2 = \mu H_5 A_5$$

$$\Phi_1 + \Phi_2 = \mu H_3 A_3 = \mu_o Hg_3 Ag_3$$

Substituting to reduce the number of variables:

$$\ell_1 H_1 + g_1 \frac{\mu}{\mu_o} \frac{A_1}{Ag_1} H_1 + \ell_4 \frac{A_1}{A_4} H_1 + \left(g_3 \frac{\mu}{\mu_o} \frac{A_3}{Ag_3} + \ell_3 \right) \left(H_1 \frac{A_1}{A_3} + H_2 \frac{A_2}{A_3} \right) = NI$$

$$\ell_2 H_2 + g_2 \frac{\mu}{\mu_o} \frac{A_2}{Ag_2} H_2 + \ell_4 \frac{A_2}{A_4} H_2 + \left(g_3 \frac{\mu}{\mu_o} \frac{A_3}{Ag_3} + \ell_3 \right) \left(H_1 \frac{A_1}{A_3} + H_2 \frac{A_2}{A_3} \right) = NI$$

These equations have the form:

$$B_1 H_1 + B_2 H_2 = NI$$

$$C_1 H_1 + C_2 H_2 = NI$$

leading to

$$H_1 = \frac{NI(C_2 - B_2)}{B_1C_2 - B_2C_1} \qquad H_2 = \frac{NI(B_1 - C_1)}{B_1C_2 - B_2C_1}$$

The fluxes through the coils are given by:

$$\Phi_1 = \mu H_1 A_1 ; \qquad \Phi_2 = \mu H_2 A_2$$

and the inductances, by definition, are:

$$L_1 = \frac{N\Phi_1}{I} = \frac{N^2 \mu A_1 (C_2 - B_2)}{B_1C_2 - B_2C_1}$$

$$L_2 = \frac{N\Phi_2}{I} = \frac{N^2 \mu A_2 (B_1 - C_1)}{B_1C_2 - B_2C_1}$$

Suppose now that the coils are driven by a voltage source,

$$E = E_o \cos \omega t = (L_1 + L_2)\frac{dI}{dt} ; \qquad \text{then} \quad I = \frac{E_o \sin \omega t}{\omega(L_1 + L_2)}$$

and

$$H_1 = \frac{E_o \sin \omega t}{\omega N \mu \left[A_1 + A_2 \left(\dfrac{\ell_1 + g_1 \dfrac{\mu}{\mu_o} \dfrac{A_1}{Ag_1} + \ell_4 \dfrac{A_1}{A_4}}{\ell_2 + g_2 \dfrac{\mu}{\mu_o} \dfrac{A_2}{Ag_2} + \ell_4 \dfrac{A_2}{A_4}} \right) \right]}$$

$$H_2 = \frac{E_o \sin \omega t}{\omega N \mu \left[A_2 + A_1 \left(\dfrac{\ell_1 + g_2 \dfrac{\mu}{\mu_o} \dfrac{A_2}{Ag_2} + \ell_4 \dfrac{A_2}{A_4}}{\ell_2 + g_1 \dfrac{\mu}{\mu_o} \dfrac{A_1}{Ag_1} + \ell_4 \dfrac{A_1}{A_4}} \right) \right]}$$

The energy stored magnetically in the circuit is given by

$$W = \frac{1}{2}\int_V B \cdot H dV = \frac{1}{2}\mu H_1^2 A_1 \left\{ \ell_1 + \frac{A_1}{A_4}\ell_4 + \frac{\mu}{\mu_o}\frac{A_1}{Ag_1}g_1 + \frac{A_1}{A_3}\ell_3 + \frac{\mu}{\mu_o}\frac{A_1}{Ag_3}g_3 \right\}$$

$$+ \frac{1}{2}\mu H_2^2 A_2 \left\{ \ell_2 + \frac{A_2}{A_5}\ell_5 + \frac{A_2}{Ag_2}g_2 + \frac{A_2}{A_3}\ell_3 + \frac{\mu}{\mu_o}\frac{A_2}{Ag_3}g_3 \right\}$$

$$+ \mu H_1 H_2 A_2 \left\{ \frac{A_1}{A_3}\ell_3 + \frac{\mu}{\mu_o}\frac{A_1}{Ag_3}g_3 \right\}$$

The total force is now given by

$$F = \frac{\partial W}{\partial g_1} + \frac{\partial W}{\partial g_2} + \frac{\partial W}{\partial g_3}$$

The torque is given by

$$M = \ell_6 \frac{\partial W}{\partial g_1} - \ell_7 \frac{\partial W}{\partial g_2}$$

At this point it becomes worthwhile to introduce some of the relationships that hold for the actual E-cores used in order to simplify the expressions and make them more manageable:

$$\ell_1 = \ell_2 = \ell \qquad A_1 = A_2 = Ag_1 = Ag_2 = A$$

$$\ell_4 = \ell_5 = \ell' \qquad A_4 = A_5 = A'$$

$$\ell_6 = \ell_7 = \ell'' \qquad A_3 = Ag_3 = 2A$$

With these substitutions the expressions for H can be simplified considerably:

$$H_1 = \frac{T}{1 + \dfrac{K + g_1}{K + g_2}} = \frac{T(K + g_2)}{2K + g_1 + g_2}$$

$$H_2 = \frac{T(K+g_1)}{2K+g_1+g_2}$$

where

$$T = \frac{E_o \sin \omega t}{\omega N \mu A}, \qquad K = \frac{\mu_o}{\mu}\left[\ell + \ell' \frac{A}{A'}\right]$$

Making these substitutions and combining several terms, the energy expression reduces to:

$$W = \frac{1}{4}\frac{\mu^2}{\mu_o} AT^2\left[g_3 + \frac{\mu_o}{\mu}\ell_3\right] + \frac{1}{2}\frac{\mu^2}{\mu_o} AT^2\left[\frac{(K+g_1)(K+g_2)}{2K+g_1+g_2}\right]$$

$$\frac{\partial W}{\partial g_1} = \frac{1}{2}\frac{\mu^2}{\mu_o} AT^2\left[\frac{K+g_2}{2K+g_1+g_2}\right]^2$$

$$\frac{\partial W}{\partial g_2} = \frac{1}{2}\frac{\mu^2}{\mu_o} AT^2\left[\frac{K+g_1}{2K+g_1+g_2}\right]^2$$

$$\frac{\partial W}{\partial g_3} = \frac{1}{4}\frac{\mu^2}{\mu_o} AT^2$$

$$F = \frac{1}{4}\frac{E_o^2 \sin^2 \omega t}{\mu_o N^2 \omega^2 A}\left\{1 + 2\frac{(K+g_2)^2 + (K+g_1)^2}{(2K+g_1+g_2)^2}\right\}$$

$$M = \frac{\ell''}{2}\frac{E_o^2 \sin^2 \omega t}{\mu_o N^2 \omega^2 A}\left\{\frac{(K+g_2)^2 - (K+g_1)^2}{(2K+g_1+g_2)^2}\right\}$$

Numerically:

$\ell = .0278$ meters $\quad A = 2.30 \times 10^{-5}\ m^2 \quad \omega = 6.4 \times 10^{3}$ radians sec^{-1}

$\ell' = .0112$ meters $\quad A' = 1.90 \times 10^{-6}\ m^2$

$\ell'' = .0136$ meters $\quad \ell_3 = .0166$ meters

Drive voltage is 3.9 VRMS; the inductance of both coils in series, with all gaps equal at .0010 meters, is 2.4 Henries. For the balanced case

$$L_1 = L_2 = \frac{\mu N^2}{\frac{\ell + \ell_3}{A} + \frac{\ell'}{A'} + \frac{g_1 + g_2}{A}\frac{\mu}{\mu_o}}$$

$$N = \sqrt{\frac{L}{\mu_o}\left[\left(\frac{\ell + \ell_3}{A} + \frac{\ell'}{A'}\right)\frac{\mu_o}{\mu} + \frac{2g}{A}\right]}$$

The value of μ for these cores is not known, but it makes little difference as long as it is large. Since $\mu = 25,000\,\mu_o$ is not an unusual figure for such materials, that will be used as an estimate.

$$N = \sqrt{\frac{1.20}{4\pi \times 10^{-7}}\left[\left(\frac{4.49 \times 10^{-2}}{2.30 \times 10^{-5}} + \frac{1.12 \times 10^{-2}}{1.90 \times 10^{-6}}\right)\frac{1}{2.5 \times 10^{-6}} + \frac{2.0 \times 10^{-3}}{2.30 \times 10^{-5}}\right]}$$

$$= 9.1 \times 10^{3} \text{ turns}$$

$$K = \frac{\mu_o}{\mu}\left[\ell + \frac{\ell' A}{A'}\right] = \frac{1}{2.5 \times 10^{4}}\left[(2.78 \times 10^{-2}) + (1.12 \times 10^{-2})\left(\frac{2.3 \times 10^{-5}}{1.9 \times 10^{-6}}\right)\right]$$

$$= 6.6 \times 10^{-6} \text{ meters}$$

For a fairly typical case $g_1 = .90$ mm, $g_2 = 1.10$ mm

$$\boxed{F = F_o \sin^2 \omega t}$$

$$F_o = \frac{1}{4} \frac{(3.9)^2(2)}{\left(4\pi \times 10^{-7}\right)\left(9.1 \times 10^{3}\right)^2\left(6.4 \times 10^{3}\right)^2\left(2.3 \times 10^{-5}\right)} \left\{1.00 + 2.00 \frac{(11.1)^2 + (9.1)^2}{(20.2)^2}\right\}$$

$$\boxed{F_o = 1.6 \times 10^{-4} \text{ newtons}^*}$$

$$\boxed{M = M_o \sin^2 \omega t}$$

$$M_o = \frac{\left(1.36 \times 10^{-2}\right)(3.9)^2(2)}{2\left(4\pi \times 10^{-7}\right)\left(9.1 \times 10^{3}\right)^2\left(6.4 \times 10^{3}\right)^2\left(2.3 \times 10^{-5}\right)} \left\{\frac{(11.1)^2 - (9.1)^2}{(20.2)^2}\right\}$$

$$\boxed{M_o = 1.7 \times 10^{-7} \text{ newton-meters}}$$

The force is attractive.

The sign of the torque is such as to reduce the smaller gap and increase the larger one.

MECHANICAL FORCES ACTING IN THE RMT-280

Accelerometer support wire:

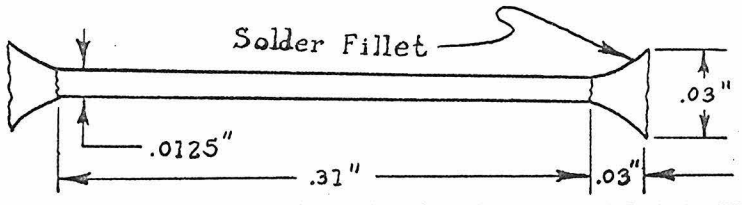

* For those more familiar with the c. g. s. system or English units, a Newton is a force equal to one kilogram meter second^{-2}, which is 10^5 dynes or roughly 1/4 pound force.

The angular twist for 1/2 g, measured at the vane is .0080 radians. Assuming rigid ends, the rate of twist of the wire is $\theta = \frac{.0080}{.31} = .0258$ radians in^{-1}. Maximum shear stress,

$$\tau_{max} = G\theta r = 1.0 \times 10^{3} \text{ psi}$$

where

G = shear modulus for phosphor bronze = 6.2×10^{6} psi

r = wire radius = .00625"

None of the standard handbooks give elastic constants for 60/40 lead tin solder, but values for other lead and tin alloys indicate a value for G of approximately 1.5×10^{6} psi. That would give $\tau = 200$ psi at the leading edge of the fillet, which is well below the yield stress of such alloys, but on the edge of the range where room temperature creep phenomena are known to occur.

For the two wires (one above, one below) the torque associated with 1/2 g is given by

$$M_t = 2\left[\theta\pi\frac{r^4}{2}G\right] = (.0258)(\pi)\left(6.25 \times 10^{-3}\right)^4\left(6.2 \times 10^{6}\right)$$

$$= 7.7 \times 10^{-4} \text{ in lb}$$

$$\boxed{M_t = 8.7 \times 10^{-5} \text{ newton meters}}$$

Total weight of the moving elements is 5.3 grams. At 1/2 g that gives a total side force:

$$\boxed{F_a = \left(5.3 \times 10^{-3} \text{Kg}\right)\left(4.9 \text{ m sec}^{-2}\right) = 2.6 \times 10^{-2} \text{ newtons}}$$

Assuming that all torque comes from the offset coil (other parts are balanced to within a small amount which varies from assembly to assembly) an approximate value can be calculated for the torque at 1/2 g:

$$M_t = \text{(coil mass) (radius to C. G.) (acceleration)}$$

$$= \left(2.3 \times 10^{-3}\right)\left(7.5 \times 10^{-3}\ \text{m}\right)\left(4.9\ \text{m sec}^{-2}\right)$$

$$= 8.5 \times 10^{-5}\ \text{newton meters.}$$

This figure is in reasonable agreement with that calculated from the measured deflections.